UNIVERSIDADE FEDERAL DO RIO GRANDE DO NORTE
CENTRO DE TECNOLOGIA
PROGRAMA DE PÓS-GRADUAÇÃO EM ENGENHARIA MECÂNICA

Performance of Fatigue Life Models Based on Reliable Estimators and an Artificial Neural Network for Materials

Joelton Fonseca Barbosa

(Tese de Doutorado)

Natal/RN
2019

Joelton Fonseca Barbosa

Performance of Fatigue Life Models Based on Reliable Estimators and an Artificial Neural Network for Materials

Tese de Doutorado apresentada ao Programa de Pós-Graduação em Engenharia Mecânica da Universidade Federal do Rio Grande do Norte, em cumprimento com as exigências legais para obtenção do título de **Doutor em Engenharia mecânica**.

Orientador: Prof. Doutor Raimundo Carlos Silverio Freire Júnior
Coorientador: Prof. Doutor José António Fonseca de Oliveira Correia

UNIVERSIDADE FEDERAL DO RIO GRANDE DO NORTE
CENTRO DE TECNOLOGIA
PROGRAMA DE PÓS-GRADUAÇÃO EM ENGENHARIA MECÂNICA

Natal/RN
2019

Universidade Federal do Rio Grande do Norte - UFRN
Sistema de Bibliotecas - SISBI
Catalogação de Publicação na Fonte. UFRN - Biblioteca Central Zila Mamede

Barbosa, Joelton Fonseca.
Performance of fatigue life models based on reliable estimators and an artificial neural network for materials / Joelton Fonseca Barbosa. - 2019.
150 f.: il.

Tese (doutorado) - Universidade Federal do Rio Grande do Norte, Centro de Tecnologia, Programa de Pós-Graduação em Engenharia Mecânica, Natal, RN, 2019.
Orientador: Prof. Dr. Raimundo Carlos Silverio Freire Júnior.
Coorientador: Prof. Dr. José António Fonseca de Oliveira Correia.

1. Fatigue - Tese. 2. Mean stress - Tese. 3. High cycle fatigue - Tese. 4. Neural network - Tese. 5. Probability - Tese. I. Freire Júnior, Raimundo Carlos Silverio. II. Correia, José António Fonseca de Oliveira. III. Título.

RN/UF/BCZM CDU 621.921

Elaborado por Ana Cristina Cavalcanti Tinôco - CRB-15/262

Tese de Doutorado sob o título "**Performance of Fatigue Life Models Based on Reliable Estimators and an Artificial Neural Network for Materials**" por **Joelton Fonseca Barbosa** e aceita pelo Programa de Pós-Graduação em Engenharia Mecânica da Universidade Federal do Rio Grande do Norte, sendo aprovada por todos os membros da banca examinadora abaixo especificada:

Prof. Dr. Raimundo Carlos Silverio Freire Júnior
Orientador
Departamento de Engenharia Mecânica
Universidade Federal do Rio Grande do Norte – UFRN

Prof. Dr. José António Fonseca de Oliveira Correia
Coorientador
Departamento de Engenharia Civil
Faculdade de Engenharia da Universidade do Porto - FEUP

Prof. Dr. Abílio Manuel Pinho de Jesus
Departamento de Engenharia Mecânica
Faculdade de Engenharia da Universidade do Porto - FEUP

Prof. Dr. Avelino Manuel da Silva Dias
Departamento de Engenharia Mecânica
Universidade Federal do Rio Grande do Norte – UFRN

Prof. Dr. Wallace Moreira Bessa
Departamento de Engenharia Mecânica
Universidade Federal do Rio Grande do Norte - UFRN

Prof. Dr. Marco Antonio Leandro Cabral
Departamento de Engenharia de Produção
Universidade Federal do Rio Grande do Norte – UFRN

Natal-RN, julho de 2019

This thesis is especially dedicated to my grandmother, mother, and wife. They are my source of strength and balance.

Acknowledgement

I thank God for giving me the opportunity to develop this doctoral project and provide conditions to overcome obstacles with perseverance and determination.

I thank my grandmother, Joanacy Pereira, for the unconditional support given to my training and all her care. My mother, Albacy Fonseca, for believing and encouraging me in the pursuit of my goals.

I thank my wife, Ligia Lislê, for the care, compression, companionship and for being the source of balance throughout the thesis construction journey.

I thank my friend and advisor, Professor Dr. Raimundo Freire Júnior, for his careful guidance, dedication, patience, and wisdom in pointing out the path of research in its most difficult times. Thank you for the encouragement and fundamentally for believing in my ability.

I thank my co-adviser Professor Dr. José A.F.O. Correia for receiving me at the Faculty of Engineering of the University of Porto for the doctoral internship. Thanks for the reviews and contributions to this project.

I would like to express my thanks to the external member of the thesis defence committee, Professor Dr. Abílio de Jesus of the Faculty of Engineering of the University of Porto, to the internal members Professors Dr. Avelino Dias and Dr. Wallace Bessa of the Graduate Program in Engineering Mechanics and Dr. Marco Antonio Leandro Cabral for reading this thesis and for contributing constructive comments.

To all who have directly and indirectly collaborated to accomplish this work, feel all victorious, just as I feel.

"If I have seen further, it is by standing upon the shoulders of giants"

(Isaac Newton)

Resumo

As falhas mecânicas de equipamentos e componentes de estruturais provocam perda de desempenho da função requerida e paradas inesperadas, ocasionando um aumento na necessidade de manutenções corretivas, o que eleva os custos de manutenção e diminui a confiabilidade dos sistemas mecânicos. O efeito da tensão média desempenha um papel importante na predição da vida à fadiga, sua influência altera significativamente o comportamento de fadiga de alto ciclo (*HCF*), diminuindo diretamente o valor do limite de fadiga com o aumento da tensão média. As descontinuidades geométricas – tais como mudança de secção transversal, furos, entalhes, canais de chavetas, entre outros – ocasiona um aumento considerável no valor das tensões nominais atuantes nas vizinhanças adjacentes do concentrador de tensão. Isso potencializa os efeitos da tensão médias positivas no dano ao longo do ciclo de vida do material, causando influência direta no cálculo do fator de redução da resistência à fadiga (K_f) do projeto. Inúmeros modelos empíricos, como o Gerber, Goodman, Soderberg e Morrow, foram desenvolvidos para corrigir o efeito da tensão média, mas apesar dos avanços não é verificado na literatura um modelo unificado que considere o comportamento estocástico da falha por fadiga que consiga predizer as tensões médias máximas suportadas na região de alto ciclo para detalhes estruturais. Desta forma, o propósito deste trabalho é desenvolver um novo modelo de diagrama de vida constante probabilístico baseado em uma rede neural artificial aplicada para materiais metálicos e detalhes estruturais, capaz de estimar o fator de redução da resistência à fadiga para diferentes tensões médias. Os resultados mostram que rede neural treinada conseguiu determinar regiões de confiabilidade de operação do material sob os aspectos da tensão média, amplitude de tensão e do comportamento estocástico do número de ciclos até a falha. Além disso, foi possível estimar os valores do fator de redução da resistência à fadiga correspondente ao limite de resistência utilizando uma pequena quantidade de dados experimentais.

Palavras chave: Fadiga, tensão média, fadiga de alto ciclo, rede neural artificial, probabilidade.

Abstract

Mechanical failures of equipment and structural components cause loss of performance of the required function and unexpected shutdowns, leading to an increased need for corrective maintenance, which increases maintenance costs and decreases the reliability of mechanical systems. The mean stress effect plays an important role in the fatigue life prediction, its influence significantly changes high-cycle fatigue behaviour (HCF), directly decreasing the fatigue limit value with increasing mean stress. Geometric discontinuities - such as cross-section shifting, holes, notches, keyways, among others - cause a considerable increase in the value of nominal stress acting in the adjacent vicinity of the stress concentrator. This enhances the positive mean stress effects on damage over the life cycle of the material, directly influencing the design fatigue strength reduction factor (K_f). Numerous empirical models, such as Gerber, Goodman, Soderberg, and Morrow, have been developed to correct the mean stress effect, but despite advances, there is no unified model in the literature that considers the stochastic behaviour of fatigue failure for prediction of the maximum means stresses supported in the high cycle region for the structural details. Thus, the purpose of this work is to develop a new probabilistic constant life diagram model based on an artificial neural network applied to metallic materials and structural details, capable of estimating the fatigue resistance reduction factor for different mean stresses. The results show that trained neural network was able to determine regions of material operation reliability under the aspects of mean stress, stress amplitude and stochastic behaviour of a number of cycles to failure. In addition, it was possible to estimate the values of the fatigue strength reduction factor corresponding to the strength limit using a small amount of experimental data.

Keywords: Fatigue, mean stress, high cycle fatigue, neural network, probability.

Publications

This section contains papers published by author in scientific journals and conferences:

- ***Scientific journals***

I. **Barbosa, J. F.** et al. Probabilistic S-N fields based on statistical distributions applied to metallic and composite materials: State of the Art. *Advances in Mechanical Engineering*, v. 11, n. 8, p. 1-22, 2019.

II. **Barbosa, J.F.** et al. Analysis of the fatigue life estimators of the materials using small samples. *The Journal of Strain Analysis for Engineering Design*, v. 53, n. 8, p. 699-710, 2018.

III. **Barbosa, J. F.** et al. A comparison between SN Logistic and Kohout-Věchet formulations applied to the fatigue data of old metallic bridges materials. *Frattura ed Integrità Strutturale*, v. 13, n. 48, p. 400-410, 2019.

IV. **Barbosa, J. F.**, et al. Fatigue life prediction considering the mean stress effects through an artificial neural network applied to metallic materials. *International Journal of Fatigue*, 2019, [accept].

- ***Scientific conferences***

1. **Barbosa, J. F.** et al, Evaluation of mean stress effects based on artificial neural network applied to the high-cycle fatigue data of the P355NL1 steel. In: XIX International Colloquium on Mechanical Fatigue of Metals, 2018, Porto, Portugal.

2. **Barbosa, J. F.** et al, A comparison between S-N logistic and Kohout-Vechet formulations applied to the fatigue data of old metallic bridges materials. 2018. In: XVI Portuguese Conference on Fracture, 2018, Covilhã, Portugal.

3. **Barbosa, J. F.** et al, Improvement of fatigue life estimation of composite materials under constant amplitude loading. In: XVI Portuguese Conference on Fracture, 2018, Covilhã, Portugal.

4. Mourao, A.; Correia, J. A. F. O.; **Barbosa, J. F.;** P, Mendes.; Neves, A.; Fantuzzi, N.; Barros, R. C.; Calçada, R.A.B. Forces on bottom-fixed offshore substructures based on different wave theories. In: First International Symposium on Risk Analysis and Safety ff Complex Structures and Components. Porto, Portugal.

5. Mourão, A.; Correia, J.A.F O.; **Barbosa, J. F.**; Castro, J. M.; Rabelo, C.; Correia, A. M. R. Fantuzzi, N.; Calçada, R. A. B. Fatigue wave loads estimation using Morison formula for an offshore jacket-type platform. In: International Colloquium on Mechanical Fatigue of Metals, 2018, Porto, Portugal.

6. Seghier, M. E. A. B.; **Barbosa, J. F.**; Correia, J.A.F.O.; Jesus, A. M. P.; Comparison of the structural reliability of corroded X52 steel pipeline using different Monte-Carlo techniques. In: XIX International Colloquium on Mechanical Fatigue of Metals, 2018, Porto, Portugal.

Contents

List of Figures

List of Tables

Nomenclature

A	Linear regression parameter
$\hat{A}$	Estimated constant
a	Geometrical parameter of the Stüssi fatigue model
a	Fitting coefficient, Geometric parameter of the material
B	Linear regression parameter; parameter related to threshold lifetime in probabilistic fatigue model
b	Geometrical exponent of the Stüssi fatigue model
$\hat{B}$	Estimated constant
b	Fit coefficients, Geometric parameters of the material
C	Material constant; parameter related to endurance limit in probabilistic fatigue model
d	Desired value
e	Produced error by ANN
z	Network response
η	Learning rate
θ	Momentum term
K_f	Fatigue resistance reduction factor
K_i	Stress intensity factor at the elementary block i
F_p	Snedecor distribution
l	Different stress or strain levels
m_i	Number of replicates per level
N	Number of cycles to failure
N^*	Normalized number of cycles
N_i	Number of cycles to crack initiation
N_f	Number of cycles to failure
N_0	Reference number of cycles; Threshold value of lifetime
N_{nor}	Normalized number of cycles
N_{max}	Maximum number of cycles
R_m	Ultimate tensile strength
S	Curve parameter
$\hat{s}^2$	Unbiased estimator of variance
S^2	Variance of population
$v,\ V$	Normalizing variable in probabilistic fatigue model

w_i	Weights
X	Logarithm of stress
$\bar{X}$	Mean of the logarithms of stress
x	Random variable
p	Probability of failure
Y	Logarithm of number of cycles
$\bar{Y}$	Mean of the Logarithm of the number of cycles
α	Location parameter of the Weibull distribution
α_s	Weibull distribution shape value of equivalent static stress data
β	Shape parameter of Weibull distribution
β_s	Weibull distribution scale parameter of equivalent static stress data
δ	Scale parameter of Weibull distribution
ψ	Fatigue damage parameter
ψ_0	Endurance fatigue limit
$\Delta\sigma$	Nominal stress range
$\Delta\sigma_{st}$	Equivalent static stress
$\Delta\sigma_i$	Stress range of the specimen i
$\Delta\sigma_0$	Endurance fatigue limit
$\Delta\sigma^*$	Normalized stress range
δ	Shape parameter of the Weibull distribution
λ	Threshold parameter of Weibull distribution
σ	Stress
σ_a	Stress amplitude
$\sigma_{a_{nor}}$	Normalized stress amplitude
$\sigma_{a_{max}}$	Maximum stress amplitude
$\sigma_{m_{nor}}$	Normalized mean stress
σ_e	Equivalent static stress
$\Delta\sigma_{smooth}$	Smooth fatigue strength
$\Delta\sigma_{notch}$	Notched fatigue strength
$\sigma_{s,ANN}(N)$	Smooth fatigue strength from the ANN as function of N
$\sigma_{d,Stussi}(N)$	Notched fatigue strength from the Stüssi fatigue model as function of N
$\sigma_M,\ \sigma_{max}$	Maximum stress
$\sigma_m,\ \sigma_{min}$	Minimum stress, mean stress
σ_{ult}	Ultimate tensile strength
$\sigma_M{}^*$	Normalized maximum stress

$\sigma_m{}^*$	Normalized minimum stress
σ_0	Cyclic yield stress
σ_∞	Fatigue limit
w	Synaptic weight

Chapter I

Introduction

1.1 Motivation

Fatigue failures in materials or structural components are primarily responsible for the loss of required function and unexpected failures. The fatigue damage caused by dynamic loading submits the material or structural component to conditions totally different from the criteria adopted for static load conditions. Progressive microscopic physical damage in the structure of the material causes a loss of load capacity, to the point that fatigue failures occur in tensions lower than monatomic stresses. Fatigue failures are characterized as a completely random phenomenon, due to the dispersions inherent to the failure times. It is an important aspect that should be considered in the engineering project to obtain safety and reliability throughout the period of operation.

Deterministic fatigue approaches have deserved a major attention of researchers despite the well-known probabilistic nature of fatigue damage. Probabilistic based approaches are mandatory alternatives since they account for scatter of fatigue results and allow us the establishment of safety margins in fatigue life predictions, constituting an important tool to assist design activities. Despite the relevance of the probabilistic approaches for fatigue, most important current design codes are still based on deterministic approaches.

The simplest way to account for scatter in fatigue is to characterize the variability of individual fatigue properties (e.g. fatigue limit), using probabilistic distributions. However, the formulation of probabilistic models is a more attractive idea. For example, it is preferable to have a general probabilistic model to describe the complete *S-N* field than dispose of a *S-N* field defined by the distribution of the fatigue limit plus a set of individual distributions for the fatigue lives under singly specific stress levels.

The great challenge of the probabilistic models of S-N curves is to be able to explain the fatigue behaviour of the materials considering the physical parameters of the material in the modelling process. A robust model can perform a good estimate with a small amount of experimental data, when the average curves of the model are close to the experimental data, from the low cycle region to the high cycle. In the adjustment of the probabilistic curves, a good fit is obtained when the probabilistic *S-N* curve is very close to the probability of failure for a certain constant stress range.

The S-N curves are a basic way that an engineer or designer can obtain information of the behaviour to the fatigue of the material under a constant average tension, however this simplicity of the model limits it to know the fatigue behaviour only for the ratio of fatigue (R) or (σ_m) that the test was performed. Estimating the fatigue behavior of the material for any region of predominance of traction loading (R = -1 to R = 1) requires a high cost of the experimental tests, since several *S-N* curves are required, each with a different mean stress value. A widely used alternative is the construction of the stress limit diagram, also known as a constant life diagram.

In this context, the motivation of the research developed in this thesis is to improve the construction models of the constant life diagrams through artificial neural networks in conjunction with improved probabilistic *S-N* curves.

1.2 Objectives

The general objective of this research project thesis is to develop a hybrid fatigue-life prediction model that uses a robust probabilistic *S-N* curve model in conjunction with artificial neural networks based on machine learning computational algorithms. The main objectives are the following:

- To compare the performance of least squares (LS), least squares weighted (WLSE), maximum likelihood (MLE) and momentum method (MOM), and to suggest a method that obtains better performance in life behaviour to fatigue with small samples. Monte Carlo simulations were performed to estimate the distribution parameters with different sample sizes and an application with real

fatigue data that compares performance using goodness-of-fit. The results of the simulations showed that the WLSE was able to generate more reliable estimators for fatigue behaviour during its useful life.

- A new formulation of a Logistic deterministic S-N curve is applied to fatigue data of metallic materials from ancient Portuguese riveted steel bridges. This formulation is based on a modified logistic relation that uses three parameters to fit the low-cycle- (LCF), finite-life- and high-cycle-fatigue (HCF) regions. This model is compared to the Kohout-Věchet fatigue model, which has a refined adjustment from very low-cycle fatigue (VLCF) to very high-cycle fatigue (VHCF). These models are also compared with other models, such as power law and fatigue-life curve from the ASTM E739 standard.

- To implement a computational algorithm with aims to estimate the probabilistic S-N fields based on Sendecyj and Stussi models. This analysis will be made using the three-parameters Weibull distribution estimation methods.

- To analyse construction models of probabilistic S-N curves and their recommendations for use, whether for composites or metals, with aims to use a fatigue life estimation model that most is appropriate for the desired level of reliability.

- To develop a new probabilistic constant life diagram model based on an artificial neural network applied to metallic materials and structural details. Additionally, the fatigue strength limits of materials and structural details for any fatigue stress R-ratio value in the quasi-static region be estimated.

- To estimate the fatigue strength reduction factor for notched details made in P355NL1 steel using stress amplitude data obtained from extrapolation of the artificial constant life diagram based on a multilayer perceptron network trained with a back-propagation algorithm, where its architecture consists of two input neurons (σ_a,N) and one output neuron (σ_m).

1.3 Organization of Thesis

This thesis is organized by an introduction (Chapter 1), a collection of four scientific articles (Chapters 2 to 5) and finally the conclusions (Chapter 6). Chapter 1, Introduction, presents the motivation, the objectives, the thesis organization, and research contribution. The main objective of the introductory part of this thesis is to describe the role of each work for the doctoral project and to offer the reader a systemic view of the research organization to achieve the expected results. The thesis is organized into two major research parts, the first part called Part A (**Figure 1.1**), related to the scientific review, comparison, analysis and implementation of computational routines of probabilistic S-N curve models. Part A is composed of Chapters 2, 3 and 4 of the thesis, so that each chapter corresponds to journal papers identified by I, II and III, respectively, as can be seen in **Figure 1.1**. The second part is called Part B, which has a purposeful characteristic of the research, which seeks to consolidate previous studies, approached in part A, with aims to propose a probabilistic constant life diagram based on an artificial neural network, as well as a new hybrid ANN-Stüssi modelling to evaluate the fatigue resistance reduction factor. Part B is structured in Chapter 5 of the thesis corresponding to journal paper IV of **Figure 1.1**. The organization of this thesis ends with Chapter 6, where conclusions and proposals for future works are presented.

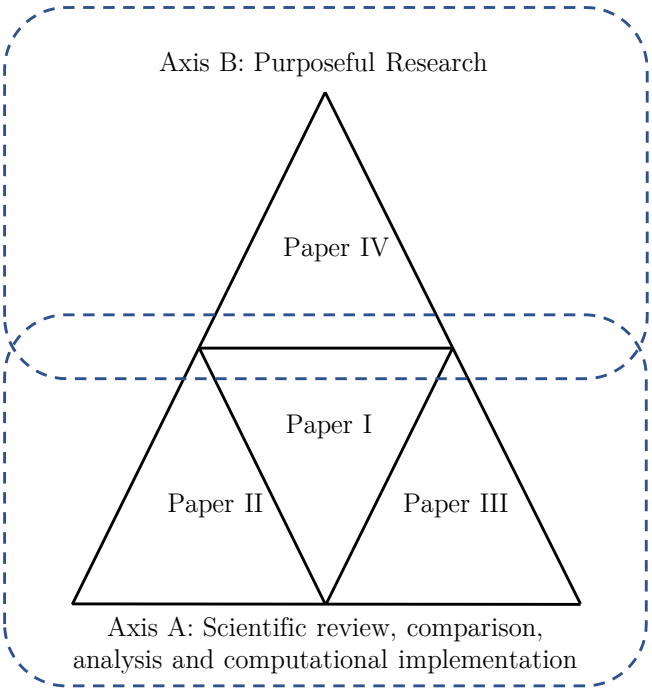

Figure 1.1: Structure and organization of the Ph.D. thesis

The relationship between the chapters (journal papers I to IV, for the construction of this thesis, can be interpreted and seen in **Figure 1.1**. It is noted that journal papers I, II and III are the basis of scientific research to support the knowledge construction of a new constant life diagram model, as well as the new hybrid ANN-Stüssi model to evaluate the fatigue resistance reduction factor, consolidated at the top of the pyramid with journal paper IV, as shown in **Figure 1.1**. The Part A on scientific review, computational implementation, analysis, and discussion of the probabilistic S-N models applied to the composite and metallic materials are made with aims to support the development of a new constant life diagram model as well as the new hybrid ANN-Stüssi model to evaluate the fatigue resistance reduction factor (Part B).
Part A is composed of the following scientific papers identified by I, II and III:

- Paper I: Probabilistic S-N fields based on statistical distributions applied to metallic and composite materials: State of the Art;
- Paper II: Analysis of the fatigue life estimators of the materials using small samples; and,
- Paper III: A comparison between S-N Logistic and Kohout-Věchet formulations applied to the fatigue data of old metallic bridges materials.

In Part B, the scientific paper designed Paper IV is titled “Fatigue life prediction considering the mean stress effects through an artificial neural network applied to metallic materials”.

In **Figure 1.2**, a summary of the proposed research activities are shown. In Paper I, a review of the models used to construct probabilistic S-N fields (P-S-N curves) and demonstrate the methodologies applied to fit the P-S-N fields that are best suited to estimate the fatigue life of the selected materials is done. A comparison of the performance of least squares (LS), least squares weighted (WLSE), maximum likelihood (MLE) and momentum method (MOM), to suggest a method that obtains better performance in fatigue life behaviour with small samples is presented (Paper II). In Paper III, a comparative study of the performance of the S-N adjustment formulations, using models such as Kohout-Věchet, Logistic, ASTM and generalized Power law, are applied to fatigue data of metallic materials is proposed, including an adjustment analysis by means of the mean quadratic error to find the model that best fits with the experimental data.

Paper I

- Monte Carlo Simulation
- Compare Weibull Estimation Methods WLSE, MLE, LSE and MOM
- Small Samples
- Composite Material
- Analysis constant stress -RMSE and Bias teste

Paper II

- S-N curves performance
- Methods: Logistic, ASTM, Khout-Vechet, Power Law Material: Metal
- LCF and HCF adjustment analysis
- Compaison graphic qualitative and quantiative by RMSE

Paper III

- Review P-S-N Methods: Sendeckyj, ASTM, Canteli, Stussi
- Analisys: Fatigue Strength limit and LCF adjustment
- Comparison: Graphical qualitative and quantitative by RMSE

Paper IV

- New model of CDL
- P355NL1 metallic material
- Stussi Probabilistic S-N Curves
- ANN backpropagtion development, training and Validation
- CLD for P355NL1
- Kf value estimation

Figure 1.2: Summary of the proposed research activities.

Finally, in Paper IV (**Figure 1.2**), a constant life diagram (CLD) based on trained artificial neural network algorithm and probabilistic Stüssi fatigue fields applied to the dog-bone shaped specimens made of P355NL1 steel is proposed. A good agreement with the high-cycle fatigue experimental data, only using the stress R-ratios equal to 0 and -0.5, is verified. Furthermore, a procedure for estimating the fatigue resistance reduction factor, K_f, for the fatigue life prediction of structural details in extrapolation regions based on machine learning artificial neural network algorithm is proposed and K_f results are presented.

1.4 Research contributions

The research contributions presented in this research project thesis are the following: Probabilistic S-N fields based on statistical distributions applied to metallic and composite materials: State of the Art.

- For a small number of experimental fatigue samples, it is recommended to use a two-parameter Weibull distribution estimated by the weighted least squares method.

- Development of the computational algorithm that allows estimating of the parameters for the probabilistic Stussi and Sendeckyj fatigue models.

- The use of Multilayer Perceptron Networks after training and validation in the analysis of fatigue behaviour of metallic and composite materials.

- Determination of material operating reliability regions under the aspects of the mean stress, stress amplitude and stochastic behaviour of the number of cycles to failure.

Chapter II

Probabilistic S-N fields based on statistical distributions applied to metallic and composite materials: State of the Art

Fatigue life prediction of materials can be modelled by deterministic equations, via mean or median S-N curve approximation. However, in engineering design it is essential to consider the influence of fatigue life scatter using deterministic-stochastic methods to construct reliable S-N curves and determine safe operation regions. However, there are differences between metals and composites that must be considered when proposing reliable S-N curves, such as distinct fracture mechanisms, distinct ultimate strengths under tension and compression loading, different cumulative fatigue damage mechanisms including low-cycle fatigue (LCF). This study aims at conducting a review of the models used to construct probabilistic S-N fields (P-S-N curves) and demonstrate the methodologies applied to fit the P-S-N fields that are best suited to estimate fatigue life of the selected materials. Results indicate that the probabilistic Stüssi and Sendeckyj models were the most suitable for composite materials, while for metallic materials only the probabilistic Stüssi model presented a good fitting of the experimental data, for all fatigue regimes.

2.1 Introduction

In this thesis, fatigue failure in materials, structural components and structures is a factor that should be considered in engineering design to ensure safety and reliability during service life. This is even more critical in structural/dynamic (mechanical) designs that

use a combination of metallic materials and polymer matrix composites, or when metallic materials are replaced by composites. It is important to underline the significant difference between the effects of cyclic stress at the microscopic and macroscopic levels, which may explain the heterogeneous fatigue behaviour of these materials. The predominance of loading, in either the region of tension or compression, leads to significant differences between the composite with a much lower tensile fatigue limit in compression-compression than tension-tension, the opposite behaviour to metals that do not undergo fatigue when compression loaded[1,2]. Fatigue damage in metals generally initiates near the surface and spreads perpendicularly to the load, behaviour linked to cyclic plasticity and its isotropic mechanical properties [3–6]. On the other hand, composites with a polymer matrix exhibit orthotropic mechanical properties, favouring far more complex fatigue damage than in metallic materials, including matrix cracking, delamination, fibre rupture and failure occurring in a synergic, cumulative and random manner[7].

Despite the differences in fatigue behaviour of metallic materials and composites, both will fail when submitted to cyclic loads lower than the monotonic strength; and the predictability of this phenomenon suffers from inherent random nature of fatigue damage. This makes fatigue life analysis more complex and difficult to understand, because even in controlled experimental environments subject to constant nominal stress, and identical samples exhibit high dispersions [8–10]. As such, the stochastic nature inherent to the fatigue process of composite and metallic materials in deterministic approaches should not be overlooked. Knowing the scatter effects on the material behaviour and its safe regions will result in reliable structural designs, since accurate predictions of material fatigue helps to explain its effect on structural elements[11] or components[11–15].

One way of synthesizing the number of factors involved in fatigue life predictions is to reduce the model to the variables that explain cause and effect. That means fitting the fatigue test cycles, N_i, (dependent variable) needed to failure for a given stress level σ_i (independent variable), using regression equations and other fitting methods with the least possible error. These techniques lead to the fatigue curves also known as *S-N* or Wöhler's curves. This purely deterministic model generates average life curves, which are not relevant for design that need to consider the influence of scatter when estimating confidence levels, in order to control the design safety factor and, in turn, costs. Thus, using deterministic-stochastic methods to construct probabilistic S-N fields (P-S-N fields) provides more reliable estimates for structural design.

In engineering, simple *P-S-N* curves are normally created by using linear regression of *log*(N) vs. *log*(σ) data and determining an average *S-N* curve with its standard deviation, assuming a log-normal distribution for the number of cycles to failure. Next, safety margins are established by applying standard deviation based corrections of 2σ or 3σ to the mean *S-N* curve, resulting in high safety levels in all fatigue regions. This is the case for most existing design codes, such as EC3, BS5400, and AASHTO, which do not take into account the statistical results of sample size, possible confidence/reliability levels required, or that the dispersion of the number of cycles to failure is far from the fatigue domain and may not be suitable for very high cycle fatigue lives. Nevertheless, this procedure is recommended by guidelines such as ASTM E739 standard[16]. However, Schijve[17] discusses the typical scatter in the S-N curves, which increases as fatigue life rises and stress amplitude declines, a property known as heteroscedasticity (see **Figure 2.1**).

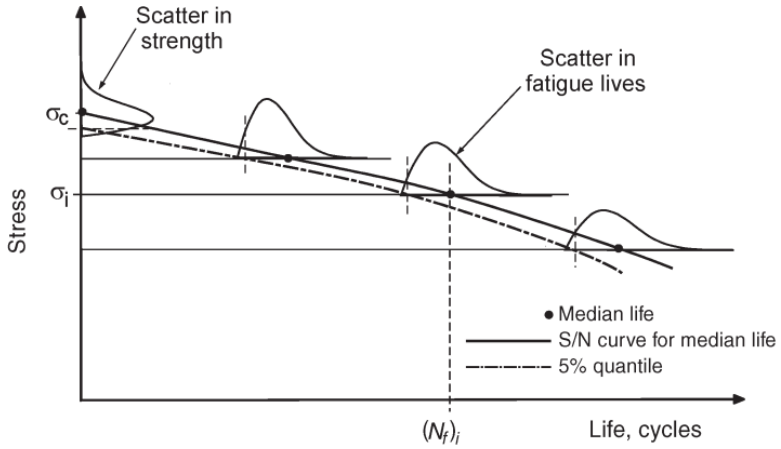

Figure 2.1: P-S-N curve model at 5% failure probability: effect of increasing variability and reducing stress with a rise in fatigue life [18].

Creating *P-S-N* curves has been the object of study of several researchers[19–24] in recent years, focusing primarily on suitable probabilistic distributions to represent fatigue life data. The most widely used probabilistic distributions for metallic materials and polymer composites are the log-normal and two and three-parameters Weibull distributions[25,26]. This was confirmed by Lee[27], who conducted a goodness-of-fit test and concluded that the two-parameters Weibull distribution best adheres to the set of carbon fibre experimental data. It is also found in the scientific work developed by Hwang and Han[28] that the two parameters Weibull distribution is more appropriate to

estimate the scatter in fatigue-life for fiberglass composites when compared to the normal and log-normal distributions.

Two-parameters Weibull distribution was used by Whitney[29] and Sendeckyj[30] to model failure cycles and build *P-S-N* curves applied to composite materials. The first author used an approach presented by Lemon[31], who normalized the data of each stress range to a single group that fits two-parameter Weibull distribution and adopted the power law to formulate the *S-N* curve. The wear-out method applied by Sendeckyj also uses a two-parameters Weibull distribution, but this model transforms fatigue data into residual strength values, using interactive optimization of the distribution parameters and *S-N* curve fitting. Other researchers (Castillo[32], Vassiloulos[33], Sakin[34] and Badi[35]) also suggest that fatigue data follows a two and three-parameters Weibull distribution. Barbosa et al.[36] also concluded that for a constant stress level the failure cycles of composite materials preferably follow a two-parameters Weibull distribution.

For the case of metallic materials, log-normal and Weibull distributions are alsowidely used. The ASTM-E739 standard is widely applied to analyze the experimental fatigue life results of metals based on log-normal statistical distribution to estimate the confidence bands for the S-N and ε-N curves[37–42]. Correia et al.[43] has used in its research work this ASTM standard with the purpose of generating the design curves for fatigue crack growth (FCG) rates applied to old steel bridges materials, demonstrating the applicability of this methodology to other laws. Raposo et al.[44] presented a methodology to generate probabilistic S-N curves applied to the structural and mechanical components, based on the fatigue crack growth modelling as a process of successive crack re-initiations, using local fatigue damage parameters (e.g. strain, SWT, etc.). Castillo & Canteli[45] proposed a probabilistic fatigue life prediction model for the stress damage parameter based on three-parameters Weibull statistical distribution. This model was widely accepted by scientific community to describe the design fatigue behaviour of the metals (see special issues, *Recent developments on experimental techniques, fracture mechanics and fatigue approaches*[46], and *Mechanical Fatigue of Metals*[47]).

Schijve[17,48], Correia[49], Zhao et al.[50] and Castillo et al[45] suggested that the Weibull distribution seems to be better suited to reproduce fatigue lifetime from a statistical standpoint, with theoretically justified distribution. Gallegos-Mayorga et al.[51] also used the Weibull distribution to evaluate the fatigue strength of double-shear

riveted connections as well as the crack growth rate for metallic materials from old bridges.

Łukaszewicz[52] suggested a fatigue life evaluation of metals based on a complex stress state. On the other hand, Su et al.[53] presented a proposal of two strategies for time-dependent probabilistic fatigue analysis considering stochastic loadings and strength degradation based on the failure transformation and multi-dimensional kernel density estimation method. Kulkarni et al.[54] proposed a statistical wind prediction and fatigue analysis for wind turbine composite material blade under dynamic loads. Fatigue reliability evaluation for steel structural details/joints can be made using probabilistic stress-life method as proposed by Kang et al.[55].

The aim of this review is to help designers in their decisions between the conventional models used to construct probabilistic *S-N* curves for composite and metallic materials, choosing the appropriate probabilistic models for the specific material. It is worth mentioning that there are several differences between composites and metals, from their composition to the failure mechanisms. This results in differences in data scatter, fatigue threshold, deterministic S-N curve inflection points and probability distributions. There are also differences between the various equations used, which may adapt better to a specific class of material, loading region set of experimental data. Thus, a more appropriate fatigue life estimation model can be used for the desired reliability level.

2.2 Fatigue Models and Methods for Statistical Analysis of Stress Life Data

2.2.1 Fatigue Models

The modelling of an S-N curve has been developed as a function of the number of parameters that constitutes the relationship between two of the main variables, the stress level ($\Delta\sigma$) and the number of cycles to failure (N), where these variables can be considered as independent and dependent variables, as well as being described in natural form of by using logarithmic transformations.

The phenomenon of fatigue was observed by engineers in metal materials in the mid-nineteenth century, due to the shortcomings of the railway wagons after a short period of work. In the 1850s a German engineer, August Wöhler, conducted the first experimental fatigue program, testing wagon shafts to failure under alternating stress. The developed loads were recorded together with the number of rotations until failure, so it was possible to formulate the first S-N diagram or Wöhler curve.

$$\log N = A - B\Delta\sigma; \quad \Delta\sigma \geq \Delta\sigma_0; \quad B \geq 0 \tag{2.1}$$

where A and B are regression parameters to obtain the linear relationship between the dependent variable *log N* and the independent variable $\Delta\sigma$. The fatigue strength limit $\Delta\sigma_0$ is a property of the know material.

In 1910 Basquin stated that the material resistance to fatigue follows a power law, with fatigue resistance being inversely correlated with the number of cycles required to the material failure. Basquin's model[56] proposes a small difference with respect to the relation proposed by Wohler, using double logarithmic coordinates:

$$\log N = A - B\log\Delta\sigma; \quad \Delta\sigma \geq \Delta\sigma_0; \quad B \geq 0 \tag{2.2}$$

Unlike the previous two models that are linear, the model of the Strohmeyer[57] model is not linear, since it proposes a smoothing of the linear models, inserting more parameters in the equations and making the estimation more complex:

$$\log N = A - B\log\left(\Delta\sigma - \Delta\sigma_0\right); \quad \Delta\sigma \geq \Delta\sigma_0; \quad B \geq 0 \tag{2.3}$$

Although the fatigue limit ($\Delta\sigma_0$) may not exist for some materials [58], Strohmeyer inserted it into the Basquin relation.
Palmgren[59] added a parameter in the dependent term of the Strohmeyer relation, that is, *log* (*N+D*):

$$\log\left(N + D\right) = A - B\log\left(\Delta\sigma - \Delta\sigma_0\right); \quad \Delta\sigma \geq \Delta\sigma_0; \quad B \geq 0 \tag{2.4}$$

The **Equations (2.3)** and **(2.4)** were the basis of the first analytical models used in the fatigue life prediction of bearings, according to scientific studies developed by Palmgren[59].

The S-N curves proposed by Weibull[60], incorporated the static stress ($\Delta\sigma_{st}$) in the **Equation (2.4)**, increasing the complexity to solve the proposed relation:

$$\log(N+D)=A-B\log\left(\left(\Delta\sigma-\Delta\sigma_0\right)/\left(\Delta\sigma_{st}-\Delta\sigma_0\right)\right); \qquad B\geq 0 \tag{2.5}$$

In this way, this proposal makes it necessary to know and/or evaluate the five parameters, where, two are constants of the material ($\Delta\sigma_{st}$, $\Delta\sigma_0$) and the remaining three parameters are regression parameters (A, B and D).

Kohout and Vechet[61] proposed a model based on the geometric modeling of the Basquin S-N curve, with smoothing in the high- and low-cycle fatigue regions, supported by the following relation:

$$\sigma(N)=\sigma_1\left(\frac{1+N/B}{1+N/C}\right)^b \tag{2.6}$$

where σ_1 is the ultimate tensile strength, b, B and C are material constants (C is characterized as a value equivalent to $\Delta\sigma_0$), and N is the number of cycles to failure. This model is based on the fatigue behaviour of metals in both the low- and high-cycle regions.

The previous models developed from the Basquin relation were modified using the fatigue limit of the metals to estimate the fatigue behaviour throughout the life cycle. However, when it comes to composite materials, it is not possible to model an S-N curve by limiting to the fatigue limit parameters.

In the composites is predominantly used models that considers the *log N* as independent variable and σ as dependent variable. The modification of the Basquin equation often used to create S-N curves of the composite materials is the generalized Power Law that obtained smaller estimation errors according to the scientific work developed by Freire and Belísio[25]:

$$\log\sigma = A - B\log(N)^c \tag{2.7}$$

where C is an exponential parameter of the material able to smooth the fall of the fatigue resistance in the low-cycle region.

The logistic S-N curve model was developed by Mu[62] through the use of the logistic distribution to describe the fatigue life behaviour of composite materials, since this function is very similar to the S shape, commonly observed in S-N curves (natural-logarithm). The logistic distribution adapted to model the S-N curve, is given by **Equation (2.8)**:

$$\sigma_N = \frac{1-c}{(1-a)+ae^{-b(\log N)}} + c \tag{2.8}$$

where a, b and c are material constants obtained by nonlinear least squares, σ_N is the normalized stress amplitude $\left(\sigma_N = \sigma_{max}/\sigma_{ult}\right)$ and N is the number of cycles until failure.

2.3 Methods for Statistical Analysis

2.3.1 ASTM Standard Practice

The ASTM E739-91 standard is a common standard in *S-N* or ε-*N* curve construction, which considers the linear behaviour of the curve on a semi-logarithm (**Equation 2.9**) and log-log scale (**Equation 2.10**). Curves are limited to the region of available experimental data and should not be extrapolated to predict fatigue life for a specific stress or strain ranges for reliability levels above 95% or failure likelihoods below 5%. The relationships between *S-N* curves are linear or linearized according to the expression desired for fitting:

$$\log(N) = a + b\sigma \tag{2.9}$$

$$\log(N) = a + b\log(\sigma) \tag{2.10}$$

In these equations, stress, given by σ, can be the maximum stress or stress amplitude, and can be replaced by strain if the aim is to find the S-N counterpart relation. The value of N corresponds to the number of cycles to failure, and in practice, including the samples that did not fail (run-out) in this model is not recommended. The values of "a" and "b" are the best-fitting parameters of the S-N curve that explain the cause/effect relation between stress level (independent variable) and number of cycles to failure (dependent variable).

The probabilistic determination of fatigue life is not represented directly. To simplify this situation, the ASTM guideline assumes that the logarithms of the number of fatigue cycles are natural. Additionally, the useful life variance is constant along the S-N curve, exhibiting heteroscedasticity with low- and high-cycle regions and the same dispersion for a constant stress or strain level. Assuming that $\log(N)$ is the random dependent variable and $\log(\sigma)$ or $\log(\varepsilon)$ the independent variable, denominated Y and X respectively in a linear fit equation given by **Equation (2.11)**:

$$Y = A + BX \tag{2.11}$$

where the best-fit parameters A and B are the linear fit coefficients of the model that can be estimated by regression, considering the maximum likelihood method. To that end, **Equation (2.11)** values are substituted by those estimated in **Equation (2.12)**.

$$\hat{A} = \bar{Y} - \hat{B}\bar{X} \tag{2.12}$$

where $\hat{A}$ and $\hat{B}$ are the estimated constants, $\bar{X} = \sum_{i=1}^{k} X_i/k$ and $\bar{Y} = \sum_{i=1}^{k} Y_i/k$ the mean values of $\log(\sigma_i)$ and $\log(N_i)$, respectively. The value of B is approximated by its estimator ($\hat{B}$) in **Equation (2.13)** given:

$$\hat{B} = \frac{\sum_{i=1}^{n}\left(X_i - \bar{X}_i\right)\left(Y_i - \bar{Y}\right)}{\sum_{i=1}^{n}\left(X_i - \bar{X}\right)^2} \tag{2.13}$$

Given that the model of the guideline stipulates that the number of cycles to failure follow a log-normal distribution, variance is given by **Equation (2.14)**:

$$\hat{s}^2 = \frac{\sum_{i=1}^{n}\left(Y_i - \hat{Y}_i\right)^2}{n-2} \tag{2.14}$$

in which $\hat{Y}_i = \hat{A} + \hat{B}X_i$ and $(n-2)$ is the term used instead of n to make $\hat{s}^2$ an unbiased estimator of the normal variance of population s^2 of the number of cycles. A confidence range can be determined for the entire median length of the *S-N* or *-N* curve, and can be estimated by **Equation (2.15)**:

$$\hat{A} + \hat{B}X \pm \sqrt{2F_p}\hat{\sigma}\left[\frac{1}{k} + \frac{\left(X - \bar{X}\right)^2}{\sum_{i=1}^{k}\left(X_i - \bar{X}\right)^2}\right]^{1/2} \tag{2.15}$$

in which F_p is the Snedecor distribution value contained in ASTM E739[16], using degrees of freedom to find reliability levels of 95% or 99%.
Although F_p values for 99% are provided, they are not recommended. The linear relation of the material ($Y = A + BX$) should be met when the F_p value exceeds its computed counterpart (**Equation (2.16)**), given that l are the different stress or strain levels and m_i the number of replicates per level. Further, information on the linearity hypothesis is contained in ASTM E739[16].

$$\frac{\sum_{i=1}^{l} m_i\left(\bar{Y}_i - \bar{Y}_i\right)^2/(l-2)}{\sum_{i=1}^{l}\sum_{j=1}^{m_i}\left(\bar{Y}_{ij} - \bar{Y}_i\right)^2/(n-l)} \le F_p \tag{2.16}$$

The ASTM E739 standard[16] recommends a minimum number of specimens for the application of this standard practice that depends on the type of test program. For exploratory research and development tests as well as research and development testing of components and specimens, a minimum number of specimens ranged of 6-12 are required. For design allowables and reliability data, 12-24 specimens need to be conducted. The number of specimens for each material used in this study can be found in Table 1 and are within the limits indicated by the ASTM E739 standard.

Figures 2.2 and 2.3 show examples of the generation of S-N reliability curves using experimental fatigue data (stress *R*-ratio equal to -1) of metallic material from the Luiz

I Bridge in Portugal[63] and experimental data of laminate DD16 (stress R-ratio equal to 0.8) collected from Mandell[64], respectively. The laminate DD16 is a glass fibre-reinforced plastic, manufactured by the resin transfer process using an orthopolyester matrix, reaching a fibre volume ratio of 36%. Its configuration is $[90/0/\pm45/0]_s$ and in the 0 and 90° layers, D155 glass fibre fabric (527 g/m^2) is used, and at ± 45°, DB120 (393 g/m^2)[64]. A good agreement can be observed between experimental data and with the percentile curves corresponding to probabilities of failure of 5% and 50% for both materials under consideration. In **Table 2.1**, the obtained parameters using ASTM standard for both materials are showed.

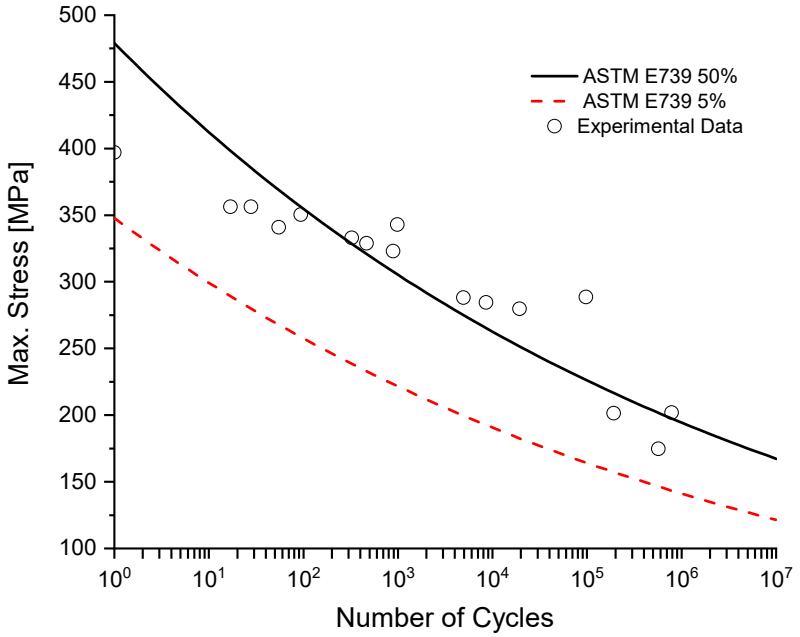

Figure 2.2: *S-N* reliability curve based on ASTM E739 standard for the experimental fatigue data of the metallic material from the Luiz I Bridge, *R=-1*.

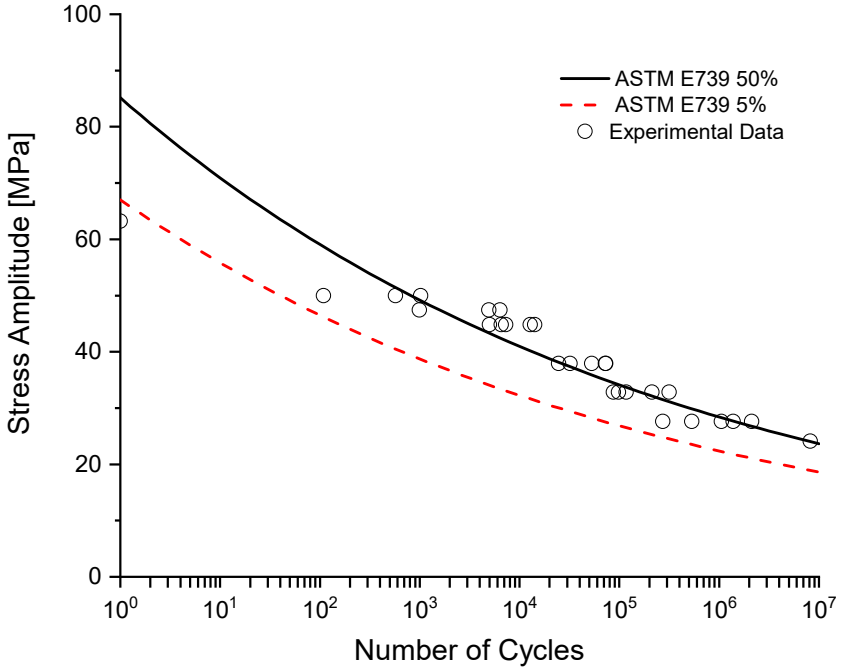

Figure 2.3: *S-N* reliability curve based on ASTM E739 standard for the experimental data of laminate DD16 collected from Mandell[64], *R=0.8*.

Table 2.1: Fatigue curve constants based on ASTM standard.

Material	n	A	B	$\bar{X}$	$\bar{Y}$	$\hat{\sigma}$
Luiz I Bridge R=-1	16	41.07	-15.32	2.4709	3.2094	0.7557
DD16 R=0.8	29	24.29	-12.58	1.5709	4.5227	0.4966

The S-N curve drawn according to the ASTM guidelines at probabilities of failure of 5%-95% would represent a confidence band, similar to the confidence interval, which uses the log-normal distribution (two parameters) to estimate the confidence band of estimators A and B. ASTM R739-91 standard does not recommend that the S-N or ε-N curves can be extrapolated outside the interval of testing.

Despite the simple application of ASTM E739 and the need for a small experimental dataset, its limitations include being unable to describe the fatigue behaviour of the material, restricting application to the region where the experimental data are found; being unable to simultaneously assess regions with low- and high-fatigue cycles, as reported by Barbosa et al.[63]; and only allowing the use of log-normal distribution, neglecting the recognized importance of the Weibull distribution in failure analysis.

2.3.2 Sendeckyj's Wear-Out Model

Sendeckyj's[30] wear-out or strength degradation model is based on three assumptions. The first is that the deterministic *S-N* equation is based on a physical phenomenon that considers damage accumulation with the application of cyclic loads. The second is that the material loses strength as damage accumulates, creating a cause and effect relation between the number of cycles and residual strength of the material. Finally, it assumes that static strength data can be described by a two-parameters Weibull distribution. To model *S-N* curves using the Sendeckyj method, deterministic equation parameters must be fit (**Equation (2.17)**) simultaneously with the Weibull distribution parameters. Fatigue data (N_i) are converted to equivalent static stress (σ_e using the *S-N* equation (**Equation (2.17)**). Next, the Weibull distribution parameters are calculated for equivalent static strength data by applying the maximum likelihood method. *S-N* curve parameter fitting optimization occurs until the maximum point is reached. The following deterministic **Equation (2.17)** was used to convert static fatigue strength data into equivalent static fatigue:

$$\sigma_e = \sigma_{\max}\left[\left(\frac{\sigma_r}{\sigma_{\max}}\right)^{1/S} + (N-1)C\right]^S \tag{2.17}$$

In **Equation (2.17)**, σ_e is the equivalent static stress, σ_{max} maximum cyclic stress, σ_r residual stress, N the number of cycles, and S and C are *S-N* curve parameters to be determined. For particular cases where $\sigma_r = \sigma_{max}$ and $N = N_{f,}$ **Equation (2.17)** is reduced to **Equation (2.18)**:

$$\sigma_e = \sigma_{\max}\left(1 - C + CN\right)^S \tag{2.18}$$

Parameter C of the previous equation (**Equation (2.18)**) determines the *S-N* curve fitting in the low-cycle fatigue region. For C=1, the *S-N* curve equation is reduced to the power law model. For C>1 is characterized by a high decline in static behaviour to low-cycle region (**Figure 2.5**) and C<1, it characterizes a smoothed transition from static fault behaviour to fatigue failure in the low cycle region, characterizing the expected behaviour for most of the composites. In the log-log graph (**Figure 2.4**), the S parameter determines the best-fit for clustering equivalent static stress data, that is, less dispersion.

A heuristic fit between parameters C and S and maximization of the Weibull distribution shape value (α) of equivalent static stress data should occur interactively until the lowest static data dispersion is found, resulting in the best fitting *S-N* curve to fatigue data. The two-parameters Weibull distribution is more appropriate for the static stress data. The evaluation of the Weibull parameters is made using the weighted least squares estimation method (WLSE), taking into account the good performance for few experimental data as presented by Barbosa et al[36]. The likelihood of equivalent static data's surviving is given by **Equation (2.19)**:

$$P(\sigma_e) = \exp\left[-\left(\frac{\sigma_e}{\beta}\right)^{\alpha}\right] \tag{2.19}$$

The probabilistic distribution of the fatigue life for a given maximum applied stress is obtained by combining Equations (2.18) and (2.19). This procedure can be seen in Sendeckyj[30] and the resulting equation is given by the following relation:

$$\sigma_{\max} = \beta\left\{\left[-\ln\left(P(N)\right)\right]^{\frac{1}{\alpha}}\right\}\left[\left(N + \left(\frac{1-C}{C}\right)\right)C\right]^{-S} \tag{2.20}$$

The parameters C, S, α and β of **Equation (2.20)** are estimated using an interactive optimization process. An estimation of parameters is achieved when α reaches the maximum value.

The S and C constants of material are used to fit the *S-N* curve to experimental data. Parameter S influences the slope of the equivalent static stress distribution curve (**Figure 2.4**), converging to equivalent static stress data with less dispersion. The ideal value of S_0 converges to static data distribution with less dispersion, but when $S_1 > S_0$ and $S_2 < S_0$ values do not converge to lower equivalent static stress data dispersion, the resulting *S-N* curve slopes move further away from experimental fatigue data.

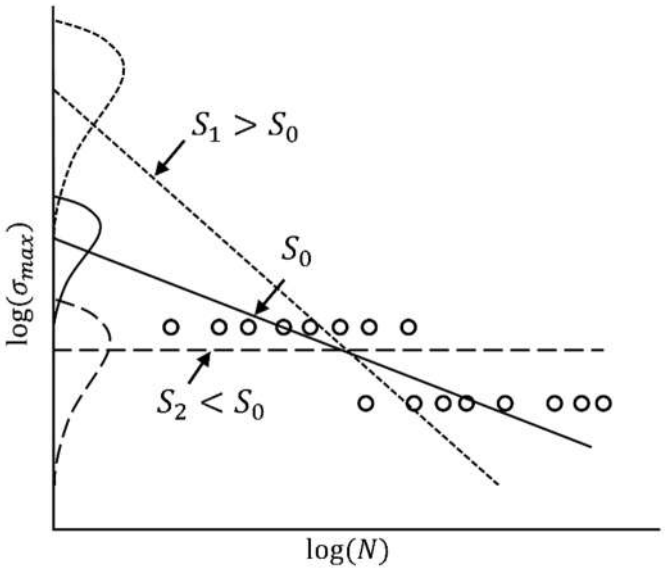

Figure 2.4**:** Effect of the slope on curve fitting and dispersion of equivalent static strength.

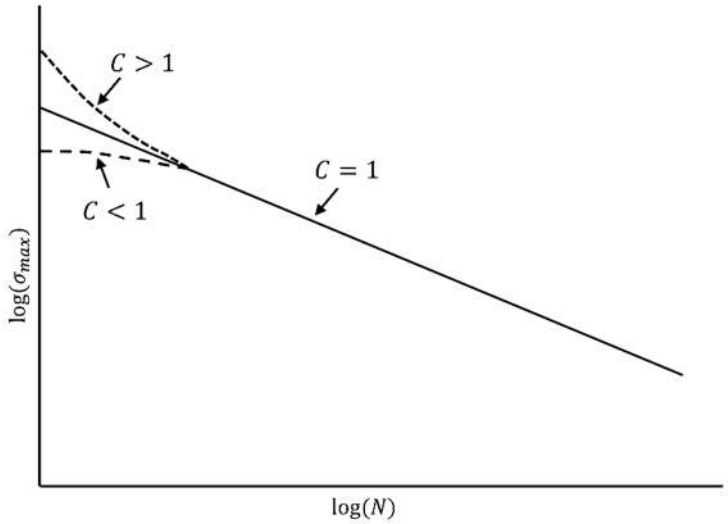

Figure 2.5**:** Effects of C parameter on *S-N* curve fitting in the low-cycle region.

An example of applying Sendeckyj's wear-out curve for both materials under consideration in this study, metallic material from the Luiz I bridge and laminate DD16, can be observed in **Figures 2.6 and 2.7**, respectively. A good agreement can be considered in all fatigue regions for the DD16 laminate. For the metallic material from the Luiz I bridge, a good agreement between quasi-static and low-medium fatigue regions is verified; however, in the medium-high cycle fatigue regime it is not observed a reasonable agreement between the experimental data and the percentile curves for 5% and 50%. In **Table 2.2**, the obtained parameters using Sendeckyj's wear-out model for both materials are showed.

Table 2.2: Fatigue curve constants based on Sendeckyj model.

Material	C	S	$\hat{\alpha}$	$\hat{\beta}$
Luís Bridge R=-1	0.2113	0.0375	13.8496	388.0149
DD16 R=0.8	0.0034	0.0932	21.2115	61.1538

In **Figures 2.8 and 2.9**, the *S-N* percentile curves of 5% and 50% obtained based on Sendeckyj's wear-out model and ASTM E739 standard for the experimental fatigue data of the metallic material from the Luiz I bridge (R=-1) and for the experimental data of laminate DD16 collected from Mandell[64] (R=0.8) are presented, respectively. For the metallic material from the Luiz I bridge (**Figure 2.8**), Sendeckyj model when compared with the ASTM E739-91 standard presents a good agreement between experimental results and percentile curves until a number of cycle to failure of 10^5. On the other hand, for the number of cycles to failure above of 10^5, high-cycle fatigue region, the ASTM standard exhibits better results. **Figure 2.9** show that Sendeckyj model produces a better fit to the experimental data in the region below 10^3, due to C parameter of **Equation (2.18)**. The ASTM E739-91 model does not fit well to the low-cycle region, compromising the analysis in this region. When deciding which of the two curves to use to analyse reliability regions for composite materials from the low-cycle region, researchers will achieve a more reliable analysis by applying the Sendeckyj method.

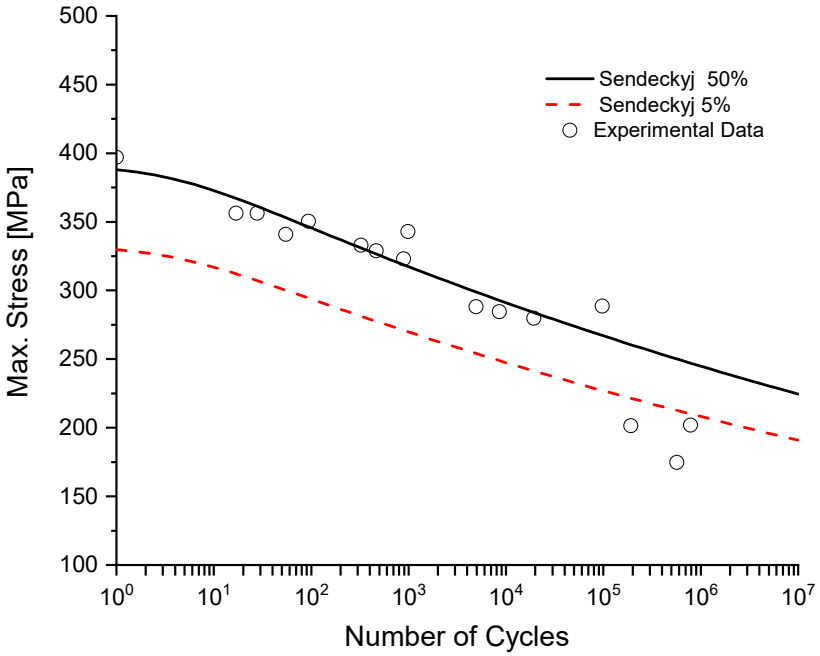

Figure 2.6: *S-N* reliability curve based on Sendeckyj's wear-out model for the experimental fatigue data of the metallic material from the Luiz I Bridge, *R=-1*.

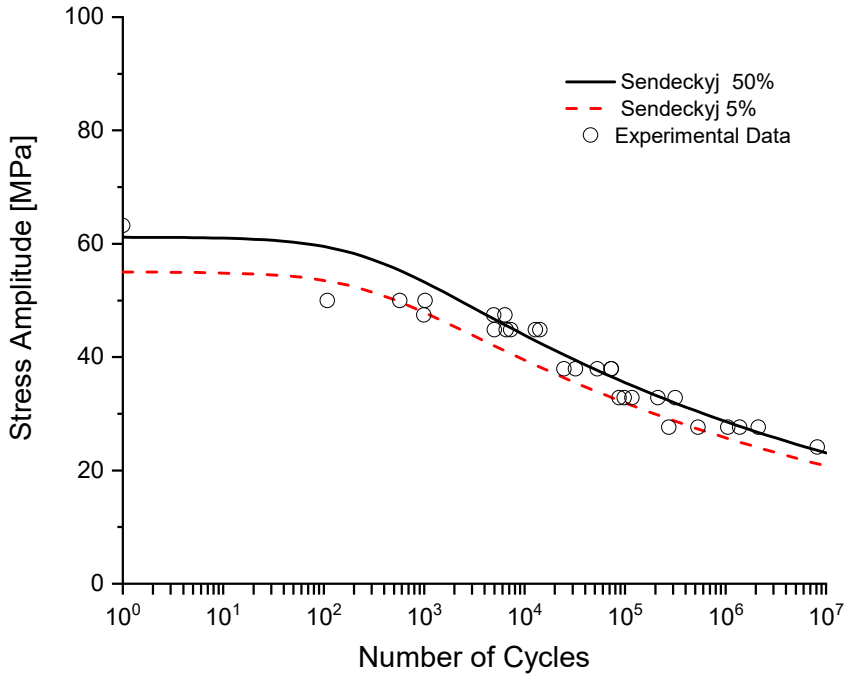

Figure 2.7: *S-N* reliability curve based on Sendeckyj's wear-out model for the experimental data of laminate DD16 collected from Mandell[64], *R=0.8*.

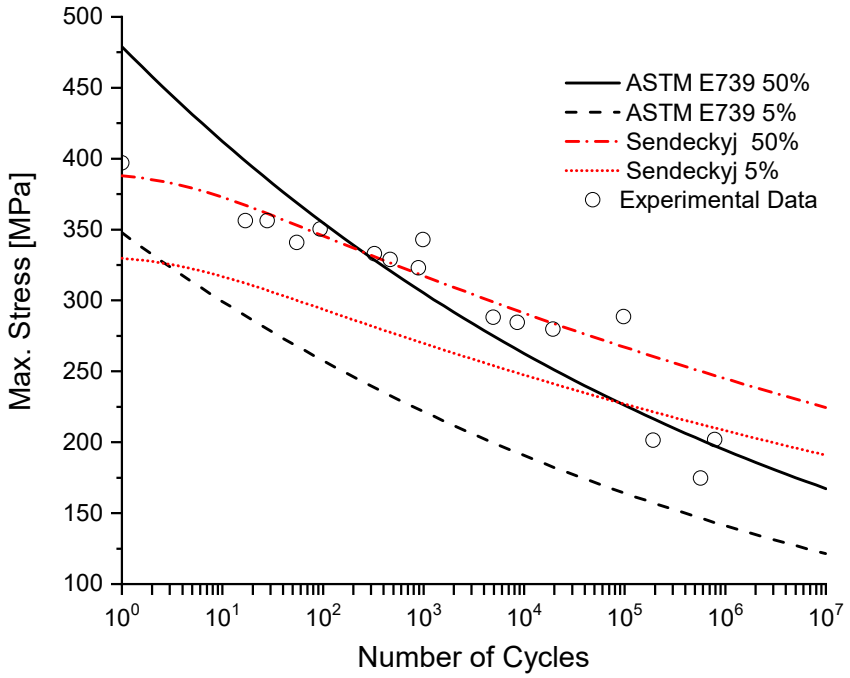

Figure 2.8**:** *S-N* reliability curves based on Sendeckyj's wear-out model and ASTM E739 standard for the experimental fatigue data of the metallic material from the Luiz I Bridge, *R=-1*.

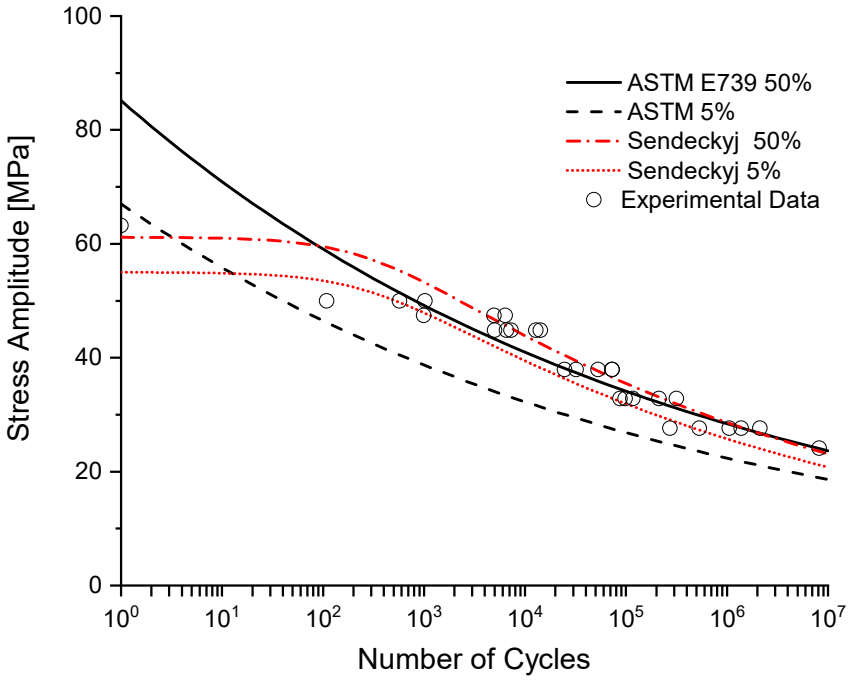

Figure 2.9**:** *S-N* reliability curves based on Sendeckyj's wear-out model and ASTM E739 standard for the laminate DD16, *R=0.8*.

Although the Sendeckyj model is currently used in composite materials, it can also be applied to metallic materials, since its three premises can be used with any material. This is due to its ability to model fatigue behaviour in low- and high-cycle regions and inclusion of the Weibull failure distribution model, which may be an interesting proposal for designers. However, it also has three drawbacks: the static strength of the material must be known in order to build the curves, the dataset cannot be small, and an interactive optimization model must be used to obtain its constants. In other words, if the dataset is not large enough and the static strength of the material is unknown, the model presented in **section 2.1** is more suitable.

2.4 Overview of probabilistic models by Castillo and Fernández-Canteli

Castillo and Fernández-Canteli proposed a set of probabilistic models for fatigue damage modelling, based on the Weibull distribution and its limiting Gumbel distribution for $\beta \to \infty$. These models are supported by both physical and statistical assumptions, leading to basic probabilistic *S-N* and ε-*N* fields, through of a reduced set of dimensionless variables, a dimensional analysis is performed and a set of compatibility conditions and

constraints are proposed for the model to be implemented[65]. These fields can be applied to describe the fatigue behaviour of both smooth and sharp notched specimens, corresponding to mechanical details and structural components, including run-outs. This model can be implemented through the ProFatigue Software in Fernández-Canteli[66].

2.4.1 Probabilistic S–N field for a fixed stress level

Castillo and Fernández-Canteli [45] derived a Weibull regression model for variable stress range and fixed stress level (e.g. stress *R*-ratio, mean stress). This model, being formulated in the stress space, is recommended for medium to high or even very high cycle fatigue. The derivation of the model is based on satisfaction of physical conditions (identification of involved variables, dimensionless analysis) and statistical requirements (weakest link principle, stability, limited range, limit behaviour). In addition, fulfilling of the necessary compatibility condition between lifetime distribution for a give stress range and stress range distribution for a given lifetime leads to a functional equation, the solution of which provides the following distribution, defining the probabilistic S-*N* field [45]:

$$F\left(\log N;\log\Delta\sigma\right)=p=1-\exp\left\{-\left[\frac{\left(\log N-B\right)\left(\log\Delta\sigma-C\right)-\lambda}{\delta}\right]^{\beta}\right\} \qquad (2.21)$$
$$\left(\log N-B\right)\left(\log\Delta\sigma-C\right)\geq\lambda$$

where: N is the lifetime; $\Delta\sigma$ is the stress level; $F()$ is the cumulative probability distribution function (*cfd*) of N for given $\Delta\sigma$; $B=log(N_0)$, N_0 being a threshold value of lifetime; $C=\log(\Delta\sigma_0)$, $\Delta\sigma_0$ being the endurance fatigue limit; and λ, β and δ are nondimensional model parameters (β: Weibull shape parameter; δ: Weibull scale parameter; λ: Weibull location parameter defining the position of the zero-percentile curve). The model defined by Equation (2.21) has been studied and successfully applied to different lifetime assessments[32,45,67,68]. **Equation (2.21)** may be rewritten for normalized number of cycles (N^*) and normalized stress range ($\Delta\sigma^*$):

$$F\left(\log N;\log\Delta\sigma\right)=p=1-\exp\left\{-\left[\frac{\log N^{*}\,\log\Delta\sigma^{*}-\lambda}{\delta}\right]^{\beta}\right\} \qquad (2.22)$$
$$\log N^{*}\,\log\Delta\sigma^{*}\geq\lambda$$

where: $N^* = N/N_0$ is the normalized number of cycles and $\Delta\sigma^* = \sigma_M^* - \sigma_m^*$ is the normalized stress range; $\sigma_M{}^* = \sigma_M/\sigma_0$ is the normalized maximum stress and $\sigma_m{}^* = \sigma_m/\sigma_0$ is the normalized minimum stress; σ_M and σ_m are respectively the maximum and minimum stresses of a cycle; N_0 and σ_o can be identified, respectively, as $\exp(C)$ and $\exp(B)$ converting the formulas dimensionless. **Figure 2.10** represents the *p-S-N* field based on three-parameters Weibull statistical distribution, with some representative percentile curves illustrated. The percentile curves are hyperbolas sharing the asymptotes $\log(N)=B$, representing the fatigue limit (horizontal asymptote) and $\log \Delta\sigma=C$, representing the lifetime threshold (vertical asymptote). The zero-percentile curve displays the minimum possible required number of cycles to achieve failure for different values of $\Delta\sigma$.

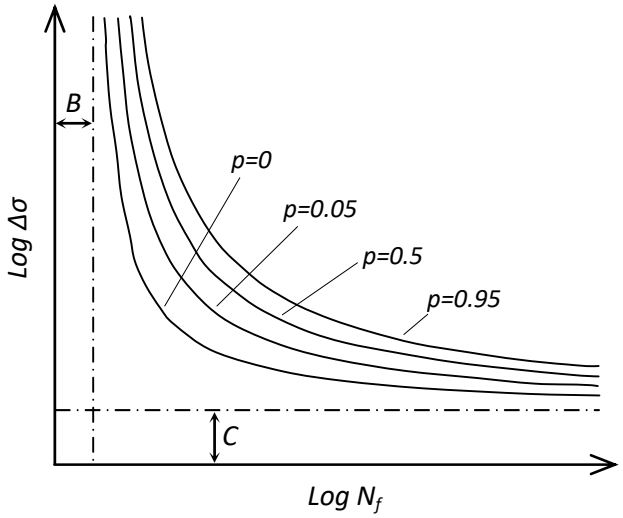

Figure 2.10**:** Probabilistic *S-N* field according to the Weibull model proposed by Castillo and Fernández-Canteli.

Both asymptotes of the *S-N* field limit its domain of applicability to specific subdomains of the field. The vertical asymptote is more controversial given that the plastic effects that appear in the region of low cycle fatigue making the real percentile curves to inflect downwards at this region. The horizontal asymptote is not controversial even for those materials that do not exhibit a clear fatigue limit as is the case of some aluminium alloys, since the model encompasses the case C=0.

An alternative for the **Equations (2.21)** and **(2.22)** were also proposed by authors, using the Gumbel distribution as a limiting case of the Weibull distribution when $\beta\rightarrow\infty$, or even for $\beta>8$:

$$F\left(\log N;\log\Delta\sigma\right)=p=1-\exp\left\{-\exp\left[\frac{\left(\log N-B\right)\left(\log\Delta\sigma-C\right)-\lambda}{\delta}\right]\right\} \tag{2.23}$$

or for non-dimensional variables:

$$F\left(\log N;\log\Delta\sigma\right)=p=1-\exp\left\{-\exp\left[\frac{\log N^{*}\log\Delta\sigma^{*}-\lambda}{\delta}\right]\right\} \tag{2.24}$$

with the same meaning of the symbols as before. Concerning the parameter identification, the process includes two steps: a) estimation of the threshold parameters B and C using the constrained least squares method, and b) estimation of the Weibull parameters, λ, β and δ by the maximum likelihood method [45], once the threshold parameter are known.

In order to illustrate the procedure, let $(\Delta\sigma_i,N_i)|\mathrm{i}=1,2,\ldots,n\}$ be a set of pairs, where $\Delta\sigma_i$ is the deterministic stress range of the specimen i, and N_i is the resulting experimental random lifetime. The procedure to estimate the threshold parameters is based on a constrained least squares method, from which result the following equation and constraints:

$$\underset{B,C,K_1,K_2,\ldots K_i}{\text{Minimize}} \quad Q_{CLS}=\sum_{i=1}^{n} w_i\left(\log N_i-B-\frac{K_i}{\left(\log\Delta\sigma_i-C\right)}\right)^2, \tag{2.25}$$

$$\begin{aligned} C &\le \min_{\mathrm{i}}\left(\log\Delta\sigma_i\right)\\ B &\le \min_{\mathrm{i}}\left(\log N_i\right)\end{aligned} \tag{2.26}$$

where w_i are the weights. The constraints listed by **Equation (2.26)** are included to guarantee that the values B and C are valid threshold values for all data points. If the sample contains run-outs, that is, right censored data points, associated with a certain given limit number of cycles, their lifetimes are not known; thus, an iterative process may be used to assign them to the expected final number of cycles [45].

Once B and C have been estimated, the Weibull constants may be evaluated using a constrained maximum likelihood method. All the data points can be pooled together, in sets of equal lengths, by calculating:

$$v_i=\left(\log N_i-B\right)\left(\log\Delta\sigma_i-C\right)=N_i^{*}\Delta\sigma_i^{*} \tag{2.27}$$

The log-likelihood for broken specimens i.e. run-outs that without loss of generality can be assumed to be the first $n_1<n$ specimens, becomes

$$\log f(v) = -\left[\frac{v-\lambda}{\delta}\right]^{\beta} + \log\beta + (\beta-1)\log\left[\frac{v-\lambda}{\delta}\right] - \log\delta, \tag{2.28}$$

$v \geq \lambda$

and for the run-outs

$$\log\left(1-F(v)\right) = -\left[\frac{v-\lambda}{\delta}\right]^{\beta} \tag{2.29}$$

$v \geq \lambda$

Finally, an optimization problem is solved,

$$\max_{\lambda,\delta,\beta} Q_l = -\sum_{i=1}^{n}\left[\frac{v_i-\lambda}{\delta_i}\right]^{\beta} + (\beta-1)\sum_{i=1}^{n_1}\log\left[\frac{v_i-\lambda}{\delta_i}\right]^{\beta} + n_1\log\beta - \sum_{i=1}^{n_1}\log\delta_i \tag{2.30}$$

subjected to,

$$\min_i v_i \geq \lambda + \delta_i\left[-\frac{1}{n}\log(1-\alpha)\right]^{1/\beta} \tag{2.31}$$

where α can be taken as 0.01. The constraint defined by **Equation (2.31)** is imposed to avoid data below the threshold value of lifetime, i.e.

$$\min_i v_i \geq \lambda \tag{2.32}$$

The solution of the maximization problem leads to an unbounded likelihood value. It states that the minimum value must be greater than its corresponding α 100 percentile value, that is,

$$F_{\min_i} x = 1-\exp\left[-\left(\frac{x-\lambda}{\delta_i n^{1/\beta}}\right)^{\beta}\right] \geq \alpha \tag{2.33}$$

More details about the parameters identification procedure can be found in reference [45].

This model was initially proposed to generate probabilistic *S-N* and ε-*N* fields[69,70]. Some authors[19],[71] taking into account the robustness of this probabilistic fatigue model, proposed a generalization of this model for several fatigue damage parameters applied to experimental fatigue results of metallic materials and steel connections.

This probabilistic fatigue model has been used to evaluate the non-linear (and/or bilinear) cumulative fatigue damage of the P355NL1 pressure vessel steel (Correia et al.[72]). Correia et al.[73] and Blasón et al.[74] evaluated the cumulative fatigue damage of riveted metallic connections with puddle iron from Fão bridge for different percentile curves with the purpose of interpreting the Miner number for fatigue life prediction. The

same path was made by Fernández-Canteli[75], where this author used the probabilistic fatigue model to evaluate the cumulative fatigue damage of the concrete.

In **Figures 2.11** and **2.12**, the *S-N* percentile curves of 5% and 50% obtained based on probabilistic fatigue model proposed by Castillo & Fernández-Canteli for the experimental fatigue data of the metallic material from the Luiz I bridge (R=-1) and for the experimental data of laminate DD16 collected from Mandell[64] (R=0.8) are presented, respectively. Based on the figures it is observed that the model exhibits good results for medium and high-cycle fatigue regions. However, for ultra-low-cycle and low-cycle fatigue regions it does not present satisfactory results due to the limitation of the model, since it has a vertical asymptote. In **Table 2.3**, the obtained parameters using probabilistic fatigue model proposed by Castillo & Fernández-Canteli for both materials are presented.

Table 2.3: Fatigue curve constants based on Castillo & Fernández-Canteli model.

Material	Weibull Parameters			Geometrical Parameters	
	λ	β	δ	B	C
Luís Bridge R=-1	-2.29	10.33	4.84	0.0	4.67
DD16 R=0.8	17.00	-3.29	-3.87	0.0	2.34

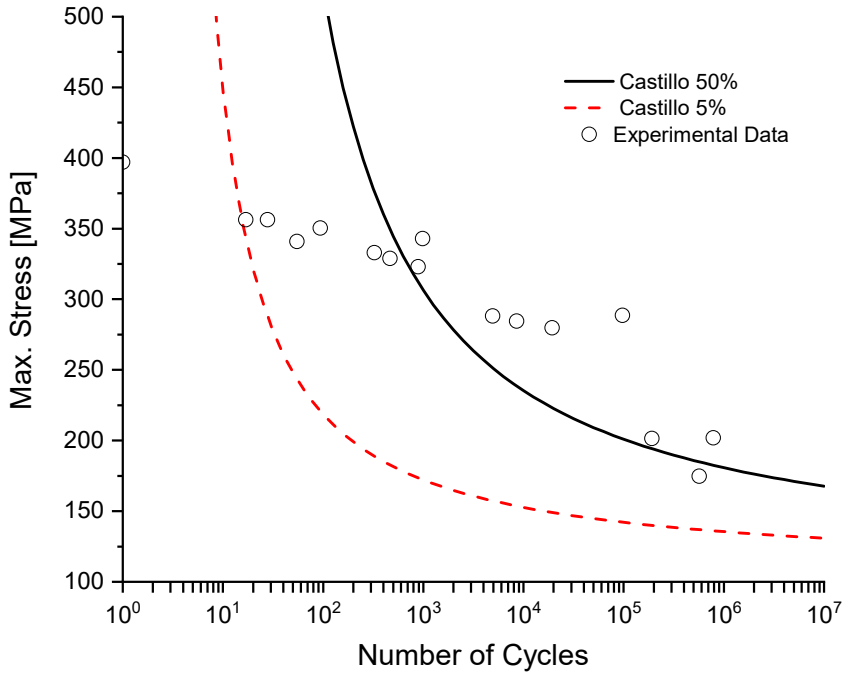

Figure 2.11: *S-N* reliability curve based on Castillo & Fernández-Canteli model for the experimental fatigue data of the metallic material from the Luiz I Bridge, *R=-1*.

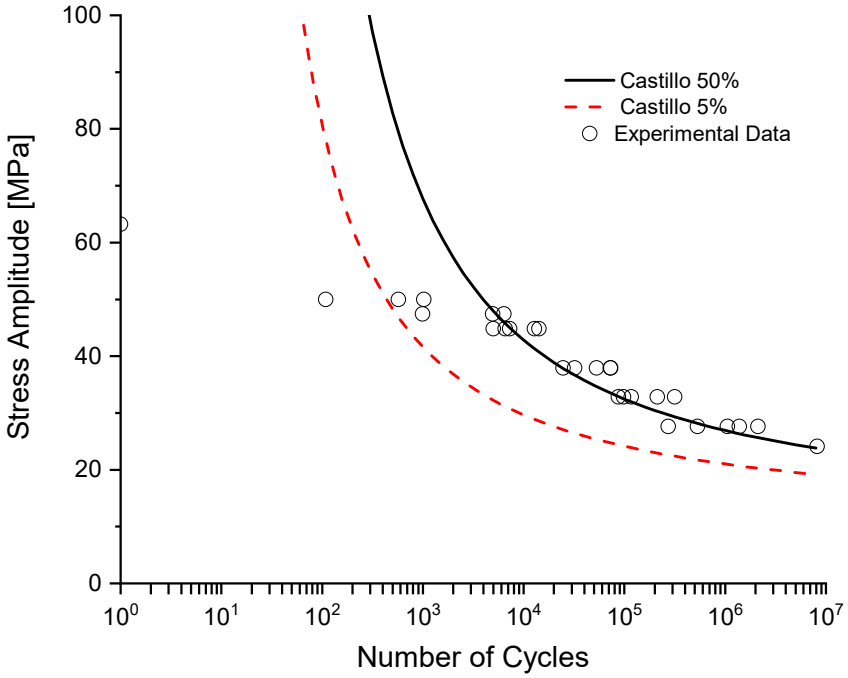

Figure 2.12: *S-N* reliability curve based on Castillo & Fernández-Canteli model for the experimental data of laminate DD16 collected from Mandell[64], *R=0.8*.

2.4.2 Generalized probabilistic model allowing for various fatigue damage variables

The fatigue damage model proposed by Castillo and Fernández-Canteli and presented in **section 2.3.1** is limited to simple fatigue damage parameters such as the stress or strain. De Jesus et al.[71] suggested the first generalization of the probabilistic fatigue model proposed by Castillo and Fernández-Canteli. These authors applied this probabilistic fatigue model to derive the probabilistic stress–life curves for a single-shear riveted connection based on a probabilistic $\varepsilon - N$ field obtained using the experimental strain-life data and based on the Neuber or Glinka rules. Correia et al[19] decided to generalize this probabilistic fatigue model to other fatigue damage parameters, such as, Smith-Watson-Topper (SWT), Walker-like strain, and energy for uniaxial and multiaxial loading conditions. This proposal proved to be feasible for fatigue damage parameters under uniaxial and multiaxial loading conditions for different metallic materials.

The onset of a macro-crack is considered a failure criterion by fatigue and can be represented by a deterministic parameter:

$$\psi = q\left(N_f\right) \tag{2.34}$$

The parameter ψ represents the fatigue damage, q is a decreasing function of the total life in terms of number of reversals to failure, $2N_f$, or number of cycles to failure, N_f. Fatigue damage can be generically rewritten by the Power law:

$$\psi = k\left(2N_f\right)^{\alpha} + \psi_0 \tag{2.35}$$

The variable ψ_0 is the limit of fatigue resistance, k and α are material constants. Through this generic damage formulation it will be possible to propose a generalization of the probabilistic fatigue model proposed by Castillo & Fernández-Canteli for several fatigue damage parameters.

Considering the same physical and statistical assumptions of probabilistic fatigue model proposed by Castillo & Fernández-Canteli[45], the modelling of the random variable of **Equation (2.27)** can be generalized to other damage parameters:

$$v = f\left(\psi\right) f\left(N_f\right) \tag{2.36}$$

This random variable v follows a three-parameters Weibull distribution $v_k \sim W(\lambda, \delta, \beta)$ and has its parameters estimated by the optimization equation of **Equation (2.30)**. The variable K represents the experiment number, $k = 1, 2, ..., T$, and T is the total number of experimental samples.

The generalized probabilistic field is then written as:

$$p = 1 - \exp\left\{-\left[\frac{\log\left(N_f/N_0\right)\log\left(\psi/\psi_0\right) - \lambda}{\delta}\right]^{\beta}\right\} \tag{2.37}$$
$$\log\left(N_f/N_0\right)\log\left(\psi/\psi_0\right) \geq \lambda$$

where p is the probability of failure, N_0 ($A = \log(N_0)$) e ψ_0 ($B = \log(\psi_0)$) are normalization values and λ, δ, and β are the Weibull distribution parameters.

The generalized probabilistic fatigue damage model can be specified using the Smith-Watson-Topper (SWT) deterministic variable in **Equation (2.37)** as proposed by Correia et al.[19]:

$$\psi = \sigma_{\max} \varepsilon_a \tag{2.38}$$

where, σ_{max} is the maximum stress and ε_a is the strain amplitude.
Other deterministic variable as the Walker-like strain damage parameter for uniaxial loading conditions can be used in **Equation (2.37)**:

$$\psi = \varepsilon_a \left(\frac{2}{1-R} \right)^{1-\hat{\gamma}} \tag{2.39}$$

where, $\hat{\gamma}$ is the Walker fitting constant, and, ε_a is the strain amplitude.

In this way, Correia et al. [19] proposed the use of energy criterion under uniaxial loading conditions suggested by Golos and Ellyin[76,77] as a generic damage variable of the generalized probabilistic fatigue model (**Equation 2.37**) and some applications were presented. The energy-based fatigue damage parameter used in their studies was the following (**Equation 2.40**):

$$\psi = \Delta W^t = \frac{1-n'}{1+n'} \Delta\sigma \, \Delta\varepsilon^P + \frac{1}{2E} \left(\frac{\Delta\sigma}{2} + \sigma_m \right)^2 \tag{2.40}$$

Correia et al[19] also demonstrated the damage parameter generalization for multiaxial proportional and non-proportional loading conditions based on an energy-based damage parameter. The multiaxial damage parameter used in his research work is recommended for non-proportional loading based on multiaxial constraint ratio ($\bar{\rho}$):

$$\psi = \Delta W^t = \frac{\Delta W^P}{\bar{\rho}} + \Delta W^{E+} \tag{2.41}$$

The multiaxial fatigue damage can also be represented by the critical plane parameters based on shear strain. Jiang et al.[78] defined this fatigue damager parameter for a material as the critical plane, and it is suitable as an energy failure criterion under multiaxial loading. The multiaxial fatigue damage parameter based on the critical plane can be presented as a damage variable, ψ, and given by:

$$\psi = \frac{\Delta\gamma}{2}\left(1 + K\frac{\sigma_{n,\max}}{\sigma_y}\right) \tag{2.42}$$

where, $\Delta\gamma/2$ is the shear strain amplitude, $\sigma_{n,max}$ is the maximum normal stress on the critical plane, K is a material constant, and, σ_y is the yield stress. An example of application of the generalization of the probabilistic fatigue model considering the damage gradient as a multiaxial parameter for both proportional and non-proportional loading was presented by Muñiz-Calvente et al.[79].

2.5 Probabilistic full-range fatigue prediction and Stüssi models based on the Weibull model proposed by Castillo et al.

The Stüssi nonlinear function was proposed to represent *S-N* curves, based on the geometric principle of material behaviour during its useful life. To that end, this model must estimate fatigue threshold and ultimate tensile strength parameters for the equation to be able to model *S-N* curve fitting in the low- (LCF) and high-cycle fatigue (HCF) regions. However, this model is based only on the average behaviour of the number of failure cycles in the material, and does not consider the randomness of failure. The nonlinear equation of the *S-N* curve for the material proposed by Stüssi is given by:

$$\Delta\sigma = \frac{R_m + aN^b\Delta\sigma_\infty}{1 + aN^b} \tag{2.43}$$

where $\Delta\sigma$ is the stress range during the fatigue test, N the number of cycles to failure, R_m ultimate tensile strength, $\Delta\sigma_\infty$ the fatigue threshold, and a and b the geometric parameters of the material.

In order to estimate the two geometric parameters (a and b) of **Equation (2.43)**, it is essential to know the two parameters of the material (R_m and $\Delta\sigma_\infty$). The first is obtained from the average ultimate tensile strength results and the second is the fatigue threshold, which can be obtained by solving **Equation (2.30)** using nonlinear optimization. After these values are obtained, the logarithm is applied in **Equation (2.26)** to linearize it,

followed by simple linear regression to estimate the values of a and b. Once the parameters of **Equation (2.26)** are known, the *S-N* curve can be obtained from the Stüssi function in its log-log scale, depicted in **Figure 2.13**. The study by Caiza[80] provides a more detailed explanation on the estimation of these geometric parameters.

Given the limitation of the model, Caiza[80] proposed to include the Stüssi function in three-parameter Weibull distribution in order to model a probabilistic method to describe *S-N* reliability curves. The three-parameter estimation model of the Weibull distribution, $W(\alpha,\beta,\delta)$, is based on the Castillo et al[45] model mentioned in **section 2.3.1**, which emphasizes the stochastic nature of fatigue, involving stress interval $\Delta\sigma$ and time to failure, given by the number of cycles as random variables [81].

The probabilistic model of Stüssi's equation is a combination of the three-parameter Weibull distribution and Stüssi function. To that end, the accumulated distribution function is used, given by:

$$F\left(x\middle|\alpha,\beta,\delta\right)=1-\exp\left[-\left(\frac{x-\alpha}{\beta}\right)^{\delta}\right], \qquad x\geq\alpha \tag{2.44}$$

and **Equation (2.43)** transformed into a random variable to be inserted into **Equation (2.44)**. The random Stüssi variable is given by:

$$x=\Delta\sigma-\frac{R_m+aN^b\Delta\sigma_\infty}{1+aN^b} \tag{2.45}$$

To obtain the probabilistic model, the random variable x (**Equation (2.45)**) is inserted into **Equation (2.44)** to obtain the probability equation for the *S-N* curve.

$$P=1-\exp\left[-\left(\frac{\Delta\sigma-\frac{R_m+aN^b\Delta\sigma_\infty}{1+aN^b}-\alpha}{\beta}\right)^{\delta}\right] \tag{2.29}$$

where, P is the failure probability; $\alpha \in \mathbb{R}$ is the Weibull localization parameter; $\beta>0$ is the Weibull scale parameter; and δ is the Weibull shape parameter.

This model was developed based on the assumption that Stüssi's random variable follows a three-parameter Weibull distribution composed of geometric and material parameters. The Castillo–Hadi[82] or PWM[83] methods can be applied to estimate the Weibull distribution parameters. Once these values are known, failure probability curves can be drawn for the material in question (**Figure 2.14**).

The Stüssi method can model plastic fatigue behaviour in the LCF region. From a geometric standpoint, **Figure 2.14** shows that this is a well-fitting model for explaining fatigue behaviour in the low-cycle regions of metals.

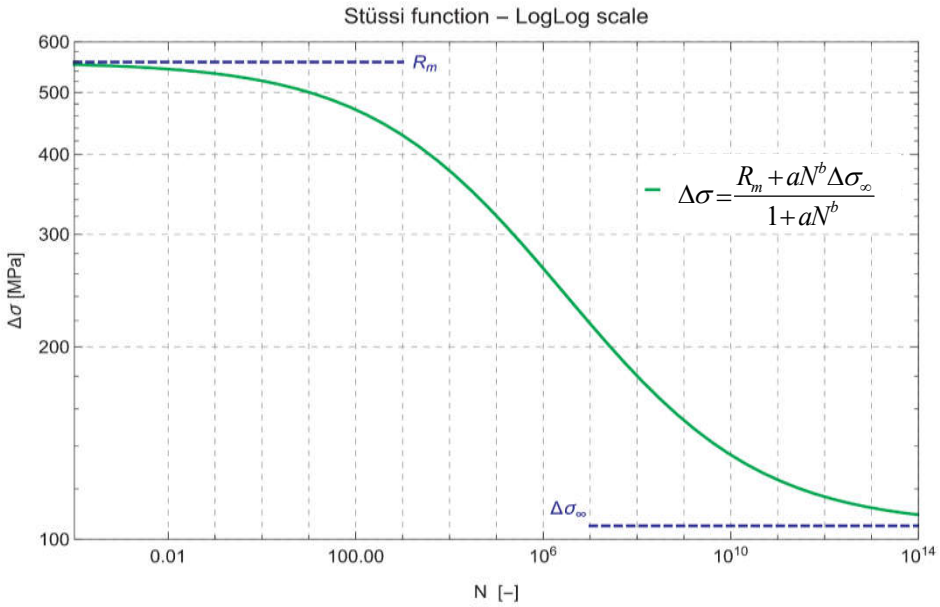

Figure 2.13**:** *S-N* curve based on the Stüssi Log-Linear scale.[1]

[1] Reprinted from International Journal of Fatigue, 117 (2018), Caiza, P.D.T., & Ummenhofer, T. A probabilistic Stüssi function for modelling the S-N curves and its application on specimens made of steel S355J2+N, 121-134, Copyright (2018), with permission from Elsevier.

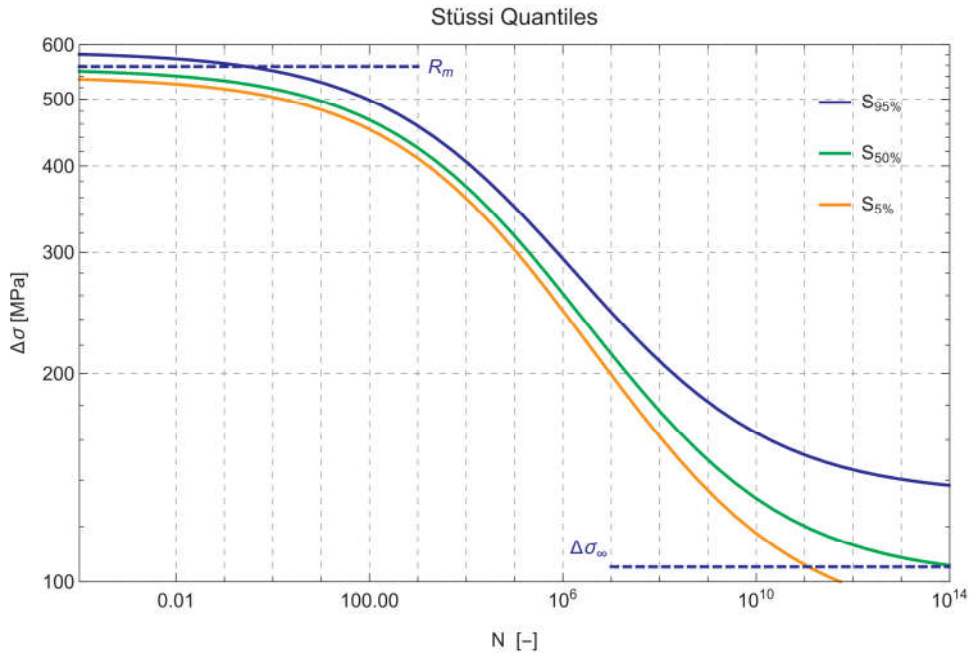

Figure 2.14: *S-N* curves based on the Stüssi model combined with a Weibull distribution. The plotted curves correspond to a failure probability of 5%, 50% and 95%.[2]

In **Figures 2.15** and **2.16**, the *S-N* percentile curves of 5% and 50% obtained based on Stüssi model combined with a Weibull distribution proposed by Caiza & Ummenhofer[80] for the experimental fatigue data of the metallic material from the Luiz I bridge (R=-1) and for the experimental data of laminate DD16 collected from Mandell[64] (R=0.8) are presented, respectively. The probabilistic fatigue analysis proposed by Caiza & Ummenhofer[80] based on Stüssi model combined with a Weibull distribution gives good results in all fatigue regions, from ultra-low- to high-cycle, for both materials under consideration. In **Table 2.4**, the obtained parameters using the Stüssi model combined with a Weibull distribution proposed by Caiza & Ummenhofer[80] for both materials are presented.

Table 2.4: Fatigue curve constants based on Stussi model.

Material	R_m	$\Delta\sigma_\infty$	Weibull Parameters			Geometrical Parameters	
	MPa	*MPa*	α	β	δ	a	b
Luís Bridge R=-1	396.6	106.79	-20.2509	23.4106	1.12439	0.0510	0.2842
DD16 R=0.8	60.2	10.34	-22.7230	23.6902	12.5096	0.0612	0.2528

[2] Reprinted from International Journal of Fatigue, 117 (2018), Caiza, P.D.T., & Ummenhofer, T. A probabilistic Stüssi function for modelling the S-N curves and its application on specimens made of steel S355J2+N, 121-134, Copyright (2018), with permission from Elsevier.

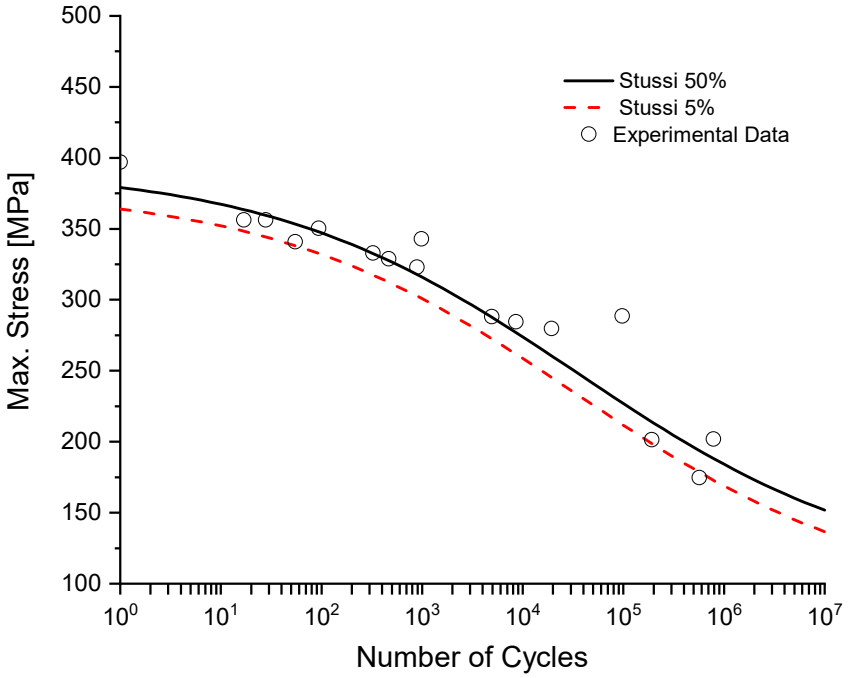

Figure 2.15: *S-N* reliability curve based on Stüssi model combined with a Weibull distribution for the experimental fatigue data of the metallic material from the Luiz I Bridge, *R=-1*.

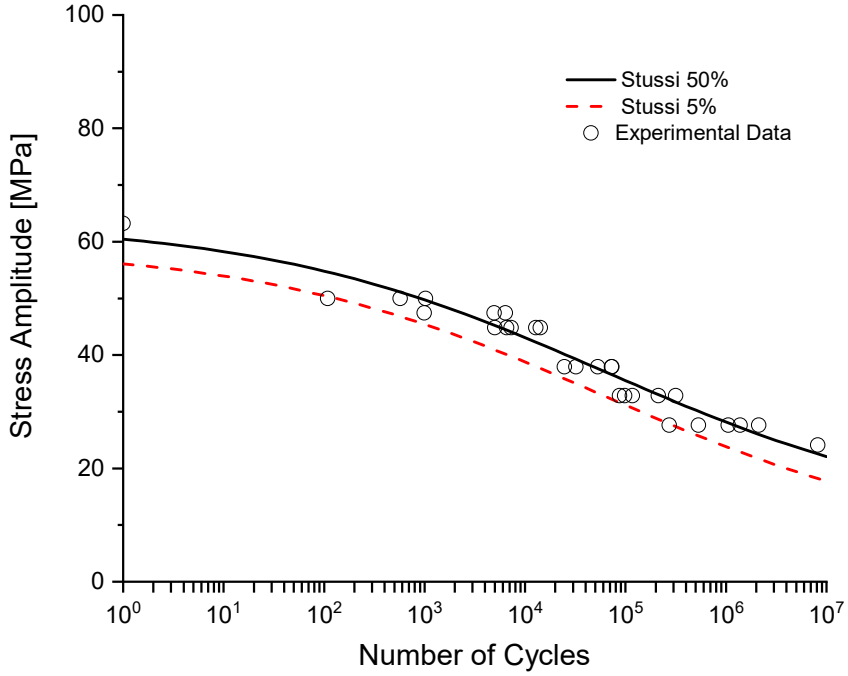

Figure 2.16: *S-N* reliability curve based on Stüssi model combined with a Weibull distribution for the experimental data of laminate DD16 collected from Mandell[64], *R=0.8*.

2.6 Results discussion: applicability of different probabilistic fatigue models

A single probabilistic *S-N* mathematical model is generally applied for the fatigue life prediction of metallic or composite materials. However, researchers and engineers should consider the differences between the two types of materials in order to determine the modelling process that best represents the stochastic fatigue life behaviour. Damage in composite laminates, with small cracks in the polymer matrix, occurs randomly and cumulatively on the surface and internally, increasing dispersion until final failure. In other hand, the fatigue crack propagation in metals is identifiable on the fracture surface, with less dispersion in the number of cycles to failure. Aspects such as sample size, dispersion of the number of cycles to failure for different stress range levels, stress range or maximum stress and the random variable(s) selected for a given probabilistic fatigue model under consideration, influence the statistical distribution[80].

The *P-S-N* curves discussed in this review are based on the two- and three-parameters Weibull and log-normal distributions. The ASTM E739 standard, Sendeckyj, Castillo & Fernández-Canteli and Stüssi models are based on different probabilistic modelling processes that allow to be used in different applications according to the specificities of the material under consideration.

For metallic materials (**Figure 2.8**), the Sendeckyj model revealed to be more efficient when the fatigue percentile curves are compared with the experimental data, for the ultra-low- until medium-cycle fatigue regions ($N_f \leq 10^5$). In another sense, the ASTM E739-91 standard exhibits a good fit for the medium- and high-cycle fatigue regions. For composite material (**Figure 2.9),** the Sendeckyj model presented a more suitable adjustment when compared with the experimental data in all fatigue regions, whereas the ASTM E739 standard is only appropriate for the medium- and high-cycle fatigue regions, such as for metallic material.

The probabilistic fatigue model based on Weibull statistical distribution for a range of variable and fixed stresses proposed by Castillo & Fernández-Canteli is recommended for the fatigue life prediction in finite life and high-cycle fatigue regions. This model is based on physical assumptions (identifying the involved variables and dimensionless analysis) and statistical requirements (weakest link principle, stability, limited reach, threshold

behaviour). According to the shown in **Figures 2.11** and **2.12**, the percentile curves are adjusted reasonably in fatigue regions with number of cycles to failure above of 10^4, for metallic and composite materials under consideration.

The Stüssi model based on three-parameter Weibull statistical distribution was proposed by Caiza & Ummenhofer. These authors used the same regression method proposed by Castillo & Fernández-Canteli, proposing the extension of the fatigue life prediction for the low-cycle fatigue (LCF) region but based on Stüssi relation. In their studies, Caiza & Ummenhofer used experimental fatigue data from the specimens made of steel S355J2+N and showed that the probabilistic Stüssi model, was able to estimate failure probabilities in the LCF region (see **Figure 2.17**). The probabilistic Stüssi model presented a good adjustment in all fatigue regions (since ultra-low fatigue to high-cycle fatigue) when compared with the probabilistic fatigue model proposed by Castillo & Fernández-Canteli (see **Figure 2.17**).

The Castillo & Fernández-Canteli model as well as probabilistic Stüssi model proposed by Caiza & Ummenhofer are more suitable for the metallic materials, since these kind of materials require the fatigue strength threshold of the material to generate reliability curves, while composite materials do not exhibit a quantifiable fatigue strength threshold.

However, in **Figures 2.15** and **2.16**, a good adjustment between the percentile curves (5% and 50%) and the range of experimental data for the metallic and composite materials, is observed, respectively. In this sense, this probabilistic Stüssi model proves to be effective for the metallic and composite materials.

In **Figures 2.18** and **2.19**, the *S-N* percentile curves of 50% and 5% obtained for all models under consideration for the experimental fatigue data of the metallic material from the Luiz I Bridge, R=-1, are presented, respectively. All models present good adjustment results with experimental data for fatigue regions with number of cycles to failure above 10^3 ($N > 10^3$), excluding the Sendeckyj model for number of cycles to failure above 10^5 ($N > 10^5$). The ASTM E739 procedures and the probabilistic fatigue model proposed by Castillo & Fernández-Canteli are not suitable for ultra-low- and low-cycle fatigue regions ($N < 10^3$). On the contrary, the probabilistic Stüssi and Sendeckyj models reveal to be effective for ultra-low- and low-cycle fatigue regions. In this sense, the probabilistic Stüssi model presents better adjustment results for all fatigue regions, from low-cycle (LCF) to high-cycle (HCF).

In **Figures 2.20** and **2.21**, the *S-N* percentile curves of 50% and 5% obtained for all methods under consideration for the experimental data of laminate DD16 collected from Mandell[64], R=0.8, are presented, respectively. All models present good adjustment results with experimental data for fatigue regions with number of cycles to failure above 10^3 ($N > 10^3$), excluding the probabilistic fatigue model proposed by Castillo & Fernández-Canteli that only shows good results for numbers of cycles to failure above 10^4 ($N > 10^4$). As with metallic materials, the ASTM E739 standard and probabilistic fatigue model proposed by Castillo & Fernández-Canteli are not suitable for ultra-low- and low-cycle fatigue regions, $N < 10^3$ and $N < 10^4$, respectively. On the contrary, the probabilistic Stüssi and Sendeckyj models reveal to be effective for ultra-low- and low-cycle fatigue regions. In this sense, for the composite materials, the probabilistic Stüssi and Sendeckyj models exhibit a good agreement with experimental data for all fatigue regions, from low-cycle (LCF) to high-cycle (HCF).

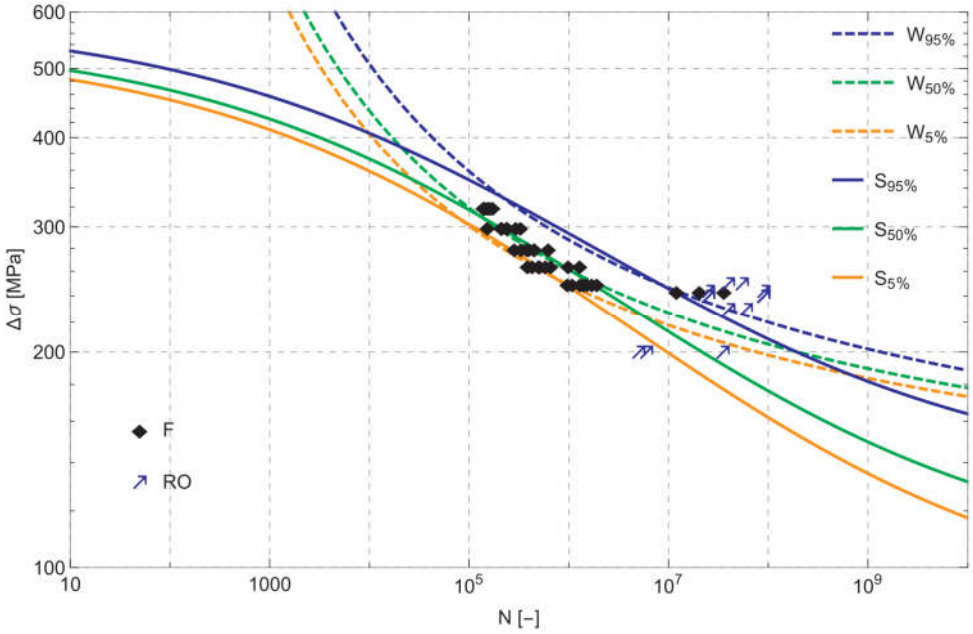

Figure 2.17: Comparison of the *S-N* quantiles based on Weibull model of Castillo et al. and Stüssi model combined with a Weibull distribution: The Weibull model considers a sample which contains only the fatigue failures without runouts.[3]

[3] Reprinted from International Journal of Fatigue, 117 (2018), Caiza, P.D.T., & Ummenhofer, T. A probabilistic Stüssi function for modelling the S-N curves and its application on specimens made of steel S355J2+N, 121-134, Copyright (2018), with permission from Elsevier.

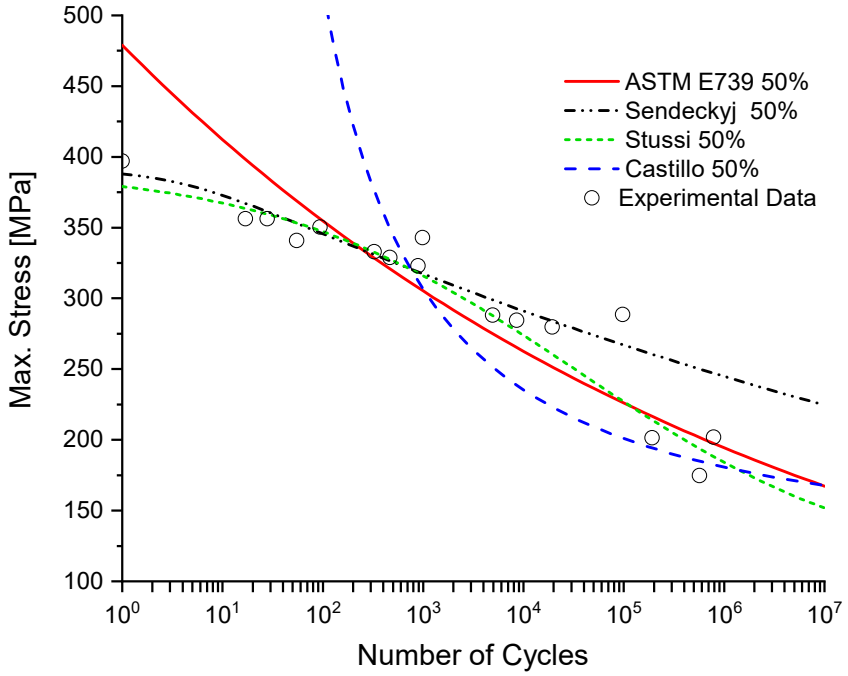

Figure 2.18: S-N reliability curves to probability of failure of 50% for all methods under consideration for the experimental fatigue data of the metallic material from the Luiz I Bridge, R=-1.

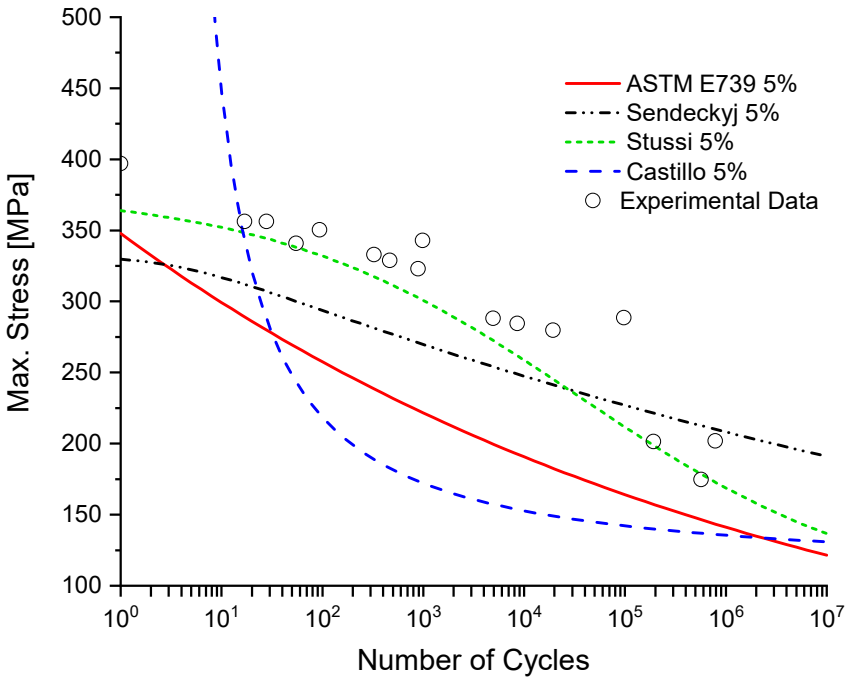

Figure 2.19: S-N reliability curves to probability of failure of 5% for all methods under consideration for the experimental fatigue data of the metallic material from the Luiz I Bridge, R=-1.

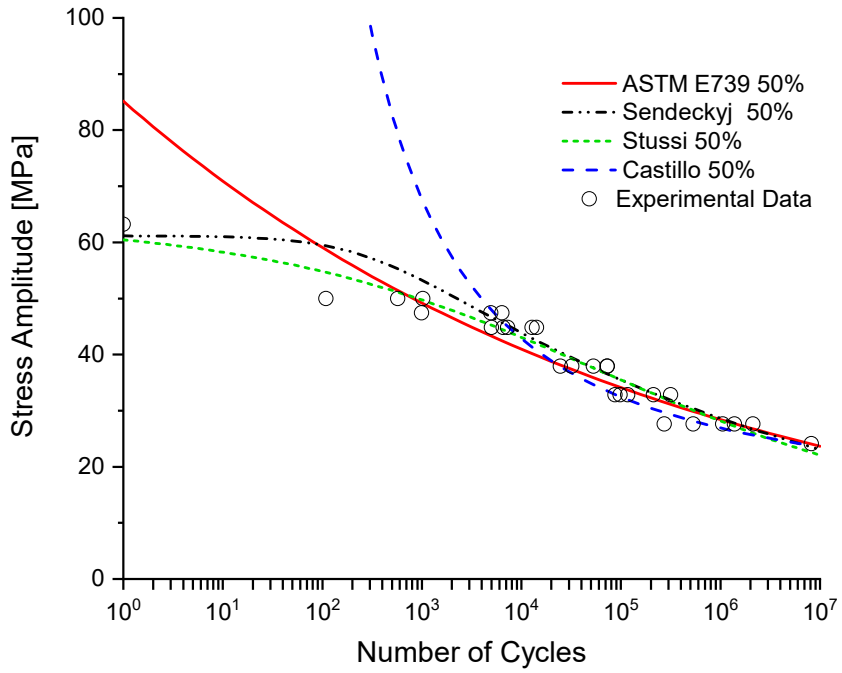

Figure 2.20: S-N reliability curves to probability of failure of 50% for all methods under consideration for the experimental data of laminate DD16 collected from Mandell[64], R=0.8.

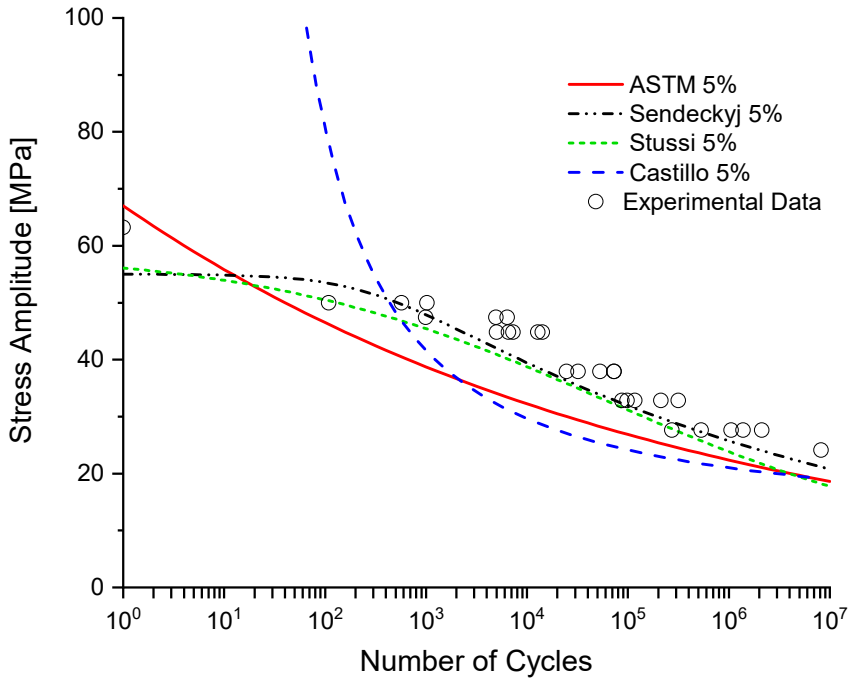

Figure 2.21: S-N reliability curves to probability of failure of 5% for all methods under consideration for the experimental data of laminate DD16 collected from Mandell[64], R=0.8.

In order to evaluate the performance of the probabilistic S-N curves according to the ASTM E739 standard[16], the probabilistic Stüssi model proposed by Caiza & Ummenhofer[80], the Sendeckyj model[30] and thee probabilistic fatigue model proposed by Castillo & Fernández-Canteli[45], the quality of fitting provided by the mean S-N curves was quantified comparing it with the available experimental data. In this way, the root mean squared error (RMSE) between $\sigma_{SN(i)}$ values (stress estimated from the mean S-N curve) and $\sigma_{exp(i)}$ values (experimental stress) are estimated by the following relation:

$$RMSE = \sqrt{\frac{1}{n}\sum_{i=1}^{n}\left(\sigma_{SN(i)} - \sigma_{\exp(i)}\right)^2} \tag{2.30}$$

where, σ_{SN} is the stress obtained by mean S-N curve, σ_{exp} is the experimental stress and n is the sample size.

The performance of the mean S-N curves (50% percentile curves) evaluated for the several models under consideration when compared with experimental fatigue data, were determined using the root mean squared error estimator separately for low- and high-cycle fatigue regions as well as for the full-range fatigue regimes.

Figures 2.22 and **2.23** present the values of the normalized root mean squared error, RMSE, for the metallic material from the Luiz I old riveted bridge and the DD16 composite material, considering separately low- and high-cycle fatigue regions ($N < 10^4$ and $N > 10^4$) as well as for full-range fatigue regimes, respectively. The values of the normalized root mean squared error, RMSE, considering separately low- and high-cycle fatigue regions as well as for full-range fatigue regimes, for the materials under study, are showed in **Tables 2.5** and **2.6**, respectively. Therefore, based on the results obtained for the normalized RMSE values, it is possible to verify that the probabilistic Sendecky model[30] presents a better fit for the Luiz I metallic material when $N < 10^4$cycles, whereas for the composite material, the probabilistic Stüssi model[80] exhibited a more adequate adjustment. For high-cycle fatigue region, $N > 10^4$cycles, the probabilistic Stüssi model exhibits better fitting for the metallic material. For the composite material in high-cycle fatigue region, the model with the best performance is the one proposed by ASTM E739 standard[16]. When the analysis is done for the full-range fatigue region, for

both metallic and composite materials, it is possible to verify that the probabilistic Stüssi model[80] proved to be the most adequate when compared to the other models under consideration.

The probabilistic fatigue model proposed by Castillo & Fernández-Canteli[45] exhibited the worst performance when compared to the experimental fatigue data available. However, the probabilistic fatigue model proposed by Castillo & Fernández-Canteli[45] presents better results when only the high-cycle fatigue data are considered according to references[19,32,44,49,65–68,79]. It is important to refer that all models were identified using the complete set of experimental fatigue data.

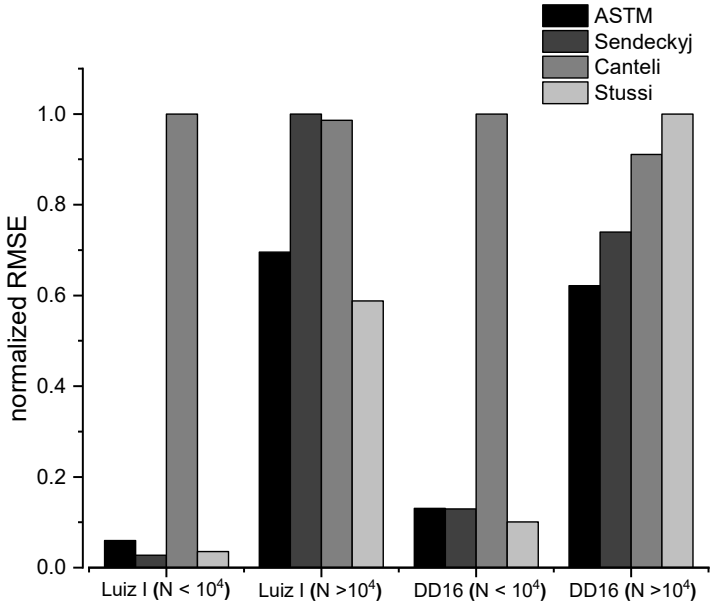

Figure 2.22: Normalized RMSE for different fatigue regions.

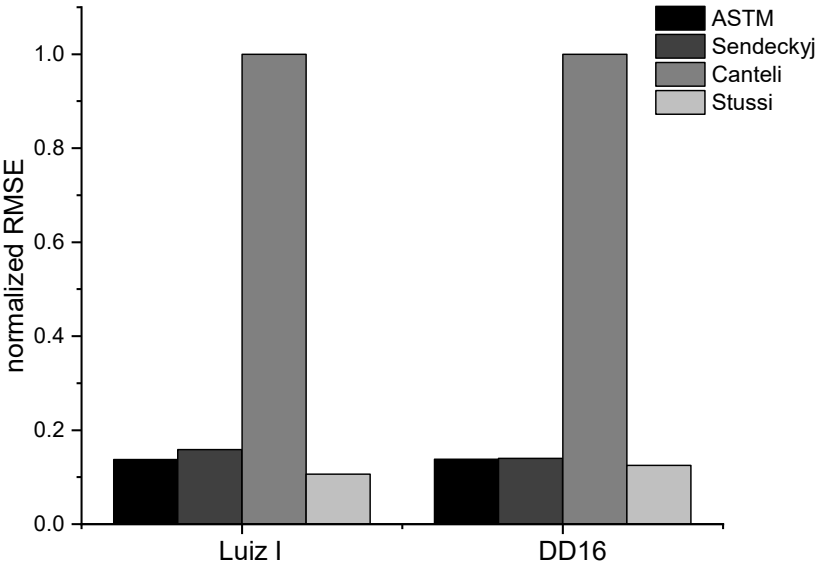

Figure 2.23: Normalized RMSE for all fatigue regimes.

Table 2.5: Normalized RMSE values for different fatigue regimes.

Material	Fatigue Region	ASTM	Sendecky	Canteli	Stüssi
Luiz I	RMSE ($N<10^4$)	0.060	**0.027**	1.000	0.036
	RMSE ($N>10^4$)	0.695	1.000	0.986	**0.588**
DD16	RMSE ($N<10^4$)	0.130	0.129	1.000	**0.101**
	RMSE ($N>10^4$)	**0.621**	0.740	0.911	1.000

Table 2.6: Normalized RMSE for all fatigue regions.

Material	Method	ASTM	Sendecky	Canteli	Stüssi
Luiz I	RMSE	0.084	0.090	1.000	**0.062**
	R	0.906	0.920	0.609	**0.948**
DD16	RMSE	0.138	0.140	1.000	**0.125**
	R	0.944	0.963	0.661	**0.971**

2.7 Conclusions

In this research work, a state of the art on probabilistic fatigue models based on statistical distributions applied to metallic and composite materials was made. In this study, the differences between probabilistic fatigue models such as ASTM E739 standard, Sendeckyj, Castillo & Fernández-Canteli, and Stüssi applied to the metallic and composite materials are presented.

For the metallic material, all models exhibit good adjustment when compared with the experimental data from low-cycle to high-cycle fatigue regimes, excluding the Sendeckyj model, which not presented a good fit for the high-cycle fatigue region. For all fatigue regions, only the probabilistic Stüssi model presented very good adjustment results when compared with experimental data. However, for metallic materials, in most practical cases (design situations), the most relevant fatigue regions are those of medium- and high-cycle with a defined fatigue limit described by Basquin law. In this way, the probabilistic fatigue models such as the Castillo & Fernández-Canteli, ASTM standard and Stüssi seem to be the most suitable.

For the composite material, the probabilistic Stüssi and Sendeckyj models reveal to be effective for all fatigue regions. The remaining models have only good adjustments to

particular fatigue regimes such as medium- and high-cycle fatigue. The probabilistic Stüssi and Sendeckyj models were the most suitable for composite materials, while for metallic materials only the probabilistic Stüssi model presented good adjustment results, for all fatigue regions (from ultra-low-cycle to high-cycle).

2.8 References

[1] Bathias C. An engineering point of view about fatigue of polymer matrix composite materials. Int J Fatigue 2006;28:1094–9. doi:10.1016/j.ijfatigue.2006.02.008.

[2] Liu H, Cui H, Wen W, Kang H. Fatigue characterization of T300/924 polymer composites with voids under tension-tension and compression-compression cyclic loading. Fatigue Fract Eng Mater Struct 2018;41:597–610.

[3] Zhu S-P, Hao Y-Z, de Oliveira Correia JAF, Lesiuk G, De Jesus AMP. Nonlinear fatigue damage accumulation and life prediction of metals: A comparative study. Fatigue Fract Eng Mater Struct 2018.

[4] Zhu S-P, Yu Z-Y, Correia J, De Jesus A, Berto F. Evaluation and comparison of critical plane criteria for multiaxial fatigue analysis of ductile and brittle materials. Int J Fatigue 2018;112:279–88.

[5] Zhu S-P, Yue P, Correia JAF de O, Blasón González S, Jesus AMP de, Wang Q. Strain energy-based fatigue life prediction under variable amplitude loadings. Struct Eng Mech 2018.

[6] Liao D, Zhu S-P, Correia JAFO, De Jesus AMP, Calçada R. Computational framework for multiaxial fatigue life prediction of compressor discs considering notch effects. Eng Fract Mech 2018;202:423–35.

[7] Vassilopoulos AP, Keller T. Fatigue of fiber-reinforced composites. Springer Science & Business Media; 2011.

[8] Zhu S-P, Huang H-Z, Wang Z-L. Fatigue life estimation considering damaging and strengthening of low amplitude loads under different load sequences using fuzzy sets approach. Int J Damage Mech 2011;20:876–99.

[9] Qian G, Lei W-S, Niffenegger M, González-Albuixech VF. On the temperature independence of statistical model parameters for cleavage fracture in ferritic steels. Philos Mag 2018;98:959–1004.

[10] Qian G, Lei W-S, Peng L, Yu Z, Niffenegger M. Statistical assessment of notch toughness against cleavage fracture of ferritic steels. Fatigue Fract Eng Mater

Struct 2018;41:1120–31.

[11] Zhu S-P, Huang H-Z, Smith R, Ontiveros V, He L-P, Modarres M. Bayesian framework for probabilistic low cycle fatigue life prediction and uncertainty modeling of aircraft turbine disk alloys. Probabilistic Eng Mech 2013;34:114–22.

[12] Lehmayr B, Staudacher S. A statistical model for scatter representation in stress life curves. Fatigue Fract Eng Mater Struct 2012;35:347–58. doi:10.1111/j.1460-2695.2011.01625.x.

[13] Mahmud M, Abdullah S, Ariffin AK, Nopiah ZM. On the need to adopt strain-based probabilistic approach in predicting fatigue life. J Brazilian Soc Mech Sci Eng 2018;40:1–13. doi:10.1007/s40430-018-1000-4.

[14] Zhu SP, Foletti S, Beretta S. Probabilistic framework for multiaxial LCF assessment under material variability. Int J Fatigue 2017;103:371–85. doi:10.1016/j.ijfatigue.2017.06.019.

[15] Zhu S-P, Huang H-Z, Peng W, Wang H-K, Mahadevan S. Probabilistic physics of failure-based framework for fatigue life prediction of aircraft gas turbine discs under uncertainty. Reliab Eng Syst Saf 2016;146:1–12.

[16] ASTM E739-10(2015). Standard Practice for Statistical Analysis of Linear or Linearized Stress-Life (S-N) and Strain-Life (ε-N) Fatigue Data. ASTM Int West Conshohocken, PA, USA 2015. doi:10.1520/E0739-10.2.

[17] Schijve J. Statistical distribution functions and fatigue of structures. Int J Fatigue 2005;27:1031–9. doi:10.1016/j.ijfatigue.2005.03.001.

[18] Harris B. Fatigue in composites: science and technology of the fatigue response of fibre-reinforced plastics. 2003.

[19] Correia J, Apetre N, Arcari A, De Jesus A, Muñiz-Calvente M, Calçada R, et al. Generalized probabilistic model allowing for various fatigue damage variables. Int J Fatigue 2017;100:187–94.

[20] Zhu S-P, Liu Q, Peng W, Zhang X-C. Computational-experimental approaches for fatigue reliability assessment of turbine bladed disks. Int J Mech Sci 2018;142:502–17.

[21] Zhu SP, Liu Q, Zhou J, Yu ZY. Fatigue reliability assessment of turbine discs under multi-source uncertainties. Fatigue Fract Eng Mater Struct 2018:1–15. doi:10.1111/ffe.12772.

[22] Zhu S-P, Liu Q, Lei Q, Wang Q. Probabilistic fatigue life prediction and reliability assessment of a high pressure turbine disc considering load variations. Int J Damage Mech 2018;27:1569–88.

[23] Qian G, Zhou C, Hong Y. A model to predict S--N curves for surface and

subsurface crack initiations in different environmental media. Int J Fatigue 2015;71:35–44.

[24] Zhu S-P, Huang H-Z, Li Y, Liu Y, Yang Y. Probabilistic modeling of damage accumulation for time-dependent fatigue reliability analysis of railway axle steels. Proc Inst Mech Eng Part F J Rail Rapid Transit 2015;229:23–33.

[25] Freire Júnior RCS, Belísio AS. Probabilistic S-N curves using exponential and power laws equations. Compos Part B Eng 2014;56:582–90. doi:10.1016/j.compositesb.2013.08.036.

[26] Kawai M, Yano K. Probabilistic anisomorphic constant fatigue life diagram approach for prediction of P-S-N curves for woven carbon/epoxy laminates at any stress ratio. Compos Part A Appl Sci Manuf 2016;80:244–58. doi:10.1016/j.compositesa.2015.10.021.

[27] Lee J, Harris B, Almond DP, Hammett F. Fibre composite fatigue-life determination. Compos Part A Appl Sci Manuf 1997;28:5–15. doi:10.1016/S1359-835X(96)00088-7.

[28] Hwang W, Han KS. Statistical study of strength and fatigue life of composite materials. Composites 1987;18:47–53.

[29] Whitney JM. Use of the lognormal distribution for characterizing composite materials. Compos. Mater. Test. Des. (6th Conf., 1982.

[30] Sendeckyj GP. Fitting Models to Composite Materials Fatigue Data. ASTM STP 734 1981:245–60. doi:10.1520/STP29314S.

[31] Wolff R V., Lemon GH. Prediction for Composite Joints-Bonded and Bolted. Gen Dyn WORTH TEX FORT WORTH DIV 1976:110.

[32] Castillo E, López-Aenlle M, Ramos A, Fernández-Canteli A, Kieselbach R, Esslinger V. Specimen length effect on parameter estimation in modelling fatigue strength by Weibull distribution. Int J Fatigue 2006;28:1047–58. doi:10.1016/J.IJFATIGUE.2005.11.006.

[33] Vassilopoulos AP, Georgopoulos EF, Keller T. Comparison of genetic programming with conventional methods for fatigue life modeling of FRP composite materials. Int J Fatigue 2008;30:1634–45. doi:10.1016/j.ijfatigue.2007.11.007.

[34] Sakin R, Ay I. Statistical analysis of bending fatigue life data using Weibull distribution in glass-fiber reinforced polyester composites. Mater Des 2008;29:1170–81.

[35] Bedi R, Chandra R. Fatigue-life distributions and failure probability for glass-fiber reinforced polymeric composites. Compos Sci Technol 2009;69:1381–7.

[36] Barbosa JF, Freire Junior RCS, Correia JAFO, De Jesus AMP, Calçada RAB. Analysis of the fatigue life estimators of the materials using small samples. J Strain Anal Eng Des 2018;53:699–710. doi:10.1177/0309324718782245.

[37] Cicero S, García T, Álvarez JA, Martín-Meizoso A, Aldazabal J, Bannister A, et al. Definition and validation of Eurocode 3 FAT classes for structural steels containing oxy-fuel, plasma and laser cut holes. Int J Fatigue 2016;87:50–8. doi:10.1016/J.IJFATIGUE.2016.01.012.

[38] Meneghetti LC, Regina Garcez M, Teixeira RM, Carlos L, Da P, Filho S. Fatigue life prediction of RC beams strengthened with FRP through MLE method. n.d.

[39] Goedel F, Mezzomo GP, Pravia ZMC. Fatigue lifespan of a fillet welded joint-Hybrid approach to obtain the SN curve with a reduced number of tests. Lat Am J Solids Struct 2018;15.

[40] Maluf O, Milan MT, Spinelli D, Martínez ME. Residual analysis applied to S-N data of a surface rolled cast iron. Mater Res 2005;8:251–5. doi:10.1590/S1516-14392005000300005.

[41] Sutherland VJ, Energy W. THE DEVELOPMENT OF CONFIDENCE LIMITS FOR FATIGUE STRENGTH DATA * †. ASME/AIAA; 2000.

[42] Kepka M. Using design s-n curves and design stress spectra for probabilistic fatigue life assessment of vehicle components. 6th Int. Conf. Integrity-Reliability-Failure , Lisbon: 2018, p. 22–6.

[43] Correia J, De Jesus AMP, Calçada R, Pedrosa B, Rebelo C, da Silva LS, et al. Statistical analysis of fatigue crack propagation data of materials from ancient portuguese metallic bridges. Frat Ed Integrità Strutt 2017;11:136–46.

[44] Raposo P, Correia J, De Jesus AMP, Calçada RAB, Lesiuk G, Hebdon M, et al. Probabilistic fatigue SN curves derivation for notched components. Frat Ed Integrita Strutt 11 2017.

[45] Castillo E, Fernández-Canteli A. A unified statistical methodology for modeling fatigue damage. Springer Science & Business Media; 2009.

[46] Correia JAFO, Lesiuk G, De Jesus AMP, Calvente M. Recent developments on experimental techniques, fracture mechanics and fatigue approaches. J Strain Anal Eng Des 2018;53:545. doi:10.1177/0309324718814097.

[47] Correia, J.A.F.O., De Jesus, A.M.P., Pariente, I.F., Belzunce J& F-C. Mechanical fatigue of metals. Eng Fract Mech 2017;185:1–300.

[48] Schijve J. Fatigue of structures and materials. 2009. doi:10.1007/978-1-4020-6808-9.

[49] Correia JAFO, Raposo P, Muniz-Calvente M, Blasón S, Lesiuk G, De Jesus AMP,

et al. A generalization of the fatigue Kohout-Věchet model for several fatigue damage parameters. Eng Fract Mech 2017;185:284–300. doi:10.1016/j.engfracmech.2017.06.009.

[50] Zhao YX, Yang B, Feng MF, Wang H. Probabilistic fatigue S--N curves including the super-long life regime of a railway axle steel. Int J Fatigue 2009;31:1550–8.

[51] Mayorga LG, Sire S, Correia JAFO, De Jesus AMP, Rebelo C, Fernández-Canteli A, et al. Statistical evaluation of fatigue strength of double shear riveted connections and crack growth rates of materials from old bridges. Eng Fract Mech 2017;185:241–57.

[52] Łukaszewicz K. Fatigue Life of Construction Elements in a Complex Stress State. Adv Mech Eng 2014;6:585262. doi:10.1155/2014/585262.

[53] Su C, Yu S, Wang Z, Tayyab Z. A time-dependent probabilistic fatigue analysis method considering stochastic loadings and strength degradation. Adv Mech Eng 2018;10:168781401878556. doi:10.1177/1687814018785560.

[54] Kulkarni PA, Hu W, Dhoble AS, Padole PM. Statistical wind prediction and fatigue analysis for horizontal-axis wind turbine composite material blade under dynamic loads. Adv Mech Eng 2017;9:168781401772408. doi:10.1177/1687814017724088.

[55] Kang D-H, Jang C, Park Y-S, Han S-Y, Kim JH. Fatigue Reliability Assessment of Steel Member Using Probabilistic Stress-Life Method. Adv Mech Eng 2012;4:649215. doi:10.1155/2012/649215.

[56] Basquin OH. The exponential law of endurance tests. Proc Am Soc Test Mater, vol. 10, 1910, p. 625–30.

[57] Stromeyer CE. The determination of fatigue limits under alternating stress conditions. Proc R Soc London Ser A, Contain Pap a Math Phys Character 1914;90:411–25.

[58] Bathias C. There is no infinite fatigue life in metallic materials. Fatigue Fract Eng Mater Struct 1999;22:559–65. doi:10.1046/j.1460-2695.1999.00183.x.

[59] Palmgren AG. Die Lebensdauer von Kugellagern (Life Length of Roller Bearings or Durability of Ball Bearings). Zeitschrift Des Vereines Dtsch Ingenieure 1924;14:339–41.

[60] Weibull W. The statistical aspect of fatigue failure and its consequences. Fatigue Fract Met Massachusetts Inst Technol John Wiley Sons New York, NY, USA 1952:182–96.

[61] Kohout J, Vechet S. A new function for fatigue curves characterization and its multiple merits. Int J Fatigue 2001;23:175–83.

[62] Mu PG, Wan XP, Zhao MY. A New S-N Curve Model of Fiber Reinforced Plastic Composite. Key Eng Mater 2011;462–463:484–8.

[63] Barbosa JF, Montenegro PA, Lesiuk G. A comparison between S-N Logistic and Kohout-Věchet formulations applied to the fatigue data of old metallic bridges materials 2019;48:400–10. doi:10.3221/IGF-ESIS.48.38.

[64] Mandell JF, Samborsky DD. DOE/MSU composite material fatigue database: test methods, materials, and analysis. 1997.

[65] Fernández-Canteli A, Castillo E, López-Aenlle M, Seitl S. Using statistical compatibility to derive advanced probabilistic fatigue models. Procedia Eng 2010;2:1131–40.

[66] Fernández-Canteli A, Przybilla C, Nogal M, Aenlle ML, Castillo E. ProFatigue: A software program for probabilistic assessment of experimental fatigue data sets. Procedia Eng 2014;74:236–41.

[67] Castillo E, Fernández-Canteli A. A general regression model for lifetime evaluation and prediction. Int J Fract 2001;107:117–37. doi:10.1023/A:1007624803955.

[68] Castillo E, Fernández-Canteli A, Ruiz-Ripoll ML. A general model for fatigue damage due to any stress history. Int J Fatigue 2008;30:150–64. doi:10.1016/J.IJFATIGUE.2007.02.011.

[69] Pyttel B, Canteli AF, Ripoll AA. Comparison of different statistical models for description of fatigue including very high cycle fatigue. Int J Fatigue 2016;93:435–42.

[70] Fernández-Canteli A, Castillo E, Argüelles A, Fernández P, Canales M. Checking the fatigue limit from thermographic techniques by means of a probabilistic model of the epsilon–N field. Int J Fatigue 2012;39:109–15.

[71] De Jesus AMP, Pinto H, Fernández-Canteli A, Castillo E, Correia JAFO. Fatigue assessment of a riveted shear splice based on a probabilistic model. Int J Fatigue 2010;32:453–62. doi:10.1016/J.IJFATIGUE.2009.09.004.

[72] de Oliveira Correia JAF, Jesus A, Blasón S, Calvente M, Fernández-Canteli A. Probabilistic non-linear cumulative fatigue damage of the P355NL1 pressure vessel steel. ASME 2016 Press. Vessel. Pip. Conf., 2016, p. V06AT06A034--V06AT06A034.

[73] Correia JAF de O, De Jesus AMP, Fernández-Canteli A, Calçada RAB. Fatigue damage assessment of a riveted connection made of puddle iron from the Fão bridge using the modified probabilistic interpretation technique. Procedia Eng 2015;114:760–7.

[74] Blasón S, Correia J, De Jesus AMP, Calçada RAB, Fernández-Canteli A. A

probabilistic analysis of Miner's law for different loading conditions. Struct Eng Mech 2016;60:71–90.

[75] Fernández-Canteli A, Blasón S, Correia J, De Jesus AMP. A probabilistic interpretation of the Miner number for fatigue life prediction. Frat Ed Integrita Strutt 2014;8:327–39.

[76] Golos K, Ellyin F. Generalization of cumulative damage criterion to multilevel cyclic loading. Theor Appl Fract Mech 1987;7:169–76.

[77] Golos K EF. A total strain energy density theory live damage. J Press Vessel Technol Trans 1988;110:36–41.

[78] Jiang Y, Hertel O, Vormwald M. An experimental evaluation of three critical plane multiaxial fatigue criteria. Int J Fatigue 2007;29:1490–502.

[79] M. Muniz Cavalcante, S Blasón, A. Fernández Canteli, A. de Jesus JC. A probabilistic approach for multiaxial fatigue criteria. Frat Ed Integrità Strutt 2017;39:160–5. doi:10.3221/IGF-ESIS.39.16.

[80] Toasa Caiza PD, Ummenhofer T. A probabilistic Stüssi function for modelling the S-N curves and its application on specimens made of steel S355J2+N. Int J Fatigue 2018. doi:10.1016/j.ijfatigue.2018.07.041.

[81] Castillo E, Galambos J. Lifetime regression models based on a functional equation of physical nature. J Appl Probab 1987;24:160–9.

[82] Castillo E, Hadi AS. Parameter and quantile estimation for the generalized extreme-value distribution. Environmetrics 1994;5:417–32.

[83] Dario P, Caiza T, Ummenhofer T. General probability weighted moments for the three-parameter Weibull Distribution and their application in S – N curves modelling. Int J Fatigue 2011;33:1533–8. doi:10.1016/j.ijfatigue.2011.06.009.

Chapter III

Analysis of the fatigue life estimators of the materials using small samples

Knowledge of the stochastic nature of fatigue life of composite materials can be modelled by the failure time with the Weibull distribution. This task becomes complex when the samples are small and scattered. In this way, it is necessary to know and to improve, robust models of estimation of the parameters of the distribution of Weibull. The aim of this work is to compare the performance of least squares (LS), least squares weighted (WLSE), maximum likelihood (MLE) and momentum method (MOM), and to suggest a method that obtains better performance in life behaviour to fatigue with small samples. Monte Carlo simulations were performed to estimate the distribution parameters with different sample sizes and an application with real fatigue data that compares performance using goodness-of-fit. The results of the simulations showed that the WLSE was able to generate more reliable estimators for fatigue behaviour during its useful life. In this way, it is possible to conclude that small samples make the real representation of life difficult to the material fatigue but using the WLSE method it is possible to obtain more estimates.

3.1 Introduction

The composite materials have a wide applicability in engineering due to their excellent structural performance and weight, considering the specific strength and stiffness. As the use of these materials in structural components increased, it was necessary to study fatigue to ensure that it does not suffer failures before the end of its useful life, because

when subjected to fluctuating or repetitive tensions [1,2], such as when subjected to cyclic stress, rupture is much lower than those subjected to static loads of traction and compression [3,4]. In most applications of fatigue these cyclic loads, cannot be avoided, making necessary to know their behaviour in depth, so that the composite materials can be used efficiently in structural designs. The high dispersion makes it difficult to explain the behaviour of the stochastic nature that composite material present when subjected to fatigue over its useful life[5,6]. In addition, due to the time required to perform a single test, it is difficult to obtain a satisfactory sample number, leaving the task more complex.

Numerous probability distributions such as normal, lognormal, exponential and Weibull are used to explain the failure time. Among these, the Weibull distribution is the most used to estimate the failure times of composite materials under cyclic loading, being flexible and capable of having characteristics of other distributions [7–10]. Confirmed by Lee [11], where the latter performed a goodness-of-fit test and concluded that Weibull has a higher adherence to the experimental data set of carbon fibres. Other researchers [2,12–14] suggest that the behaviour of fatigue data follows a Weibull distribution with two parameters.

In the use the appropriate Weibull probability distribution model, it is necessary to estimate the two parameters of this function, the form and scale parameter. Many methods are available in the literature to estimate these parameters as the method of maximum likelihood, least squares method, method of moments and weighted least squares [15]. However, there has not been an article that shows, in an applied way, which of these methods is most appropriate to analyse for a database with few samples. The limitation of sample size and the dispersion of cycle numbers to failure when working with composite materials makes necessary to choose robust models capable of estimating the shape and scale parameters of the Weibull distribution.

Many studies are advancing in improving the performance of Weibull estimation techniques of two parameters, but few studies present comparisons and performance analysis of these estimators with a reduced number of samples. Some papers present studies considering small samples of size 10 and 20 [15,16], but for the reality of the fatigue tests it is common to observe samples of size equal to 5 for a test with constant cyclical load. The maximum likelihood estimator (MLE) is generally preferred by researchers [17–19] because it presents good theoretical properties for large samples ($n > 250$) as cite by Kantar and–Zhang[15,20] cite an example in which the maximum

likelihood estimator of the model's shape parameter Weibull has an addiction when working with small samples. The moment method uses the moments matching, where it equates the sampling moments with the population moments to estimate the parameters of the desired probability distribution. The method is applicable for non-censured samples and requires numeric computation[21]. Besides, generates no-efficient estimators[16]. While the MLE method has been extensively studied in the literature, the LSE method is less discussed and has a good potential. This method uses the regression procedure based on the probability graph to estimate the parameters of the statistical distribution and is used by engineers and professionals for its simplicity of application, graphical representation and applicability in cases of complete and censored data [22–24]. However, all these techniques, mentioned previously, still do not present satisfactory results when have tried to find the shape and scaling parameters of the Weibull distribution. Note from the work of Kalili [25], who analysed different techniques of estimation of fragile materials and concluded that at least 30 samples were necessary for the characterization of this fragile material.

Recent works are developing more robust regression techniques, known as Weighted Least Squares Estimation (WLSE), capable of giving each data point its ideal weight of influence on estimation. The work of Hung [26], proposed to use the WLSE to estimate the shape parameter of the Weibull distribution and its results, by simulation, presented better performance than the techniques already mentioned. Some publications like: [27–29] compare and analyse WLSE performance, but nothing applied with real data and small samples. In the paper by Zhang [9], he proposes a WLSE model with adjusted weights that considerably improves the performance, from the estimate, to a small set of data.

In this work, it is proposed a comparative research of the performance of the LSE, WLSE, MLE and MOM estimation techniques of the shape parameter of the Weibull distribution for a small data set. In the performance evaluation of these estimators can be used the Monte Carlo Simulation. In addition, the root-mean-square error (RMSE) and bias for different sample sizes can be obtained. Thus, a comparison between numerical and experimental results using high-cycle fatigue data is made. A good performance of these estimators is verified.

3.2 Two-parameters Weibull distribution

Weibull's distribution of two parameters has a wide applicability to estimate the probability to failure of materials, due to their good flexibility in adjusting to the failure times of the datasets [7,8,30], and its density function is given by **Equation (3.1)**:

$$f(N \mid \alpha, \beta) = \frac{\alpha}{\beta^{\alpha}} N^{(\alpha-1)} \exp\left\{-\left(\frac{N}{\beta}\right)^{\alpha}\right\}, \; to\ \alpha > 0, \; and\ \beta > 0 \tag{3.1}$$

where N represents the number of cycles required to perform the total fracture of the material, β is the scale parameter and α is the shape parameter. Weibull's cumulative probability distribution of two parameters can be expressed by:

$$F(N \mid \alpha, \beta) = 1 - \exp\left\{-\left(\frac{N}{\beta}\right)^{\alpha}\right\} \tag{3.2}$$

Variations in the shape parameter are responsible for giving this versatility in the probability distribution, for example: when the parameter $\alpha = 1$ it reduces to an exponential distribution, and when $\alpha = 2$, the Weibull distribution is Rayleigh. When $\alpha = 3.48$, it becomes a distribution close to normal [10,28].

The estimation of parameters in a model is one of the main steps at the analysis of a distribution, it is known that a good estimator must be "close" in some way to the value of the true unknown parameter, that is, the estimator must be a function of sufficient statistics [31]. The four methods of estimation will be approached in this article: MLE, MOM, LSE and WLSE.

3.2.1 Method of estimation by maximum likelihood

The maximum likelihood method is the most popular estimation method because it is considered a very versatile and reliable method [22]. It is defined by treating the distribution parameters as unknown values and seeks to find the joint density of all observations of a set of data, which are assumed to be independent and identically distributed (*iid)*. Once the likelihood function is defined, its maximum value of the function is found. If the points of the experimental data are highly likely under specific

parameter values, then the product will be the "most likely" result, or the maximum probability.

For a random variable N with distribution $N \sim Weibull(\alpha,\beta)$ and density function given by **Equation (3.1)**. The likelihood function for complete samples of the distribution $N \sim Weibull(\alpha,\beta)$ is given by:

$$L(\alpha,\beta \mid N) = \prod_{i=1}^{n} f\left(N_i \mid \alpha,\beta\right) \tag{3.3}$$

$$= \prod_{i=1}^{n}\left[\frac{\alpha}{\beta^{\alpha}} N_i^{(\alpha-1)} \exp\left\{-\left(\frac{N_i}{\beta}\right)^{\alpha}\right\}\right] \tag{3.4}$$

$$= \left(\frac{\alpha}{\beta^{\alpha}}\right)^{n} \prod_{i=1}^{n}\left[N_i^{(\alpha-1)} \times \exp\left\{-\left(\frac{\sum N_i}{\beta}\right)^{\alpha}\right\}\right] \tag{3.5}$$

Then, the natural *ln* is applied in the likelihood function and obtains the log-likelihood function:

$$\ell\left(\alpha,\beta \mid N\right) = n\left[\ln\left(\alpha\right) - \alpha\ln\left(\beta\right)\right] + \left(\alpha-1\right)\sum_{i=1}^{n}\ln\left(N_i\right) - \sum_{i=1}^{n}\left(\frac{N_i}{\beta}\right)^{\alpha} \tag{3.6}$$

The estimators α and β are obtained by solving the equations resulting from equating the first two partial derivatives $\ell(\alpha,\beta \mid N)$ from zero. By maximizing the logarithmic function by means of interactive numerical methods, it is possible to find the parameter values for the Weibull distribution.

3.2.2 Moment Method

The method of moments is considered one of the oldest estimation methods, it has been used in the literature since the 18th century [31]. This method consists of matching the sampling moments to the population and the result of this operation will produce the estimates of the parameters of the studied distribution. Let $k \geq 1$ be the kth sampling moment of a random sample $N_1, \ldots, N_n$ the estimation of the sample moment μ_k is given by:

$$\mu_k = \frac{1}{n}\sum_{i=1}^{n} N_i^k \tag{3.7}$$

For $N \sim^{iid} Weibull(\alpha,\beta)$ the distribution depends on the parameter $\theta(\alpha, \beta)$, only the first two population moments (M_1, M_2) are required to perform the parameter estimation in the Weibull distribution. These moments are calculated by the following two equations:

$$M_1(t) = \beta\Gamma\left(1+\frac{1}{\alpha}\right) \tag{3,8}$$

$$M_1(t) = \beta\Gamma\left(1+\frac{1}{\alpha}\right) \tag{3.9}$$

Where $\Gamma(.)$ represents the gamma function, $\Gamma(\alpha)=\int_0^\infty x^{\alpha-1}e^{-x}dx$ where $\alpha > 0$ [32]. Equating the fraction of M_2 by the square of M_1, with their respective sampling moments, given by **Equations (3.8)** and **(3.9)**, is given by following relation:

$$\frac{\mu_2}{\mu_1^2} = \frac{\Gamma\left(1+\frac{2}{\alpha}\right)}{\Gamma^2\left(1+\frac{1}{\alpha}\right)} \tag{3.10}$$

The result is a function dependent on a single variable α, and this function corresponds to the coefficient of variation of the sample. In this way, it is possible to find the root of this function using the Newton-Raphson method[33]. The Newton–Raphson method is given by the following form:

$$1\,x_{k+1} = x_k - [F'(x_k)]^{-1}F(x_k), k = 0, 1, \ldots \tag{3.11}$$

for the solution of the nonlinear equation

$$F(x)=0 (F:X \to Y) \tag{3.12}$$

Where, X and Y are Banach spaces, and F' is the Fréchet derivative of F. More details about this method can be found in ref. [33].

3.2.3 Least squares estimation method

The Weibull cumulative probability distribution function can be transformed can be transformed into a linear model through the double application of the logarithm, in **Equation (3.2)**. Obtaining **Equation (3.13)**.

$$\ln[-\ln(1-F(N))] = \beta \ln N - \beta \ln \alpha \tag{3.13}$$

Assigning $X = \ln N$ and $Y = \ln[-\ln(1-F(N))]$, a simplified model is given by

$$Y = \beta X - \beta \ln \alpha \tag{3.14}$$

Then with the linear model it will be possible to estimate the values of α and β through simple linear regression. Estimates of the probability function values accumulated in this study will use Bernard's median rank estimator[8] , which serves to present a discrete cumulative probability value.

$$\hat{F}(N_i) = \frac{i-0.3}{n+0.4} \tag{3.15}$$

where i is the order number of failures and n is the sample size. The purpose of the least squares estimator function (LSE) is:

$$\min SS = \sum_{i=1}^{n} \left[y_i - (\beta x_i - \beta \ln \alpha) \right]^2 \tag{3.16}$$

Taking the partial derivatives of SS relative to α and β respectively and set the resulting expressions equal to zero. The estimated least squares of the parameters α and β are:

$$\hat{\beta} = \frac{r\sum_{i=1}^{r} x_i y_i - \sum_{i=1}^{r} x_i . \sum_{i=1}^{r} y_i}{r\sum_{i=1}^{r} x_i^2 - \left(\sum_{i=1}^{r} x_i \right)^2} \tag{3.17}$$

$$\hat{\alpha} = \exp\left(-\frac{\sum_{i=1}^{r} y_i - \hat{\beta} \sum_{i=1}^{r} x_i}{r\hat{\beta}} \right) \tag{3.18}$$

where the values of x_i are given by the function $x_i = \ln(N_i)$ where N_i represents the number of cycles to failure, and $y_i = \ln\left[-\ln\left(1-\hat{F}_i\right)\right]$ represents in the linear model the accumulated probability of failure, where $\hat{F}_i$ it is estimated by Bernard's median rank estimator (for the complete samples n = r).

3.2.4 Weighted Least Squares Estimation (WLSE)

This estimation model considers for a data set that each element has a specific weight, that is, each element of a given sample will have a greater or lesser contribution in the calculation of probability. The idea of the WLSE is to consider that each observation point, used in the regression analysis, has an influence on each of these points through a w_i weight [9]. The choice of the weights is maximized to improve the estimation of the parameters. The objective function of the WLSE estimator is given by:

$$\min SS' = \sum_{i=1}^{n}\left[y_i - \left(\beta x_i - \beta \ln \alpha\right)\right]^2 \tag{3.19}$$

Taking the partial derivatives of SS' relative to α and β respectively, and set the resulting expressions equal to zero. The estimated weighted least squares (WLSE) of the parameters α and β are:

$$\hat{\beta} = \frac{\sum_{i=1}^{n} w_i \cdot \sum_{i=1}^{n} w_i x_i y_i - \sum_{i=1}^{n} w_i x_i \cdot \sum_{i=1}^{n} w_i y_i}{\sum_{i=1}^{n} w_i \cdot \sum_{i=1}^{n} w_i x_i^2 - \left(\sum_{i=1}^{n} w_i x_i\right)^2} \tag{3.20}$$

$$\hat{\alpha} = \exp\left(-\frac{\sum_{i=1}^{n} w_i y_i - \hat{\beta}\sum_{i=1}^{n} w_i x_i}{\hat{\beta}\sum_{i=1}^{n} w_i}\right) \tag{3.21}$$

The values of x_i and y_i are obtained in the same manner as for the LSE model. The values of the weights w are modelled through a polynomial model that realizes a relation between F_i and w_i to carry out the proposed approximation. In the reference Hung W-L[26] the approximations of the weights are given by:

$$w_i = 0.076 + 3.610\hat{F}_i - 6.867\hat{F}_i^{\,2} + 13.54\hat{F}_i^{\,3} - 9.231\hat{F}_i^{\,4} \tag{3.22}$$

where the values of F_i are obtained by **Equation (3.12)** in i is the order number of failures and n is the size of the sample.

3.3 Monte Carlo simulation and comparison of methods

3.3.1 Estimates of α and β values

The exact values of the Weibull distribution parameters α and β originate from their population. In case of choosing N random samples of this population and estimate the parameters will verify that their values are different from the population. But the closer the value of the sample parameters is to the population, the more efficient the estimation will be. To evaluate the performance of the estimation methods for reduced samples, it is necessary to compare the different methods through the Monte Carlo simulation and its performance will be evaluated using bias and root-mean-square error (RMSE).

The Monte Carlo simulation will generate random numbers, which will compose samples with sizes n (3;4;5;6;7;8;9;10;20;30;50;100;150;200}. These samples will be replicated 10,000 times each, with Weibull distribution parameters set at α = 1.5, 2.0 and β = 50,000. The range of values adopted in this simulation for α was based on the document of the Federal Aviation Administration [34], where it was found that the result of many samples had, for the most part, values in this range. The value of β that has a relation with the average number of cycles until the breakup, it was decided to adopt a value of β = 50,000 that will approximate the average value of the number of cycles obtained in the literature [11].

For each combination of n, α and β, R = 10,000 (number of Monte Carlo replicates) will be generated with estimates of $\hat{\alpha}_1, \hat{\alpha}_2, ..., \hat{\alpha}_{10.000}$ and $\hat{\beta}_1, \hat{\beta}_2, ..., \hat{\beta}_{10.000}$, through which we obtain the (E), bias and root mean square error (RMSE) **Equations (3.23)** to **(3.28)**.

$$E\left(\hat{\beta}\right) = \frac{1}{10.000}\sum_{i=1}^{10.000}\hat{\beta}_i \tag{3.23}$$

$$E\left(\hat{\alpha}\right) = \frac{1}{10.000}\sum_{i=1}^{10.000}\hat{\alpha}_i \tag{3.24}$$

$$bias\left(\hat{\beta}\right) = E\left(\hat{\beta}\right) - \beta \tag{3.25}$$

$$bias\left(\hat{\alpha}\right) = E\left(\hat{\alpha}\right) - \alpha \tag{3.26}$$

$$RMSE\left(\hat{\beta}\right) = \left(\frac{1}{10.000} \sum_{i=1}^{10.000} \left(\hat{\beta}_i - \beta\right)^2 \right)^{1/2} \tag{3.27}$$

$$RMSE\left(\hat{\alpha}\right) = \left(\frac{1}{10.000} \sum_{i=1}^{10.000} \left(\hat{\alpha}_i - \alpha\right)^2 \right)^{1/2} \tag{3.28}$$

As previously stated, the Monte Carlo simulation yielded the RMSE and bias results for each sample size n, as shown on **Tables 3.1** and **3.2**, for the shape parameter (α) and the scale parameter (β), respectively.

There was a decrease in bias and RMSE values with increasing sample size for all methods. However, it was possible to identify that bias $(\hat{\alpha})$ usually increases with increasing α values. The bias in the MLE and MOM methods presented a reduction with the increase of n values, but for the LSE and WLSE methods a change pattern was not observed as a function of the n increase. For $n \leq 5$, the Weighted Least Squares Estimation (WLSE) showed better bias performance than all other methods.

Table 3.1 shows the relative performance of the methods in relation to root mean square (RMSE). Using small samples, the MOM and MLE methods performed poorly compared to the other methods, but between them there is a very similar behaviour. It is interesting to note that although the MLE is inferior, when the RMSE is evaluated, as the sample size increases, its performance begins to improve rapidly from the sample $n \geq 100$, surpassing MOM, WLSE and LSE. But for samples smaller than $n \leq 50$ the method the WLSE method was the one that presented better performance.

Analyzing **Table 3.2**, the values of β have a much greater variability, both of RMSE and bias, than the values of α, since the scale parameter is closely linked to the probability of failure of the material. When analysing the results, it was observed that with the increase of α from 1.5 to 2.0 the values of root mean square error tend to decrease in all methods, although with respect to bias it is not possible to affirm such behaviour. It is also possible to observe that the RMSE decreases with increasing n. For bias, it is not possible to verify the same type of behaviour. In the estimation of the parameter β the overall performance of the MLE and MOM was better than the other methods, especially when the bias is observed, but when analysed the RMSE verifies A

very small difference that reaches the maximum of 5% in the performance of the WLSE in relation to the MLE for a $n = 5$, $\alpha = 1.5$.

Table 3.1: Bias and RMSE of the estimated shape parameters of the Weibull distribution

α=1.5 and β=50 000								
Methods	MLE		WLSE		MOM		LSE	
n	RMSE	Bias	RMSE	Bias	RMSE	Bias	RMSE	Bias
3	5,955	1,909	3,061	0,522	3,369	1,678	3,629	0,613
4	2,165	0,979	1,281	0,140	1,951	0,963	1,358	0,205
5	1,347	0,658	0,827	-0,001	1,346	0,669	0,891	0,080
6	1,062	0,503	0,701	-0,038	0,978	0,501	0,746	0,020
7	0,867	0,402	0,590	-0,066	0,829	0,414	0,631	-0,012
8	0,721	0,331	0,506	-0,078	0,698	0,344	0,563	-0,035
9	0,645	0,290	0,460	-0,087	0,645	0,296	0,530	-0,037
10	0,597	0,269	0,440	-0,083	0,575	0,273	0,481	-0,058
20	0,329	0,115	0,288	-0,069	0,327	0,122	0,332	-0,064
50	0,181	0,042	0,178	-0,027	0,187	0,048	0,216	-0,048
100	0,122	0,020	0,130	-0,010	0,129	0,025	0,157	-0,038
200	0,085	0,011	0,091	-0,006	0,089	0,010	0,111	-0,025
α=2.0 and β=50 000								
3	2,625	11,536	4,828	0,820	2,128	4,137	4,147	0,841
4	1,282	2,736	1,927	0,192	1,197	2,503	1,646	0,236
5	0,862	1,824	1,268	0,034	0,869	1,832	1,184	0,095
6	0,659	1,394	0,872	-0,060	0,615	1,281	0,974	0,029
7	0,527	1,125	0,763	-0,085	0,528	1,135	0,845	-0,015
8	0,430	0,944	0,693	-0,095	0,425	0,938	0,754	-0,041
9	0,401	0,878	0,619	-0,114	0,370	0,834	0,698	-0,053
10	0,343	0,775	0,586	-0,110	0,323	0,748	0,642	-0,067
20	0,146	0,432	0,389	-0,083	0,145	0,428	0,442	-0,078
50	0,056	0,243	0,242	-0,035	0,054	0,239	0,295	-0,059
100	0,028	0,164	0,175	-0,016	0,028	0,162	0,209	-0,042
200	0,014	0,113	0,123	-0,009	0,016	0,115	0,149	-0,032

Table 3.2: Bias and RMSE of the estimated scale parameters of the Weibull distribution

α=1.5 and β=50 000								
Methods	MLE		WLSE		MOM		LSE	
n	RMSE	Bias	RMSE	Bias	RMSE	Bias	RMSE	Bias
3	19927	-765	20752	2296	19887	-242	21283	3436
4	17335	-547	17809	1660	17342	25	18532	2953
5	15303	-394	16051	1193	15339	60	16656	2736
6	14225	-91	14346	863	13891	29	15333	2628
7	13102	-183	13227	539	13107	-146	14230	2672
8	12352	-65	12713	559	12341	-116	13185	2134
9	11672	-148	11762	572	11655	-73	12448	2023
10	10981	-60	11195	525	10982	-139	11719	2036
20	7716	56	7922	173	7830	-13	8362	1266
50	4977	-39	4992	95	4928	67	5270	771
100	3505	-46	3514	65	3526	22	3676	514
200	2482	-28	2529	30	2500	-53	2588	270
α=2.0 and β=50 000								
3	14705	-1099	15191	763	14840	-1266	15352	1496
4	13022	-867	13227	601	12927	-838	13651	1963
5	11679	-647	11784	313	11520	-558	12233	1600
6	10611	-546	10927	249	10645	-452	11128	1498
7	9840	-394	10042	37	9789	-409	10318	1362
8	9221	-472	9311	175	9149	-407	9709	1471
9	8715	-322	8847	110	8776	-325	9131	1248
10	8347	-213	8421	234	8283	-339	8659	1264
20	5822	-167	5890	118	5886	-73	6214	928
50	3747	-106	3784	31	3744	-46	3905	575
100	2646	-16	2666	62	2651	-31	2778	338
200	1871	-8	1899	12	1861	-2	1932	221

3.3.2 Estimation of the number of cycles up to the break (lifetime)

The parameters of the Weibull distribution as well as the number of cycles, (N), for each failure probability of the material, was obtained by the inverse Weibull distribution (equation 3.28). The advantage of analyzing the result of the random variable in detriment to the parameters of the equation is that by analyzing separately, each parameter, it is difficult to evaluate which of these influences in a more significant way

the capacity of precision of the estimators. E.g., if the parameter α presents displays a result that is conflicting with that obtained by the β parameter, it is not possible to say which of the two will influence more significantly the final result, since the Weibull equation is nonlinear. On the other hand, analysing the random variable, it proved be that the obtained result approaches a predetermined value (target value) with more confidence in the analysis.

$$N = F^{-1}(p \mid \alpha, \beta) = \beta\left[-\ln(1-p)\right]^{(1/\alpha)} \tag{3.29}$$

In **Equation (3.29)**, α and β are the estimated parameters of the Weibull distribution and p is the probability of failure up to a given number of N cycles. In this work, we will adopt the values of 1% and 5% of the probability of failure as target values of Numbers of cycles. Table 3.3 shows the values for each of the cases previously mentioned using the inverse Weibull distribution (**Equation (3.29)**).

Table 3.3: Values of $\widehat{N}$ at 1% and 5% probability

β=50.000		
p	α=1.5	α=2.0
1%	2329	5013
5%	6903	11324

As previously stated the Monte Carlo simulation will generate 10,000 replicates of the estimates of $\hat{\alpha}_1, \hat{\alpha}_2, ..., \hat{\alpha}_{10.000}$ and $\hat{\beta}_1, \hat{\beta}_2, ..., \hat{\beta}_{10.000}$, according to the equations already mentioned in **section 3.1**. Which will obtain, through **Equation (3.28)**, estimates of the numbers of cycles required until failure, and the estimated value will be given by the average number of cycles $E(\widehat{N})$ in **Equations (3.23)** and **(3.24)**.

$$\hat{N}_i = \hat{\beta}_i\left[-\ln(1-p)\right]^{(1/\hat{\alpha}_i)} \tag{3.30}$$

The values of $E(\widehat{N})$ should converge to the values in **Table 3.3**, the closer the estimated values are to the reference value N, the better the estimator. In the performance evaluation of the $\hat{\alpha}$ and $\hat{\beta}$ estimators in the calculation of the value of N cycles until the rupture, the performance of the estimated values of $\widehat{N}$ in terms of bias and root of the mean square error will be analyzed at the reference values (**Table 3.3**). As shown in **Tables 3.5** and **3.6** for 1% and 5% probability of failure, respectively.

Table 3.4: Bias and RMSE of $\widehat{N}$ at 1% probability

α=1.5 and β=50 000								
Methods	MLE		WLSE		MOM		LSE	
n	RMSE	Bias	RMSE	Bias	RMSE	Bias	RMSE	Bias
3	13042	7530	8384	2720	12984	7442	8842	3040
4	9347	5059	5734	1373	9258	5057	6196	1758
5	7253	3745	4266	690	7061	3763	4790	1145
6	6090	3043	3634	418	5712	2977	4044	785
7	5045	2442	3093	215	4930	2490	3471	579
8	4384	2077	2737	111	4228	2102	3099	391
9	3976	1822	2448	12	3876	1828	2874	341
10	3661	1693	2331	-1	3510	1688	2559	199
20	1977	748	1474	-132	1954	774	1664	-34
50	1027	273	931	-48	1057	310	1047	-105
100	670	127	684	-5	710	160	756	-108
200	462	67	479	-9	484	66	537	-83
α=2.0 and β=50 000								
3	14004	8300	9490	2653	13747	8009	9760	2933
4	10582	5874	6952	1043	10071	5428	7103	1434
5	8475	4422	5629	403	8489	4374	5991	874
6	7203	3585	4796	-3	6904	3397	5167	535
7	6221	2975	4350	-158	6273	2992	4713	312
8	5497	2498	3954	-239	5399	2466	4271	136
9	5188	2364	3562	-389	4949	2194	3918	38
10	4719	2071	3403	-373	4536	1939	3757	-21
20	2760	927	2363	-334	2742	927	2584	-232
50	1582	360	1522	-142	1554	351	1739	-229
100	1064	183	1107	-57	1057	182	1237	-184
200	737	93	787	-33	745	106	886	-152

Tables 3.4 and 3.5 shows that the MLE and MOM method decrease their bias values by increasing the sample size n, but for the WLSE and LSE methods this cannot be stated. However, bias values of the WLSE and LSE methods are much smaller than MLE and MOM, taking as an example the comparison between MLE and WLSE, for $\alpha = 2.0$, $p = 1\%$ and $n = 3$ the difference in terms of bias between them to be greater than 5,600 cycles, which is 212% greater the bias of the MLE in relation to the WLSE. This shows that the number of cycles estimated by the WLSE has a rapid convergence to the expected values when compared to the other methods.

Table 3.5: Bias and RMSE of $\widehat{N}$ 5% probability

α=1.5 and β=50 000								
Methods	MLE		WLSE		MOM		LSE	
n	RMSE	Bias	RMSE	Bias	RMSE	Bias	RMSE	Bias
3	15587	8908	10778	2509	15515	8978	11249	2978
4	11994	6327	8135	984	11898	6478	8696	1628
5	9790	4866	6650	183	9565	5026	7250	952
6	8579	4081	5909	-129	8154	4095	6401	513
7	7366	3332	5301	-353	7242	3475	5747	291
8	6650	2887	4891	-434	6467	2985	5276	44
9	6121	2555	4488	-525	5986	2608	4988	15
10	5734	2411	4304	-514	5570	2444	4609	-179
20	3476	1123	2966	-502	3454	1173	3271	-356
50	1983	418	1891	-189	2033	488	2124	-320
100	1337	193	1388	-62	1412	254	1538	-265
200	939	103	982	-43	983	99	1085	-188
α=2.0 and β=50 000								
3	15062	8459	11227	1715	14790	8165	11444	2125
4	12058	6208	9008	110	11456	5749	9148	729
5	10057	4795	7708	-490	9973	4752	8074	197
6	8801	3942	6917	-869	8514	3771	7221	-93
7	7803	3319	6406	-983	7843	3354	6744	-308
8	7065	2799	5923	-992	6940	2783	6201	-447
9	6707	2697	5448	-1122	6465	2506	5816	-526
10	6236	2378	5212	-1039	6019	2216	5638	-561
20	3946	1085	3701	-727	3926	1097	4025	-608
50	2392	424	2395	-305	2353	419	2710	-446
100	1644	222	1727	-130	1636	220	1916	-320
200	1152	113	1233	-74	1162	132	1363	-244

The WLSE presented better performance in the RMSE values for samples of $n \leq 50$ for a $p = 1\%$, and for $p = 5\%$ the WLSE performed better with $n \leq 20$. Thus, performing the interpretation of all these results It was found that WLSE presented the best overall performance for estimation of Weibull distribution parameters with small sample size.

Analysing the dispersion of the data obtained by the Monte Carlo method to 1% probability of failure (**Figure 3.1**) using $\alpha = 1.5$ and $\beta = 50{,}000$, for the four estimation methods with 2.5%, 50% and 97.5% 95% of the data, it was noticed that there is a

tendency of the curves, for all the evaluated methods, to converge to the reference value ($N = 2{,}329$ cycles).

By the methods analysed, only the LSE and WLSE have an average result (50% curve) close to the target value for small samples for other methods (MLE and MOM), this only occurs when the sample has at least 8 values.

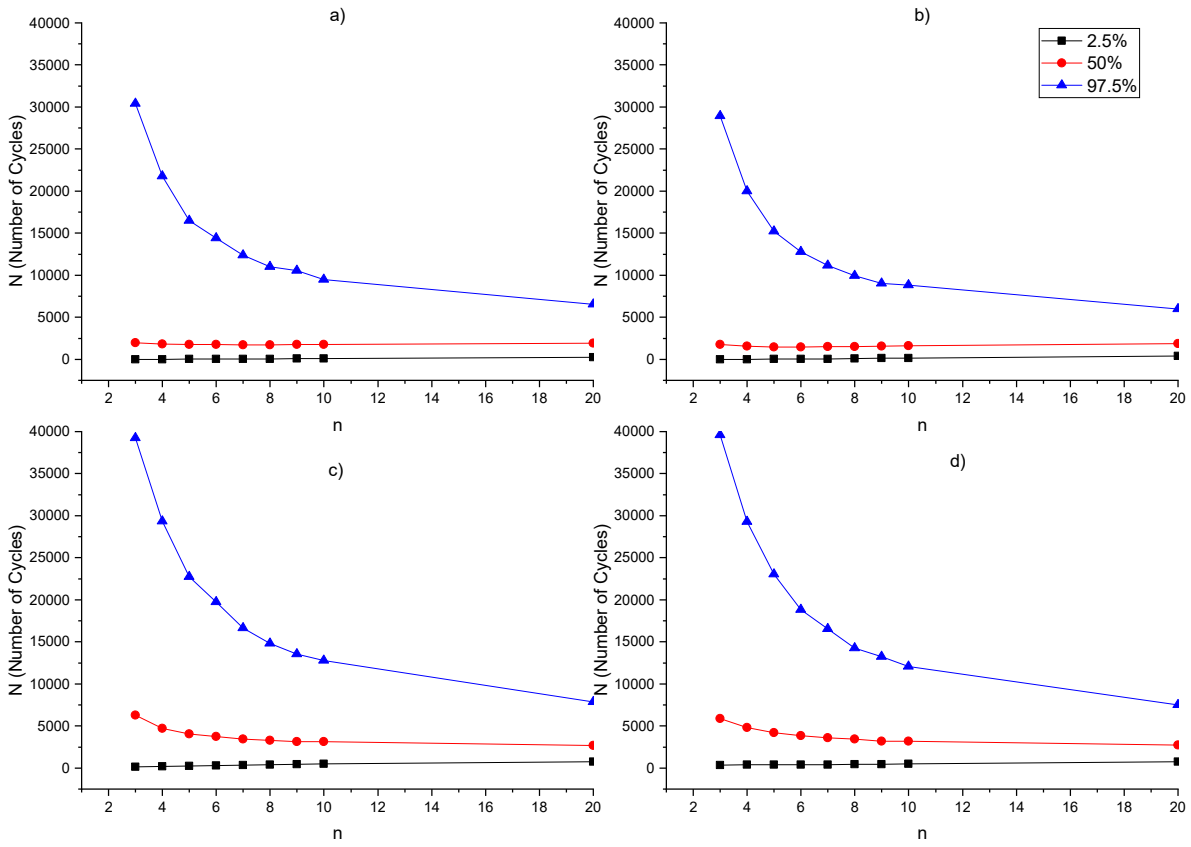

Figure 3.1: Comparison for $p = 1\%$ a) LSE, b) WLSE, c) MLE and d) MOM

In addition, the 97.5% percentile curve shows that the WLSE method produces the best results, because for all values of n this method produces the smallest dispersions. From the results presented, the best values obtained in the dispersion with a sample greater than 10 have a small contribution in the final result. In order to compare the performance difference between the methods, the logarithm was applied in the data of the percentile curve to 97.5% and its performance was compared in percentage terms of its difference in relation to the results obtained for $n = 200$ (The logarithmic value was used because the values obtained in number of cycles were high). With this, it was possible to compare the methods and verify that the MLE methods needed to use 8 samples to obtain a

similar estimate to the WLSE with 5 samples (with a percentage difference verifying that for the estimation of the WLSE for an $n = 5$ the MLE method We have to perform a sampling of $n = 8$ to have a similar result. When we compare the performance between LSE and WLSE it is verified that the LSE needs at least one more sample to obtain the same performance of the WLSE. In this context, WLSE method is able to provide more accurate and more economical estimates, because with a smaller number of samples it is possible to obtain better performance than the other methods.

3.4 Application to the Experimental Fatigue-Life Data

In the previous items, an analysis was performed of the ability of the estimators to obtain the parameters of the Weibull distribution by the Monte Carlo method. However, the experimental data were not used in analysis. In this item, a set of experimental data will be used, based on results of the work of Lee [11] using the 982[a] epoxy matrix composite reinforced with 16-layer HTA fiberite carbon fibre and with unidirectional fibre loaded with a stress amplitude of 1.6 GPa (73% of the tensile strength) and with a fatigue ratio of 0.1. The reason for choosing this data is that it has a large amount of experimental data (sample size 50), that helps in comparisons of goodness-of-fit tests. This analysis of the performance of the estimation methods with the fatigue data holds the following steps:

Step 1 - Removal of random samples from the data set: From the data set size 50 experimental values of material HTA/982A. Random samples of size 3, 4 and 5 of the fatigue life data of the HTA/982A composite will be taken so that the different estimation methods generate estimates of the real data with small samples. It is generated 10,000 samples of sizes n=3, n=4 e n=5, simple random sampling is used without replacement of the populations of $C_{50,3}$, $C_{50,4}$ and $C_{50,5}$.

Step 2 - Estimates of the α and β parameters of the Weibull distribution: Through the **Equations 3.23** and **3.24** the estimates of α and β of the methods are known: MLE, WLSE, MOM and LSE. Making possible the comparison of the estimates between the methods and sample size.

Step 3 - Graphical analysis of the Weibull probability paper (WPP) and cumulated distribution (CDF): In this step, a graphical analysis will be carried out to

observe the level of adjustment of the probability distribution functions estimated from step 2 to the data set of the fatigue test. Comparing the distributions generated by the MLE, WLSE, MOM and LSE methods with the experimental values verifying which of these methods has the highest level of adherence to the data set.

Step 4 - Evaluation of the Weibull distribution adherence to the experimental data using Goodness-off-fit statistics**:** Using three different goodness-of-fit statistics tests, the Kolmogorov-Smirnov, Cramer-von Mises and Anderson-Darling presented in **Table 3.6** will measure the distance between the obtained parametric distribution and the empirical distribution vivificating their level of adjustment to experimental data [35].

Table 3.6: Goodness-of-fit statistics as defined by D'Agostinho and Stephens [35].

Statistic	General formula	Computational formula
Kolmogorov-Smirnov (KS)	$\sup \lvert F_n(x) - F(x) \rvert$	$\max(D^+, D^-)$ with $D^+ = \max_{i=1,\ldots,n} \left(\frac{i}{n} - F_i\right)$ $D^- = \max_{i=1,\ldots,n} \left(F_i - \frac{i-1}{n}\right)$
Cramer-von Mises (CvM)	$n \int_{-\infty}^{\infty} (F_n(x) - F(x))^2 dx$	$\frac{1}{12n} + \sum_{i=1}^{n} \left(F_i - \frac{2i-1}{2n}\right)^2$
Anderson-Darling (AD)	$n \int_{-\infty}^{\infty} \frac{(F_n(x) - F(x))^2}{F(x)(1-F(x))} dx$	$-n - \frac{1}{n} \sum_{i=1}^{n} (2i-1) \log(F_i(1 - F_{n+1-i}))$

where $F_i \triangleq F(x_i)$

3.4.1 Application to Fatigue Data Set

When performing the procedures of **steps 1** and **2**, the values of the Weibull distribution parameters estimated by the MLE, WLSE, MOM and LSE methods were obtained on **Table 3.7**.

Table 3.7: Weibull distribution parameters estimated by each method

n	*3*		*4*		*5*	
Method	α	β	α	β	α	β
MLE	2,712	45600	2,354	45663	2,141	45834
WLSE	1,791	48236	1,592	47614	1,483	47358
MOM	2,720	46072	2,379	46104	2,176	46250
LSE	1,830	49385	1,639	49181	1,527	49111

At this stage it is not possible to say which of the Weibull distributions generated by the parameters in **Table 3.7** will have a better fit to the fatigue dataset, but it will be possible to draw these distributions on a graph and compare them.

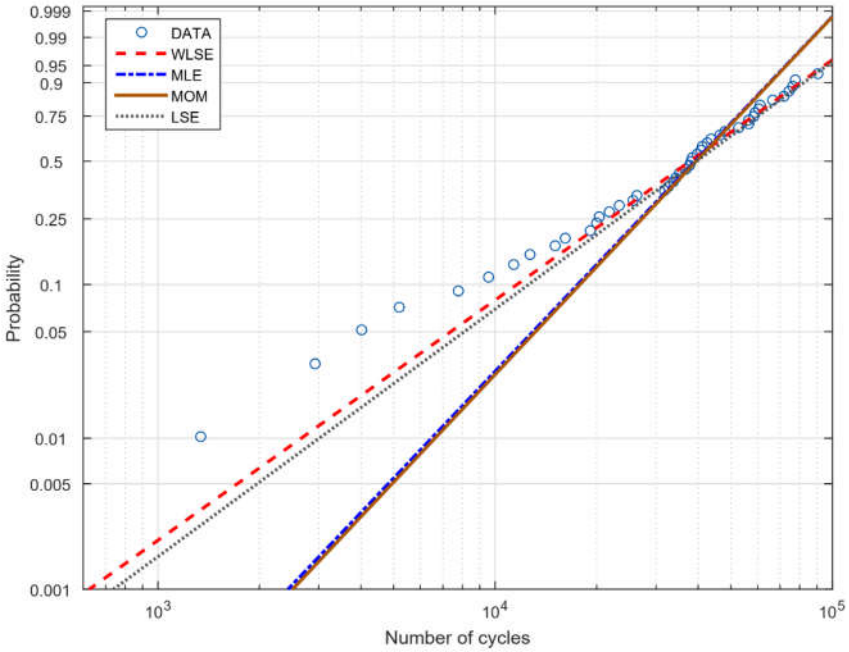

Figure 3.2: Comparison of the cumulative Weibull distribution function for n=4

Analysing **Figure 3.2**, it can be verified that the WLSE method has a higher level of adhesion, and the distribution line estimated by WLSE is closer to the data. The MLE and MOM estimation methods are well separated for data below 10^4 Cycles. This shows that these parameters are not well adjusted in the distribution tails. Another way of visualizing these results is shown in **Figure 3.3**, where it presents the estimated distribution using only 4 samples.

From **Figure 3.3**, it can be see that the moment and maximum likelihood methods were not able to obtain a good fit in the tails of the Weibull cumulative distribution. However, the WLSE and LSE methods were more adjusted to the data set, and the WLSE method was slightly more adhered to the dataset than the LSE. In order to quantitatively measure the results presented in **Figures 3.2** and **3.3**, the values obtained by goodness-of-fit statistics for the four analysed methods were presented in **Table 3.8** and by their results it was noticed that the WLSE method had the best And the MLE and MOM methods should not be used for a small amount of sample data because, as shown in the

Anderson-Darling statistic, the results show a low adjustment This occurred due to the weight given by this method on distribution tails.

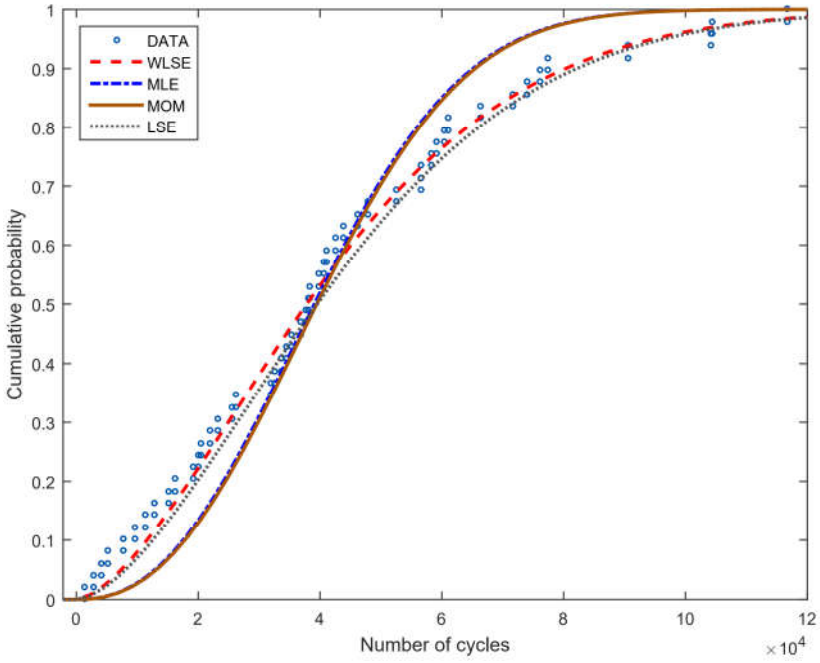

Figure 3.3: Comparison of the cumulative Weibull distribution function

3.5 Conclusion

In this paper, it was possible to compare and suggest a method of estimating the Weibull distribution parameters to represent the fatigue life behaviour of composite materials when they have small size samples. For fatigue tests it is common to have samples smaller than or equal to 5, in this case the WLSE method presented superior performance in estimating the shape parameter under the aspect of centrality and dispersion of the estimator. However, in the analysis of the probabilities of failure at 1% and 5% of useful life, it was observed that the WLSE and LSE methods have a rapid convergence in terms of bias, although in terms of RMSE the WLSE was superior to all other methods, showing a more reliable estimation. This could be confirmed in the graphical analysis, WPP and CDF of Weibull, that the WLSE obtained superior performance. Confirming the graphical analysis quantitatively it was possible to verify that the WLSE also obtained better performance in Goodness-of-fit statistics for size 3, 4 and 5 samples when compared with the experimental data.

In this way, it is concluded that small samples can give a distorted view of the fatigue life behaviour of materials, with aims to minimize the errors and to improve reliability in the estimation of the two-parameters Weibull distribution. Additionally, it is recommended the using of the weighted least squares method in experimental results from high-cycle fatigue tests for composites materials.

3.6 References

[1] Wicaksono S, Chai GB. A review of advances in fatigue and life prediction of fiber-reinforced composites. Proc Inst Mech Eng Part L J Mater Des Appl 2013;227:179–95. doi:10.1177/1464420712458201.

[2] Castillo E, Fernández-Canteli A. A unified statistical methodology for modeling fatigue damage. Springer Science & Business Media; 2009.

[3] D'Amore A, Giorgio M, Grassia L. Modeling the residual strength of carbon fiber reinforced composites subjected to cyclic loading. Int J Fatigue 2015;78:31–7.

[4] Makkar U, Rana M, Singh A. Analysis of fatigue behavior of glass/carbon fiber epoxy composite. Nternational J Res Eng Technol 2015;4:211–6.

[5] Zhu SP, Liu Q, Zhou J, Yu ZY. Fatigue reliability assessment of turbine discs under multi-source uncertainties. Fatigue Fract Eng Mater Struct 2018:1–15. doi:10.1111/ffe.12772.

[6] Zhu SP, Foletti S, Beretta S. Probabilistic framework for multiaxial LCF assessment under material variability. Int J Fatigue 2017;103:371–85. doi:10.1016/j.ijfatigue.2017.06.019.

[7] Sakin R, Ay I. Statistical analysis of bending fatigue life data using Weibull distribution in glass-fiber reinforced polyester composites. Mater Des 2008;29:1170–81.

[8] Freire Júnior RCS, Belísio AS. Probabilistic S-N curves using exponential and power laws equations. Compos Part B Eng 2014;56:582–90. doi:10.1016/j.compositesb.2013.08.036.

[9] Zhang LF, Xie M, Tang LC. On Weighted Least Squares Estimation for the Parameters of Weibull Distribution. Recent Adv. Reliab. Qual. Des., London: Springer London; 2008, p. 57–84. doi:10.1007/978-1-84800-113-8_3.

[10] Nixon-Pearson OJ, Hallett SR. An experimental investigation into quasi-static and

fatigue damage development in bolted-hole specimens. Compos Part B Eng 2015;77:462–73.

[11] Lee J, Harris B, Almond DP, Hammett F. Fibre composite fatigue-life determination. Compos Part A Appl Sci Manuf 1997;28:5–15. doi:10.1016/S1359-835X(96)00088-7.

[12] Castillo E, López-Aenlle M, Ramos A, Fernández-Canteli A, Kieselbach R, Esslinger V. Specimen length effect on parameter estimation in modelling fatigue strength by Weibull distribution. Int J Fatigue 2006;28:1047–58. doi:10.1016/j.ijfatigue.2005.11.006.

[13] Vassilopoulos AP, Georgopoulos EF, Keller T. Comparison of genetic programming with conventional methods for fatigue life modeling of FRP composite materials. Int J Fatigue 2008;30:1634–45.

[14] Bedi R, Chandra R. Fatigue-life distributions and failure probability for glass-fiber reinforced polymeric composites. Compos Sci Technol 2009;69:1381–7.

[15] Kantar YM, Şenoğlu B. A comparative study for the location and scale parameters of the Weibull distribution with given shape parameter. Comput Geosci 2008;34:1900–9.

[16] Teimouri M, Hoseini SM, Nadarajah S. Comparison of estimation methods for the Weibull distribution. Statistics (Ber) 2013;47:93–109.

[17] Correia J, Apetre N, Arcari A, De Jesus A, Muñiz-Calvente M, Calçada R, et al. Generalized probabilistic model allowing for various fatigue damage variables. Int J Fatigue 2017;100:187–94.

[18] De Jesus AMP, Pinto H, Fernández-Canteli A, Castillo E, Correia JAFO. Fatigue assessment of a riveted shear splice based on a probabilistic model. Int J Fatigue 2010;32:453–62.

[19] Mayorga LG, Sire S, Correia JAFO, De Jesus AMP, Rebelo C, Fernández-Canteli A, et al. Statistical evaluation of fatigue strength of double shear riveted connections and crack growth rates of materials from old bridges. Eng Fract Mech 2017;185:241–57.

[20] Zhang LF, Xie M, Tang LC. A study of two estimation approaches for parameters of Weibull distribution based on WPP. Reliab Eng Syst Saf 2007;92:360–8.

[21] Rinne H. The Weibull distribution: a handbook. Chapman and Hall/CRC; 2008.

[22] Mert Kantar Y. Estimating Variances in Weighted Least-Squares Estimation of Distributional Parameters. Math Comput Appl 2016;21:7. doi:10.3390/mca21020007.

[23] Zhang L-F, Xie M, Tang L-C. Robust Regression using Probability Plots for

Estimating the Weibull Shape Parameter. Qual Reliab Eng Int 2006;22:905–17. doi:10.1002/qre.778.

[24] Apetre N, Arcari A, Dowling N, Iyyer N, Phan N. Probabilistic model of mean stress effects in strain-life fatigue. Procedia Eng 2015;114:538–45.

[25] Khalili A, Kromp K. Statistical properties of Weibull estimators. J Mater Sci 1991;26:6741–52.

[26] Hung W-L. Weighted least-squares estimation of the shape parameter of the Weibull distribution. Qual Reliab Eng Int 2001;17:467–9. doi:10.1002/qre.423.

[27] Lu HL, Chen CH, Wu JW. A note on weighted least-squares estimation of the shape parameter of the Weibull distribution. Qual Reliab Eng Int 2004;20:579–86. doi:10.1002/qre.570.

[28] Yavuz AA. Estimation of the shape parameter of the Weibull distribution using linear regression methods: Non-censored samples. Qual Reliab Eng Int 2013;29:1207–19. doi:10.1002/qre.1472.

[29] Kantar YM, Ibrahim A, Ilhan U, YEN\.ILMEZ I. Comparison of some estimation methods of the two parameter Weibull distribution for unusual wind speed data cases. Int J Informatics Technol 2016;9:81.

[30] Li Y, Hu C, Yu Y. Interfacial studies of sisal fiber reinforced high density polyethylene (HDPE) composites. Compos Part A Appl Sci Manuf 2008;39:570–8.

[31] Bolfarine H, Sandoval MC. Introdução à inferência estatística. vol. 2. SBM; 2001.

[32] Casella G, Berger RL. Statistical inference. vol. 2. Duxbury Pacific Grove, CA; 2002.

[33] Ben-Israel A. A Newton-Raphson method for the solution of systems of equations. J Math Anal Appl 1966;15:243–52.

[34] Tomblin J, Seneviratne W. Determining the fatigue life of composite aircraft structures using life and load-enhancement factors. Final Report, Air Traffic Organ Washingt DC, USA 2011.

[35] Stephens MA. Tests based on EDF statistics. Goodness-of-Fit Tech 1986;68:97–193.

Chapter IV

A comparison between S-N Logistic and Kohout-Věchet formulations applied to the fatigue data of old metallic bridges materials

A new formulation of a Logistic deterministic S-N curve is applied to fatigue data of metallic materials from ancient Portuguese riveted steel bridges. This formulation is based on a modified logistic relation that uses three parameters to fit the low-cycle- (LCF), finite-life- and high-cycle-fatigue (HCF) regions. This model is compared to the Kohout-Věchet fatigue model, which has a refined adjustment from very low-cycle fatigue (VLCF) to very high-cycle fatigue (VHCF). These models are also compared with other models, such as, power law and fatigue-life curve from the ASTM E739 standard. The modelling performance of the S-N curves was made using the fatigue data considering the stress fatigue damage parameter for the materials from the Eiffel, Luiz I, Fão and Trezói riveted steel bridges. Using a qualitative methodology of graphical adjustment analysis and another quantitative using the mean square error, it was possible to evaluate the performance of the mean S-N curve formulation. The results showed that the formulation of the S-N curve using the Logistic equation applied to the metallic materials from the old bridges resulted in a superior performance when compared with others models under consideration, both in the estimation of fatigue behaviour in the low-cycle fatigue (LCF) region and in the lowest mean square error.

4.1 Introduction

The knowledge about the fatigue life expectancy of materials and structural components in engineering design is of great importance for the determination of load bearing during

operation. Prediction of failure through mathematical and statistical modelling is a complex activity that attempts through an analytical model to consider the effects of cyclic stresses, stress intensity, predominance between traction and compression loading, frequency, number of experimental samples and the effects of manufacturing processes. Therefore, fatigue assessment is a difficult and still attractive challenge that remains in many situations an open problem.

One way to synthesize the number of factors involved in the fatigue life prediction is to reduce the model to the variables that are able to explain cause/effect, i.e. to fit a fatigue test to a stress level σ_i (independent variable) to explain the number of cycles N_i (dependent variable) required until failure. This fatigue model is known as S-N curves or Wöhler's curves, widely used in standards and standardization manuals such as ASTM E-739-10[1], ISO 12107:2012[2], EN 1993-1-9[3], BS5400[4], AASHTO[5], for engineering design of material and structural details. These standards are based on the Basquin equation[6,7] suggested in 1910, aiming at characterizing the fatigue behaviour in the high- (HCF) and low-cycle fatigue (LCF) regions.

Typically, fatigue data for preliminary design are studied in regions of 10^3 to 10^7 cycles. However, depending on the application, there is a need to prioritize estimation in the LCF or HCF regions. For extrapolation of estimates in HCF region, one must observe the adjustment equation and insert more fatigue data for regions of unknown space. For LCF region, the combination between the static strength and low-cycle fatigue data can be used to better fit the model. Concepts of engineering design for low-cycle fatigue regimes have been important to the use of advanced materials in different applications in mechanical designs. Civil engineering structures, railway and roadway bridges, offshore and ground structures, logistic structures, among others, are designed for the HCF regimes. Recently, a series of failures of these structures cannot be explained only with the HCF regime, taking into account the extreme loading conditions to which the structural elements are subject (e.g., earthquakes). Recent studies[8,9] suggest the use of S-N or ε-N curves covering both the LCF and HCF regimes.

The models used to estimate the S-N and ε-N curves, which have a good adjustment capacity in the low-cycle region, will provide greater reliability in estimating the fatigue damage parameters such as Smith-Watson-Topper, Strain, Walker-Like and energy-based criteria, among others. These approaches will allow the fracture mechanics to be able to predict crack onset by fatigue and residual life, more accurately. In addition, S-

N curve with good adjustment in the low-cycle fatigue region allows the generalization of probabilistic fatigue models, and in this way, it is possible to estimate the load limit and reliability of the material or structural component at the beginning of the operation. The use of S-N curves in the fatigue life prediction can be related to fracture mechanics based approaches. Additionally, probabilistic approaches can be implemented to handle the uncertainties associated to the materials or models as observed in the research works [10–13] that have been applied and compared with existing fatigue data from the Portuguese riveted metallic bridges.

With the principle of meeting the most accurate estimates for the low-cycle fatigue regions, ranging from ultimate tensile strength to the high-cycle fatigue region, the Kohout-Věchet S-N curve is currently being proposed. This model has been increasingly used in fatigue life assessment of existing bridge structures[6,14,15]. Another model very similar to Kohout-Věchet relation is the model that was proposed by Mu et al[16], which proposes a multi-slope model capable of adjusting the S-N curve in the three target regions, low-cycle-, finite-life- and high-cycle-fatigue, using a logistic function of three parameters. However, the analysis of Mu's work was limited to testing the model only for the T300/QY8911 carbon/epoxy composite. Knowing that this model has a wide adjustment capacity, in this research it will be applied to represent the fatigue behaviour of metallic materials from the ancient bridges, and in this way verify the performance of the S-N Logistic formulation.

A comparative study of the performance of the S-N adjustment equations, using models such as Kohout-Věchet, Logistic, ASTM and generalized Power law, will be applied to fatigue data from the old Portuguese riveted metallic bridges (Eiffel, Luiz I, Fão and Trezói). By means of a graphical adjustment analysis and the mean quadratic error, it will be possible to find the model that best fits with the experimental data. The results will be presented and discussed for a better recommendation on using the model in predicting fatigue of old bridges.

4.2 Methods used in the modelling of the S-N curves

4.2.1 Power Law

The generalized power law model is a derivation of the power law model of two terms, commonly used for the interpretation of fatigue data of composite and metallic materials.

These models are of direct application[17] and not based on any assumptions, even in limited databases. The estimation of the model parameters is based on the linear regression analysis that can be performed by simple calculations. The generalized power law is given by **Equation 1**:

$$\log(\sigma_{max}) = A - B\log\left(N\right)^{C} \tag{4.1}$$

where σ_{max} is the maximum stress amplitude parameter, N is the number of cycles until the material failure, whereas A, B, and C are the parameters of the fatigue model derived by linear regression analysis, resulting from the adjustment of the equation to the experimental data. The constant C is an adjustment exponent that can smooth the S-N curve in the low-cycle fatigue region.

The S-N curve proposed by ASTM E739 standard[1] is widely used by researchers for their reliable and simple modelling process. This model does not recommend an extrapolation outside the experimental data region. The representation of the model can be done by linearized form (*log-log*) given by **Equation 2**:

$$\log(N) = A + B\log(\sigma_{max}) \tag{4.2}$$

The equations of the power law and ASTM E739 standard have similar structures for estimating the parameters of the curve in the linearized model (log-log); however these models have two relevant differences. The first difference presented by ASTM E739 standard when compared with the Power Law is to consider fatigue stress as a dependent variable, while the power law considers the fatigue stress an independent variable (the number of cycles to failure, N_f, is assumed as dependent variable). The second difference is the presence of a constant C, included in power law, able to smooth the fit in the low-cycle fatigue region.

4.2.2 Logistic Function

The logistic S-N curve model, developed in the research work of Mu [16], uses a logistic function to describe fatigue life behaviour of composite materials, since this function is very similar to the S shape, commonly observed in S-N curves (lin-log). The logistic function is adapted to model the S-N curve and is given by **Equation 4.3:**

$$\sigma_N = \frac{1-c}{(1-a)+ae^{-b(\log N)}} + c \tag{4.3}$$

where a, b and c are the material constants, obtained by nolinear least squares, σ_N is the normalized stress amplitude $\sigma_N = \sigma_{max}/\sigma_{ult}$and N is the number of cycles until failure. σ_{ult} is the ultimate tensile strenght.

4.2.3 Kohout-Věchet Model

The full-amplitude S-N curve, based on the stress-damping parameter proposed by Kohout and Věchet, has been increasingly used in assessing the fatigue life of existing bridge structures[18]. The Kohout and Věchet S-N curve is a model based on geometric technical adjustment of fatigue behaviour, based on stress or other damage linked parameter, which can achieve a good fit to the experimental data. The Kohout-Věchet fatigue model (KV) can estimate the behaviour of the material in low-cycle (LCF) and high-cycle (HCF) regions[6], being able to cover the estimate from the ultimate tensile strength to the permanent fatigue limit. This KV model can be expressed by the following **Equation 4.4**:

$$\sigma_{\max} = a\left[\frac{(N+B)C}{N+C}\right]^b \tag{4.4}$$

where a and b are the similar to Basquin parameters, B is the number of cycles corresponding to the intersection of the tangent line of the finite life region and the horizontal asymptote of the total tensile strength, and C is the number of cycles corresponding to the intersection of the tangent line of the region of the finite life and the horizontal asymptote of the fatigue limit. The details for obtaining the parameters can be obtained in ref. [[6]].

4.3 Normalized stress ranges

The normalized stress ranges were suggested by Taras and Greiner[19] with aims to take into account the mean stress effects. The research work was developed for fatigue experimental results of riveted joints. This approach can be applied for fatigue results

from metallic bridge materials to allow the comparison of experimental fatigue data from distinct mean stresses. The normalized stress ranges can be determined by

$$\Delta\sigma_{norm} = \frac{\Delta\sigma}{f(R)} \tag{4.5}$$

where, $\Delta\sigma_{norm}$ is the normalized stress range, $\Delta\sigma$ is the tested stress range, and $f(R)$ is a normalization function to account for stress ratio effects, defined as a function of the material.

For wrought/puddle iron and mild steel manufactured before 1900, $f(R)$ is defined as:

$$\begin{aligned} f(R) &= \frac{1-R}{1-0.7\cdot R} \Leftarrow -1 \le R \le 0 \\ f(R_\sigma) &= \frac{1-R}{1-0.75\cdot R} \Leftarrow R > 0 \end{aligned} \tag{4.6}$$

For mild steel after 1900, the normalization function to be used is the following:

$$\begin{aligned} f(R) &= \frac{1-R}{1-0.4\cdot R} \Leftarrow -1 \le R \le 0 \\ f(R_\sigma) &= \frac{1-R}{1-0.6\cdot R} \Leftarrow R \end{aligned} \tag{4.7}$$

However, the proposed normalization functions are only valid for high-cycle fatigue regimes, hence, they are not valid for low- and medium-cycle fatigue regimes. In this sense, fatigue design curves based on Goodman[20] , Soderberg[21] and Gerber[22] diagrams become of high importance for the fatigue life evaluation of old metallic bridges using local approaches.

4.4 Comparison of the modelling performance of the S-N curves formulations

A comparison of the modelling performance of the S-N curves was made using the fatigue data of the materials from the ancient Portuguese riveted steel bridges (Eiffel, Luiz I, Fão and Trezói bridges). The performance of the mean fatigue curves was based on two methodologies of analysis. The first analysis the adjustment of the S-N curve is based on direct graphical observation, where the degree of adjustment in the LCF and HCF regions is empirically assessed. The second analysis, quantitative, estimates the quality of the curve adjustment to the experimental fatigue data by means of the mean square errors (MSE). This parameter was calculated for each fatigue model by defining the error as

the difference between the logarithms of the experimental and estimated values for the cyclic stresses, based on following equation:

$$MSE = \frac{1}{n}\sum_{i=1}^{n}\left(\log\left(\sigma_{\exp}\right) - \log\left(\sigma_{est}\right)\right)^2 \tag{4.8}$$

where σ_{exp} and σ_{est} are the experimental cyclic stress and the estimated cyclic stress levels of the S-N curves, respectively, for all models considered in this research. The stress levels correspond to the same number of cycles, *N*, of the experimental data. Therefore the comparison between fatigue models was evaluated qualitatively and quantitatively. Acquisition of each model was examined for its accuracy in modeling, ability to extrapolate and interpolate, number of model parameters, sensitivity to available experimental data, etc.

The MSE normalized calculation related with the adjustment of the presented S-N models to the experimental fatigue data, can be observed in **Table 4.1**. To facilitate the comparison between the S-N curve models, the results of the normalized MSE values were shown in **Table 4.1**. The normalization expression is given by

$$\mathrm{MSE_{NORM}} = \mathrm{MSE}/\mathrm{MSE_{MAX}} \tag{4.9}$$

where MSE_{max} is the largest MSE (**Equation 4.8**) between the Logistic, Kohout-Věchet, Power Law and ASTM E739 models when compared by the bridge model.

Table 4.1: Normalized calculation of the mean squared error of the derived S-N curves.

Material	Normalized mean squared error (MSE)				
	Logistic	Kohout-Věchet	Power Law	ASTM	*n*
Eiffel (R=0)*	0,4946	**0,4943**	0,5138	1	16
Eiffel (R=-1)**	0,6246	0,6741	**0,6214**	1	27
Luiz I (R=-1)**	**0,4312**	0,6450	0,4343	1	16
Fão (R=0)**	0,8618	0,9776	**0,8341**	1	21
Fão (R=-1)**	0,5268	**0,4400**	0,5705	1	14
Trezói (R=-1)**	0,5823	1,0000	**0,3960**	0,8455	10
All bridges(R=-1)***	**0,6682**	0,7312	0,6788	1	66

* Fatigue tests under stress-controlled conditions; ** Fatigue tests under strain-controlled conditions; *** Only bridges R=-1.

The obtained S-N curve based on ASTM E739 standard did not present a satisfactory performance when compared with the other models, such as, Logistic formulation, Kohout-Věchet model and Power law. The fatigue model proposed by generalized Power Law obtained a smaller error in four of the seven fatigue data of the analyzed bridge materials, resulting in a better approximation of the S-N curve to the experimental data set. This method obtained the best estimate considering the MSE value computed for the material from the Trezoi bridge (see **Table 4.2**). The logistic model that uses only three parameters in the equation obtained a lower MSE value when all the experimental fatigue data are analyzed together, considering only the data of the fatigue tests under strain-controlled conditions at R=-1. In the individual analysis of each bridge material it can be observed that the performance of the model was very similar to that of generalized Power Law model. For a set of fatigue experimental data with few data, it is possible to observe that some equations can't obtain such precise estimates. This situation is verified for the material from the Trezói Bridge at R=-1 (fatigue test under strain-controlled conditions) with a sample of 10 specimens, where the Kohout-Věchet model obtained a very high MSE value when compared to Logistic formulation and Power Law. In general, the S-N curve using the Logistic formulation obtained satisfactory performance in terms of MSE values for all samples with size lower than 16.

In the low-cycle fatigue region (LCF), Logistic, Khout-Věchet and Power Law curves achieved better adjustments than the ASTM standard. This can be seen in **Figure 4.1** related with the material from the Eiffel bridge at R=0 (fatigue test under stress-controlled conditions), where these models are able to flatten and smoothen the inflection of the S-N curve in this region. The improvement of the S-N curve in the low-cycle region for the Logistic, Power Law and Kohout-Věchet models is justified by Basquin fatigue exponent included in the models. For the materials from the Eiffel (**Figures 4.1 and 4.2**) and Luiz I bridges (**Figure 4.3**), it is possible to verify the robustness of adjustment of these formulations in the LCF region; in some cases the S-N curve becomes very close to the experimental values.

The improvement of the S-N curve in the low cycle region for Logistic, Power Law and Kohout-Věchet models is justified by the exponent of these equations, responsible for smoothing the rate of degradation in this region.The improvement of the S-N curve in the low cycle region for Logistic, Power Law and Kohout-Věchet models is justified by the exponent of these equations, which is responsible for smoothing the transition of elasto-plastic behavior.

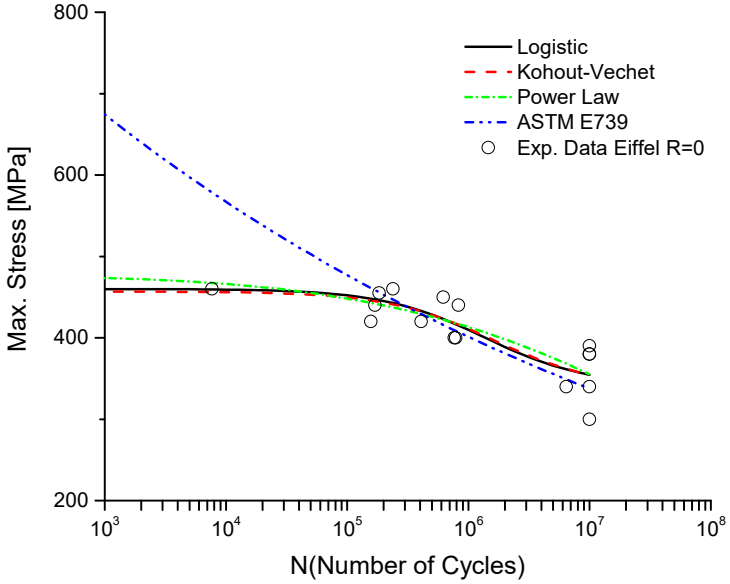

Figure 4.1: Comparison of the S-N curves for the fatigue data of the metallic material from the Eiffel bridge, R=0 (fatigue tests under stress-controlled conditions).

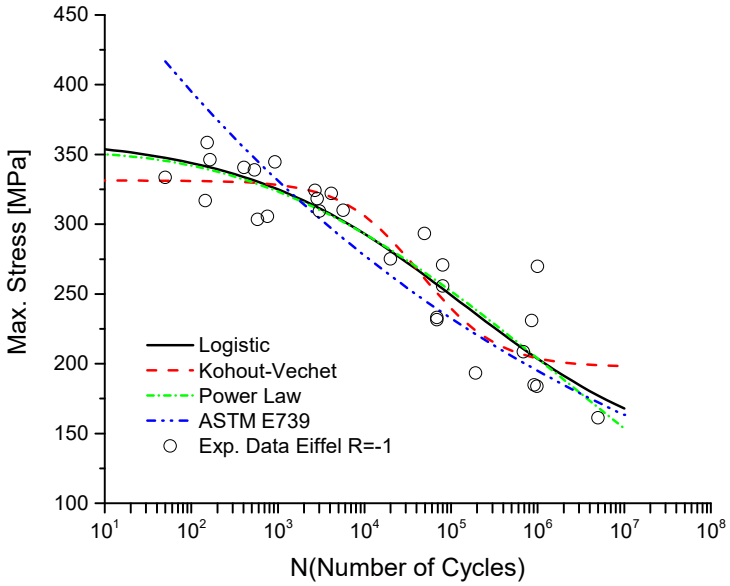

Figure 4.2: Comparison of the S-N curves for the fatigue data of the metallic material from the Eiffel bridge, R=-1 (fatigue tests under strain-controlled conditions).

Figure 4.2 presents the fatigue data of the marerial from the Eiffel bridge tested at R = -1 (fatigue test under strain-controlled conditions), where it can be seen that the S-N curve based on ASTM E739 standard does not achieve a good approximation in the low-

cycle fatigue region (LCF), even with data availability for the region smaller than 10^3 cycles. In this region, the Logistic and Power Law curves performed slightly better than the Kohout-Věchet model. In the high-cycle fatigue region (HCF) the generalized Power Law curve presented a very pronounced degradation rate. The Kohout-Věchet and ASTM models presented a coherent behaviour in the HCF region and are recommended to better indicate the fatigue limit of the material.

As regards the metallic material from Luiz bridge tested at R=-1 (fatigue test under strain-controlled conditions), which can be seen in **Figure 4.3**, the fatigue curves for the Power Law and Logistic model obtained very similar performance. The differences between them becoming more evident only in number of cycles higher than 10^6. In the low-cycle fatigue region, for the Power Law, Logistic and Kohout-Věchet curves a very similar adjustment is observed. A poor performance of the S-N curve obtained from the Kohout-Vechet model for numbers of cycles to failure between 10^5 and 10^6 is verified, improving estimates to values above 10^6. By analyzing the adjustement of the curve of the ASTM standard to the experimental data in the LCF region, it is verified an increasing distances between the experimental data and predictions, and consequently increasing the MSE value, making this model with the largest mean square error.

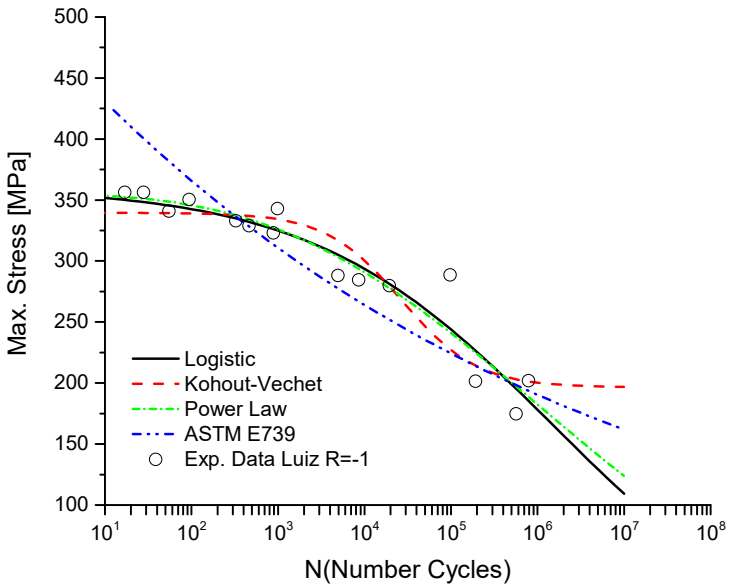

Figure 4.3: Comparison of the S-N curves for the fatigue data of the metallic material from the Luiz I bridge, R=-1 (fatigue test under strain-controlled conditions).

The available fatigue data from the material from the Trezoi Bridge consists on only 10 experimental points. Therefore, the conclusions to be obtained for the LCF and HCF

regions are limited. **Figure 4.4** shows a marked difference in the fit of the analyzed S-N curves in the HCF region. The Power Law formulation obtained the lowest MSE (**Table 4.1**) followed by the Logistic model. These models achieved a good agreement with the experimental fatigue data above 10^6 cycles. The ASTM standard and Kohout-Věchet methods did not provided good estimates in the HCF region. However, it is not possible to assert that the Logistic and Power Law formulations better describe the fatigue life behavior, due to the lack of data mainly in the high-cycle fatigue region. For a more complete analysis of this material, it is necessary to perform further experimental fatigue tests in stress levels between 400MPa and 300MPa.

Regarding the fatigue data from the material of Fão bridge, two strain ratios, R, were explored, namely R=0 and R=-1 (fatigue test under strain-controlled conditions). The S-N Kohout-Věchet formulation and Power Law resulted in the lowest MSE values and very close to each other. The only perceptible difference in a qualitative analysis of the S-N curves at fatigue strain ratio equal to 0, is in the HCF region, where the possible extrapolation to the permanent fatigue limit of the Logistic S-N Curve would present a more adequate behaviour (**Figure 4.5**).

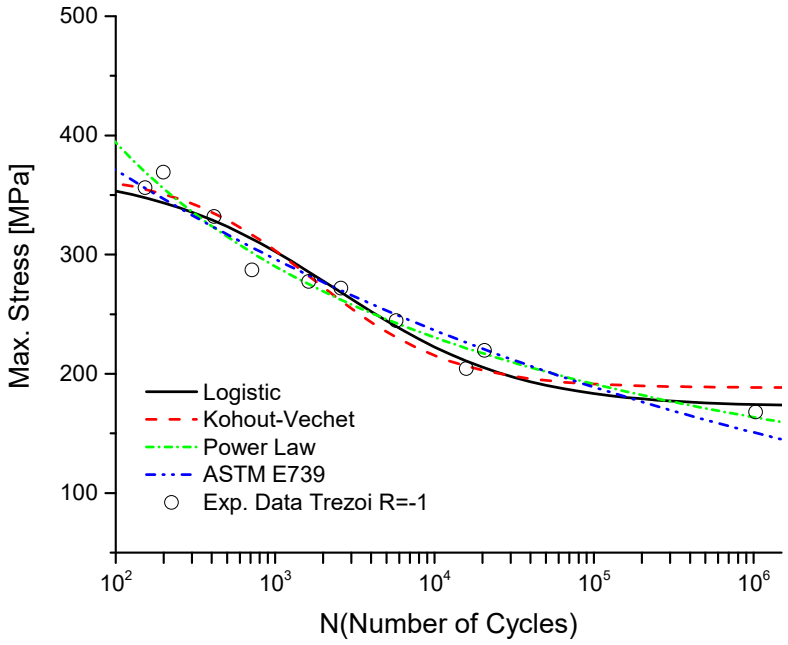

Figure 4.4: Comparison of the S-N curves for the fatigue data of the metallic material from the Trezói bridge, R=-1 (fatigue test under strain-controlled conditions).

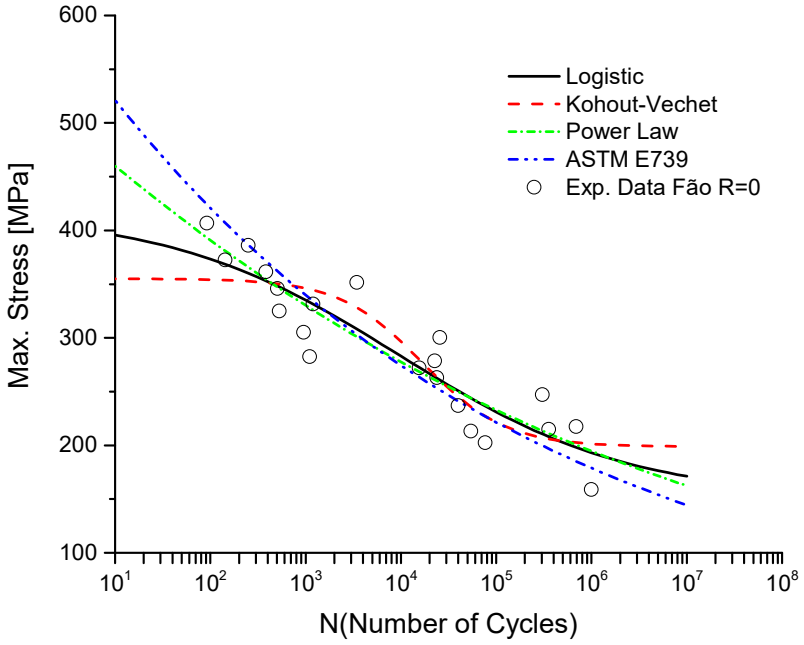

Figure 4.5: Comparison of the S-N curves for the fatigue data of the metallic material from the Fão bridge, R=0 (fatigue test under strain-controlled conditions).

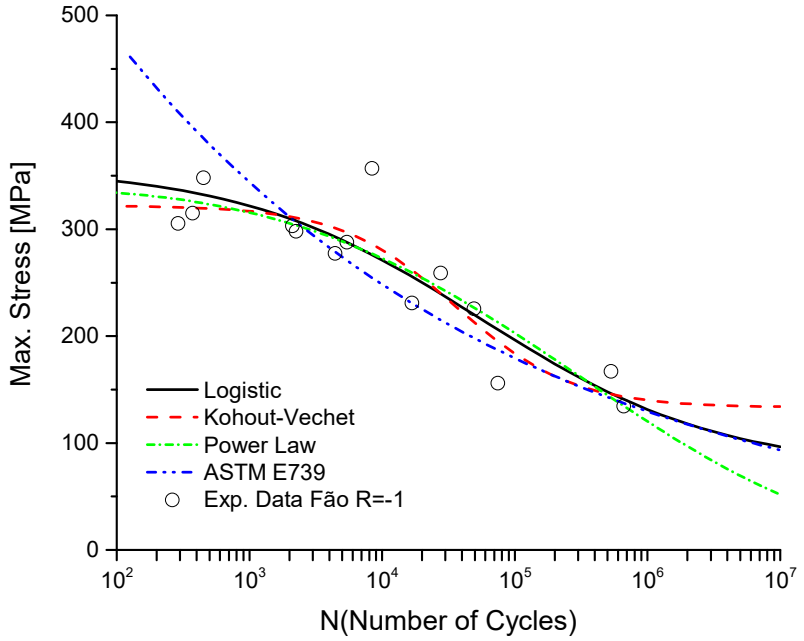

Figure 4.6: Comparison of the S-N curves for the fatigue data of the metallic material from the Fão bridge, R=-1 (fatigue test under strain-controlled conditions).

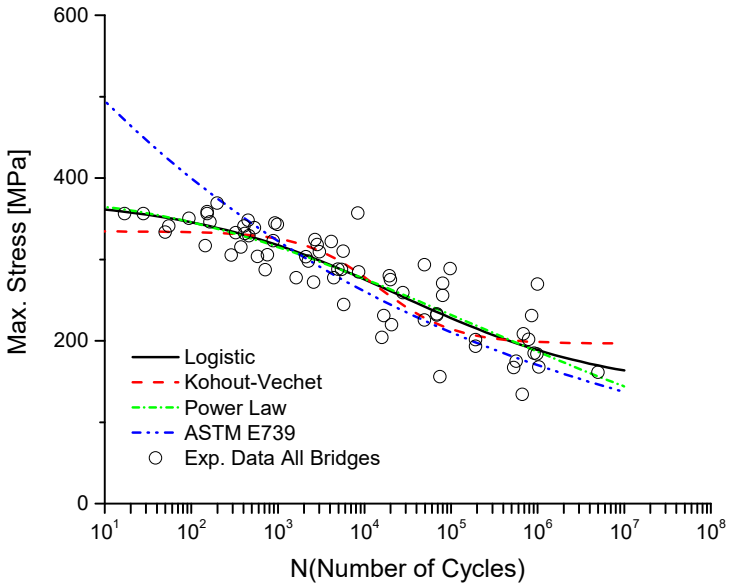

Figure 4.7: Comparison of the S-N curves for the fatigue data at R=-1 (strain ratio) of the metallic materials from the all bridges.

In **Figure 4.6**, regarding to the fatigue data of the Fão bridge at R=-1, the estimation in the LCF region of the Power Law, Logistic and Kohout-Věchet curves obtained similar and well-adjusted results, while in the HCF region the curve of Kohout-Věchet obtained a conservative result.

Based on **Figures 4.5** and **4.6**, it is possible to report that the Kohout-Věchet curve is very conservative in the HCF region justified by high MSE values. In the same way, the adjustment results based on the ASTM standard leads to excessively conservative values in the LCF region as well as reported by mean square error (MSE) values.

In **Figure 4.7** is presented a comparison between the S-N curves generated based on different fatigue formulations, such as ASTM standard, Power Law, Logistic and Kohout-Věchet models, for the fatigue data at R=-1 (under strain-controlled conditions) of the metallic materials from the several bridges under consideration in this research.

A single S-N curve was estimated for each studed method considering a total of 66 experimental data available. These old metallic materials were extracted of members from the ancient metallic bridges of the 19th century, so this research sought to propose the method that is best suited to these materials. This analysis aims to consolidate what

has already been observed in previous cases. The ASTM standard does not provide a good approximation in the low-cycle region even though experimental data are available in this region. The Power Law, Logistic and Kohout-Věchet S-N models obtained good adjustments to the low-cycle region when compated with the experimental data, as shown in **Figure 4.7**. For the HCF region the Logistic, ASTM and Power Law methods presented a similar performance, however, only the Kohout-Věchet model didn't obtain a good agreement to the fatigue data in the region above 10^6 cycles. In general the Logistic and Power Law method obtained the best fit according to the MSE estimation, however it is not conclusively due to the lack of data in regions above 10^6 cycles.

4.5 Conclusion

The formulations of the S-N curves, using Logistic method, Kohout-Věchet model, Power Law and ASTM E739 standard, applied to the metallic materials of old bridges, obtained different performances mainly in the LCF and HCF regions. The ASTM standard does not perform well in estimating fatigue life in the low-cycle region. All analyzed graphs showed discrepant values of maximum stresses corresponding to the LCF region. Even following the recommendations of the ASTM E739 standard, of not extrapolating analysis beyond the experimental data, it is perceptible the difficulty of the method in approaching the LCF fatigue data. In the low-cycle region, the Logistic, Kohout-Věchet and Power Law methods presented satisfactory performance when compared with experimental data, however it is not possible to say which one has the best fit. A greater amount of experimental fatigue data would be needed in the LCF region to complete such analysis. In the high-cycle region, there is also a lack of experimental data, but assuming that the extrapolation of this region is expected to follow the permanent fatigue limit, it can be concluded that the Kohut-Vechet method presented a very conservative performance. The S-N curves of this model are distant from experimental fatigue data in regions above 10^5 cycles. The generalized simple Power Law model can yield good approximations in the low-cycle region and in some cases in the region above 10^5 cycles. The S-N logistic curve formulation, which was initially applied only to composite materials, obtained an interesting performance when applied to the metallic materials of old bridges. In terms of MSE, this model obtained similar performance to the results of the Kohout-Věchet model, using only 3 parameters in the equation. Both models presented a good agreement with little experimental data. The

largest difference between these models is in HCF region. The logistic model allowed a better approximation to the experimental data in HCF region and a graphical analysis showed better results for a possible extrapolation of the analysis.

The achieved results showed that the S-N curve formulation using the Logistic and Power Law equations obtained a better performance in the LCF and HCF regions and lower MSE values when compared to the generalized Power Law formulations and the ASTM E739 standard. It was also observed that the Logistic, Kohout-Věchet and Power Law equations are able to obtain smaller errors for the cases with a reduced number of experimental data. However, in order to generalize which model has a better fit, it is necessary to carry out an exhaustive study with a greater amount of experimental data of fatigue of other metallic materials.

4.6 References

[1] ASTM Committee and others. Standard Practices for Statistical Analysis of Linear or Linearized Stress-Life (S-N) and Strain-Life (ε-N) Fatigue Data. ASTM Int West Conshohocken, PA, USA 2004.

[2] ISO BS. 12107: 2003,"Metallic materials--Fatigue testing--Statistical planning and analysis of data." Int Organ Stand 2012.

[3] EN B, others. Eurocode 3: Design of Steel Structures-Part 1-9: Fatigue. Eur Comm Stand 2004.

[4] BSI B. 5400 Steel, concrete and composite bridges, Part 10: Code of practice for fatigue. Br Stand Inst 1980.

[5] Specifications A-LBD. American Association of State Highway and Transportation Officials (AASHTO). Washington, DC 2004.

[6] Kohout J, Vechet S. A new function for fatigue curves characterization and its multiple merits. Int J Fatigue 2001;23:175–83.

[7] Weibull W. Fatigue Testing and Analysis of Results: Publ. for and on Behalf of Advisory Group for Aeronautical Research and Development, North Atlantic Treaty Organisation. Pergamon Press; 1961.

[8] Chaminda SS, Ohga M, Dissanayake R, Taniwaki K. Different approaches for remaining fatigue life estimation of critical members in railway bridges. Steel Struct 2007;7:263–76.

[9] Kajolli R. A new approach for estimating fatigue life in offshore steel structures. University of Stavanger, Norway, 2013.

[10] De Jesus AMP, Pinto H, Fernández-Canteli A, Castillo E, Correia JAFO. Fatigue assessment of a riveted shear splice based on a probabilistic model. Int J Fatigue 2010;32:453–62. doi:10.1016/J.IJFATIGUE.2009.09.004.

[11] Jesus AMP de, Silva ALL da, Figueiredo M V., Correia JAFO, Ribeiro AS, Fernandes AA. Strain-life and crack propagation fatigue data from several Portuguese old metallic riveted bridges. Eng Fail Anal 2011;18:148–63. doi:10.1016/J.ENGFAILANAL.2010.08.016.

[12] Correia J, Apetre N, Arcari A, De Jesus A, Muñiz-Calvente M, Calçada R, et al. Generalized probabilistic model allowing for various fatigue damage variables. Int J Fatigue 2017;100:187–94.

[13] Muniz-Calvente M, de Jesus AM., Correia JAFO, Fernández-Canteli A. A methodology for probabilistic prediction of fatigue crack initiation taking into account the scale effect. Eng Fract Mech 2017;185:101–13. doi:10.1016/J.ENGFRACMECH.2017.04.014.

[14] Kohout J, Vechet S. Some Estimations of Tolerance Bands of SN Curves. Mater Sci 2008;14:202–5.

[15] Zapletal J, Věchet S, Kohout J, Obrtlík K. Fatigue lifetime of ADI from ultimate tensile strength to permanent fatigue limit. Strength Mater 2008;40:32–5.

[16] Mu PG, Wan XP, Zhao MY. A New S-N Curve Model of Fiber Reinforced Plastic Composite. Key Eng Mater 2011;462–463:484–8. doi:10.4028/www.scientific.net/KEM.462-463.484.

[17] Freire Júnior RCS, Belísio AS. Probabilistic S-N curves using exponential and power laws equations. Compos Part B Eng 2014;56:582–90. doi:10.1016/j.compositesb.2013.08.036.

[18] Correia JAFO, Raposo P, Muniz-Calvente M, Blasón S, Lesiuk G, De Jesus AMP, et al. A generalization of the fatigue Kohout-Věchet model for several fatigue damage parameters. Eng Fract Mech 2017;185:284–300. doi:10.1016/j.engfracmech.2017.06.009.

[19] Taras A, Greine R. Development and application of a fatigue class catalogue for riveted bridge components. Struct Eng Int J Int Assoc Bridg Struct Eng 2010. doi:10.2749/101686610791555810.

[20] Goodman J. Mechanics Applied to Engineering. 9th ed. London: Longmans Green and Co; 1930.

[21] Soderberg CR. Factor of Safety and Working Stress. Trans Am Soc Test Matls

1930;52:146.

[22] Morrow JD. fatigue design handbook, section 3.2. SAE Adv. Eng., 1968. doi:http://dx.doi.org/10.1521/jscp.21.4.441.22597.

Chapter V

Fatigue life prediction considering the mean stress effects through an artificial neural network applied to metallic materials

The mean stress effect plays an important role in the fatigue life predictions, its influence significantly changes high-cycle fatigue behaviour, directly decreasing the fatigue limit with the increase of the mean stress. Fatigue design of structural details and mechanical components must account for mean stress effects in order to guarantee the performance and safety criteria during their foreseen operational life. The purpose of this research work is to develop a new methodology to generate a constant life diagram (CLD) based on assumptions of Haigh diagram and artificial neural networks, using the probabilistic Stüssi fatigue S-N fields, for metallic materials. This proposed methodology can estimate the safety region for high-cycle fatigue regimes as a function of the mean stress and of the stress amplitude in regions of the predominance of tensile loading, using fatigue S-N curves only for two stress R-ratios. In this approach, the experimental fatigue data of the P355NL1 pressure vessel steel available for three stress R-ratios (-1, -0.5, 0), is used. A multilayer perceptron network has been trained with the back-propagation algorithm; its architecture consists of two input neurons (σ_a, N) and one output neuron (σ_m). The proposed constant life diagram (CLD) based on trained artificial neural network algorithm and probabilistic Stüssi fatigue fields applied to the dog-bone shaped specimens made of P355NL1 steel showed a good agreement with the high-cycle fatigue experimental data, only using the stress R-ratios equal to 0 and -0.5. Furthermore, a procedure for estimating the fatigue resistance reduction factor, K_f, for the fatigue life prediction of structural details in extrapolation regions based on machine learning artificial neural network algorithm is proposed and K_f results are presented.

5.1 Introduction

Mechanical failures of machine equipment and structural components cause loss of required function performance and unexpected stops, resulting in an increase in the need for corrective maintenance, which increases maintenance costs and reduces the reliability of mechanical systems. Fatigue damage is the cause of most of the failures of materials from structural elements or machine components, which during their operational life are subjected to cyclic loads with the presence of mean stresses capable of causing microscopic physical damage [1,2].

The mean stress effects play an important role in fatigue life prediction, its influence significantly changes the fatigue behaviour in high-cycle fatigue regimes (HCF), directly decreasing the fatigue limit with the increase of the mean stress. This may be explained by the observation that positive mean stress increases the crack opening and accelerates the fatigue damage accumulation, while compressive mean stresses are beneficial in terms of fatigue strength [3,4].

The potential damage that mean stresses may cause in mechanical and structural details depends on the microstructure of the material. For example, brittle materials are very influenced by the effects of mean tensile stresses when compared with ductile materials [5]. Additionally, the geometric discontinuities such as a change of cross-section, holes, notches, key channels, among others, can cause a considerable increase in the value of the applied stresses in the vicinity of the stress concentration. These potential effects of the positive mean stress on the fatigue damage of the materials can cause a direct influence on the calculation of the fatigue stress concentration factor (K_t) to be used in the engineering design. In order to improve the estimation of the mean stress effects in the high-cycle fatigue (HCF) regime, between 10^6 and 10^8 cycles, several researchers such as Gerber [6], Goodman [7], Soderberg [8], Morrow [9] and Smith [10] proposed empirical models for mean stress correction [11]. In the opposite way to the proposed empirical models, other researchers have proposed new approaches considering physical phenomena into their models attempting to account for mean stress effects on fatigue behaviour of the materials under different loading conditions. Zhu et al. [1] proposed a new strain energy model considering the mean stress effects. This model led to good results when the mean stress sensitivity parameter was considered. Niesłony and Böhm [12] investigated the influence of the mean stress on fatigue resistance, considering these

effects thru a function of the number of cycles to failure. Ince [2] proposed a new fatigue model including the mean stress influence based on the distortion energy. Lu et al. [3] developed a modified Walker model to explain the mean stress effects on the fatigue life prediction for aeroengine disks. The evaluation of the mean stress effects on the fatigue crack initiation behaviour, under different loading conditions for various metallic materials, was investigated by Correia et al. [13], Zhu et al. [1] and Koutiri et al. [14]. Despite the innovation of these recent models, few studies have taken into account the stochastic fatigue behaviour in the modelling of the mean stress effects and generation of stress limit diagrams applied to metals.

The S-N or Wöhler curves are used by engineers to evaluate the fatigue behaviour of the metallic materials under a constant mean stress; however the Basquin model, because of its simplicity, is only applicable to the same fatigue conditions of the test data used in its identification, i.e., the same stress R-ratio (R) or mean stress for which it was identified [15]. The fatigue behaviour estimation of metallic materials for any region with the predominance of tensile loading ($R = -1$ to $R = 1$) requires time consuming and expensive experimental tests, with the aim of generating several S-N curves, each obtained fatigue curve corresponding to one mean stress value. Alternatively, a stress limit diagram also known as constant life diagram (CLD) – Haigh diagram, or modified Goodman diagram, can be built. This diagram allows the representation of mean stress effects with the decreasing of the stress amplitude, for the materials without failures. When these diagrams are built using a small number of fatigue data, the simulated fatigue damages can be underestimated or overestimated [16]. This kind of situation may lead to the need for further experimental tests covering other stress R-ratios. Recently, Freire Júnior, Neto and Aquino [16,17] have proposed the use of artificial neural networks (ANNs) to develop the constant life diagram (CLD) applied to composite materials. In their research works, the authors showed that the proposed approach led to good results using a reduced number of fatigue curves, when compared with the experimental data and deterministic laws. A new application based on ANN, aiming to assess the mean stress effects on the fatigue resistance of a steel reinforced aluminium electrical cable was presented by Pestana et al. [18].

The purpose of this research is to develop a new probabilistic constant life diagram (CLD) based on an artificial neural network applied to metallic materials and structural details. It is possible to obtain the fatigue strength limits of the material for any stress R-ratio in the region with predominant tensile loading. This CLD model uses a small

amount of fatigue data aiming at developing a probabilistic diagram, capable of providing designers with safe and reliable high-cycle fatigue (HCF) strength data. Additionally, the estimated probabilistic CLD diagrams obtained for the P355NL1 steel and notched detail made of the same steel, can be used to obtain the fatigue resistance reduction factor, K_f. A comparison between deterministic and ANN values is presented.

5.2 Experimental fatigue data of P355Nl1 Steel and notched detail

In this research work, experimental fatigue data of the P355NL1 pressure vessel steel, widely used in the pressure vessels, boilers and storage tanks industry, as well as of a notched detail made of the same steel was collected and used [19]. The mechanical properties are summarized in **Table 1** [19]. In **Figures 1** and **2**, the geometry and dimensions of the smooth dog-bone shaped specimens and notched detail are shown [19]. In **Figure 3**, the experimental fatigue data for the stress R-ratios, R=-1, R=-0.5 and R=0, of the dog-bone shaped specimens made of P355NL1 steel, collected from the ref. [19], are presented. For the notched detail made of the same steel, **Figure 4** shows the collected fatigue data for various stress R-ratios, namely R=0, R=0.15 and R=0.30 [19].

Table 5.1: Mechanical properties of the P355NL1 steel [19].

σ_{ult} (MPa)	σ_y (MPa)	E (GPa)	v (-)
568	418	205.2	0.275

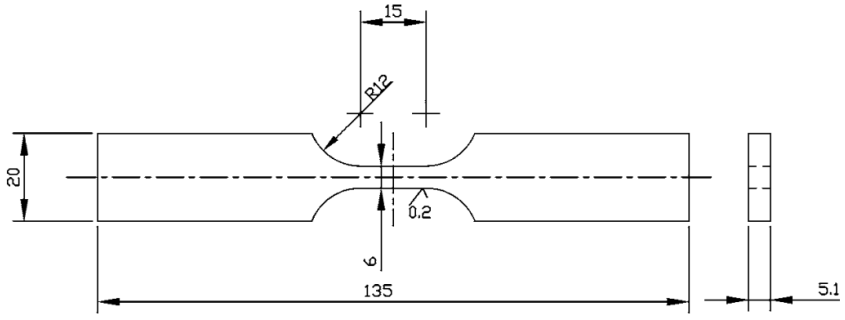

Figure 5.1: Geometry and dimensions of the dog-bone shaped specimens used in the fatigue tests (dimensions in mm).

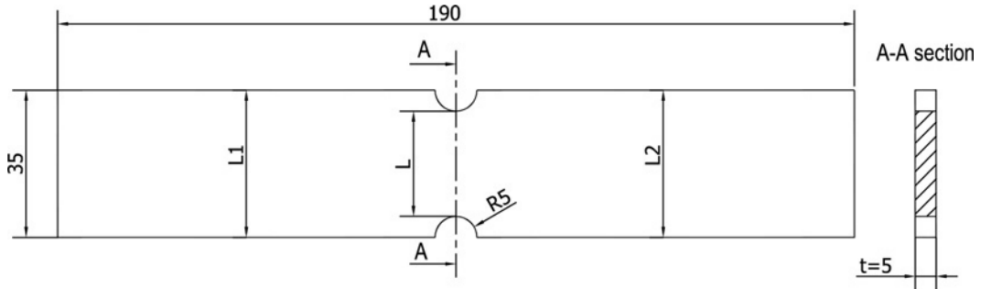

Figure 5.2: Geometry and dimensions of the notched geometry made of P355NL1 steel (dimensions in mm).

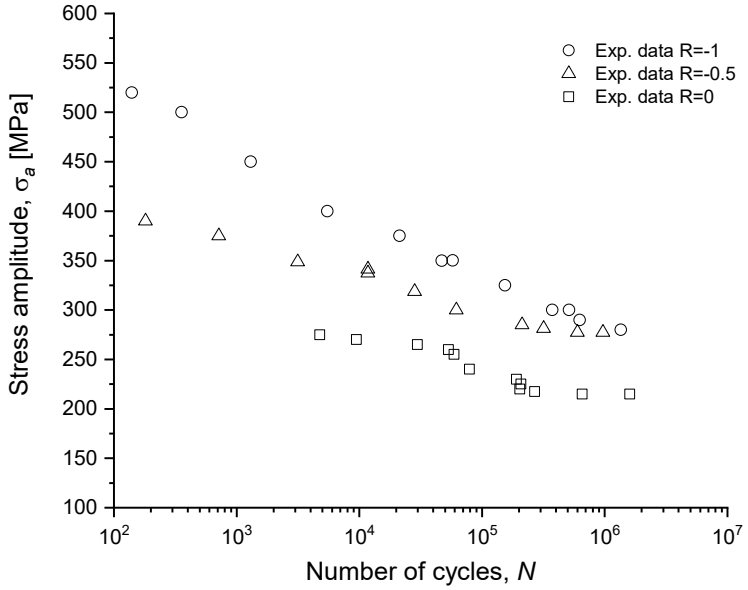

Figure 5.3: Experimental S-N fatigue data of the dog-bone shaped specimens made of P355NL1 steel, for the stress R-ratios, R=-1, R=-0.5 and R=0.

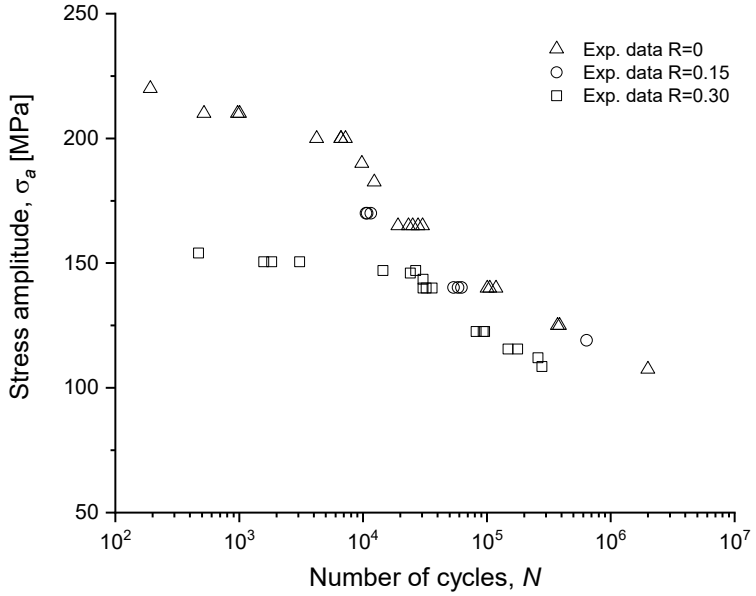

Figure 5.4: Experimental S-N fatigue data of the notched plate made of P355NL1 steel, for stress R-ratios, R=0, R=0.15 and R=0.30.

5.3 Probabilistic Stüssi fatigue model

The Stüssi nonlinear function [20] was proposed to represent the full-range S-N curve, describing the fatigue resistance in all fatigue regimes from low-cycle (LCF) to high-cycle fatigue (HCF) regimes. This model requires the estimation of parameters of the fatigue limit and ultimate tensile strength, aiming at performing a good adjustment to the experimental fatigue data in all fatigue regimes. However, this fatigue model proposed by Stüssi [20] is only based on the deterministic fatigue behaviour of the metallic materials and/or structural details, i.e., it does not take into account the random nature of the failure time. The full-range fatigue model applied to the metallic materials and details proposed by Stüssi [20] and evaluated by Barbosa et al. [21], is given by:

$$\Delta\sigma = \frac{R_m + aN^b \cdot \Delta\sigma_\infty}{1 + aN^b} \tag{5.1}$$

where, $\Delta\sigma$ is the nominal stress range, N is the number of cycles to failure, R_m and $\Delta\sigma_\infty$ are two material parameters, respectively the ultimate tensile strength and fatigue limit, and finally, a and b the geometric variables so-called Stüssi geometrical parameters of the metallic materials and details. The estimation of the two Stüssi geometrical parameters is performed by applying a linear regression according to ref. [20]:

$$\Delta\sigma a N^b = \frac{R_m - \Delta\sigma}{\Delta\sigma - \Delta\sigma_\infty}$$

or

$$\log N = \frac{1}{b}\log\left(\frac{R_m - \Delta\sigma}{\Delta\sigma - \Delta\sigma_\infty}\right) - \frac{1}{b}\log(a) \tag{5.2}$$

The R_m parameter is given by the mean value of tensile tests. In order to estimate the fatigue limit ($\Delta\sigma_\infty$), n experimental points given by the stress amplitude and number of cycles to failure should be considered:

$$\begin{aligned} N_i &= \{N_1, N_2, \dots, N_n\} \\ \Delta\sigma_i &= \{\Delta\sigma_1, \Delta\sigma_2, \dots, \Delta\sigma_n\} \end{aligned} \tag{5.3}$$

In this way, the probabilistic fatigue model based on three-parameters Weibull distribution proposed by Castillo & Fernández-Canteli [22] can be a good choice to estimate the fatigue limit ($\Delta\sigma_\infty$). This model requires two parameters, $B = \log N_0$ and $C = \log \Delta\sigma_0$, corresponding to the threshold value for N and fatigue limit, respectively. The regression equation proposed by Castillo & Fernández-Canteli [22] is given by:

$$E[\log N - B | g(\Delta\sigma_i) - C] = \frac{\mu}{g(\Delta\sigma_i) - C} \tag{5.4}$$

Base on the Equations (4), the estimation of B and C is made by an optimization-non-linear process by minimizing of the Equation (5.6):

$$Q = \sum_{i=1}^{n}\left(\log N_i - B - \frac{\mu}{g(\Delta\sigma_i) - C}\right)^2 \tag{5.5}$$

The initial estimates to solve B, C and μ can be made by the following equation:

$$\mu_i = \frac{1}{n}\sum_{i=1}^{n}\log N_i = B + \frac{\mu}{g(\Delta\sigma_i) - C};\ \ i = 1, 2, \dots, n \tag{5.6}$$

The optimization process can be found in detail in ref. [22]. In this research, in the optimization process, a semi-logarithmic scale is used, where the stress amplitude is in linear scale and the number of cycles in logarithmic scale of base 10.

The probabilistic Stüssi fatigue modelling is generated combining the three-parameters Weibull distribution and the Stüssi function [21]. In this way, the cumulative distribution function need to be used and is given by

$$F(x|\alpha,\beta,\delta) = 1 - exp\left[-\left(\frac{x-\alpha}{\beta}\right)^{\delta}\right], x \geq \alpha \tag{5.7}$$

With the random variable x given transforming the Equation (5.1) in the following Equation (5.8):

$$x = \Delta\sigma - \frac{R_m + aN^b \cdot \Delta\sigma_\infty}{1 + aN^b} \tag{5.8}$$

Then, combining Equations (5.7) and (5.8), the probabilistic Stüssi fatigue modelling can be made using the following equation:

$$p = 1 - exp\left[-\left(\frac{\Delta\sigma - \frac{R_m + aN^b \cdot \Delta\sigma_\infty}{1 + aN^b} - \alpha}{\beta}\right)^{\delta}\right] \tag{5.9}$$

where p is the probability of failure, $\alpha > x$ and $\alpha \in R$, $\beta > 0$ and $\delta > 0$ are the location, scale and shape Weibull parameters. The main assumption of this model is the Stussi parameter to be assumed as a random variable in the three-parameters Weibull distribution. The Weibull distribution parameters are normally estimated by the Castillo–Hadi method [23] or using probability-weighted moment (PWM) [24] methods. In this research work, the PWM method [24] was used to estimate the α, β and δ parameters, according to the recommendations proposed by Caiza & Ummenhofer [24].

In **Table 5.2**, the geometrical and material/detail parameters of the Stüssi function as well as the α, β and δ parameters from the three-parameters Weibull distribution for the dog-bone shaped specimens and notched details under consideration are presented. In **Figures 5.5** and **5.6**, the probabilistic S-N curves based on Stüssi model combined with the three-parameters Weibull distribution for the dog-bone shaped specimens made of P355NL1 steel (stress R-ratios R=0, R=-0.5 and R=-1) and notched details made of the same material (stress R-ratios R=0, R=0.15 and R=0.3) are shown. These results are used in the methodologies proposed in **Sections 5.4** and **5.5**, aiming at estimating

the artificial fatigue life surface and constant life diagram (CLD) for the dog-bone shaped specimens made of P355NL1 steel, for failure probabilities and fatigue strength reduction factor as a function of the number of cycles to failure for failure probabilities of the notched detail under consideration, respectively. In **Figures 5.5** and **5.6**, a good agreement between the experimental fatigue results and the Stüssi fatigue curves, for the probability of failure of 50% for all stress R-ratios of the specimen geometries under consideration, is observed.

Table 5.2: Fatigue curve constants based on probabilistic Stüssi model.

Specimen	R	R_m	$\Delta\sigma_\infty$	a	b	α	β	δ
Dog-bone	-0,5	426	260.4	2.13E-02	0.441	-8.881	9.390	1.370
shaped	-1	568	252	2.87E-02	0.407	58.617	-54.734	-10.510
specimens	0	284	210	1.07E-06	1.233	-16.927	17.837	3.526
	0.3	162,4	109	4.25E-06	1.161	-73.633	73.517	18.534
Notch detail	0.15	197,2	117	7.16E-05	0.954	-2.077	2.299	2.077
	0	230	107	1.38E-03	0.653	-15.982	16.792	3.199

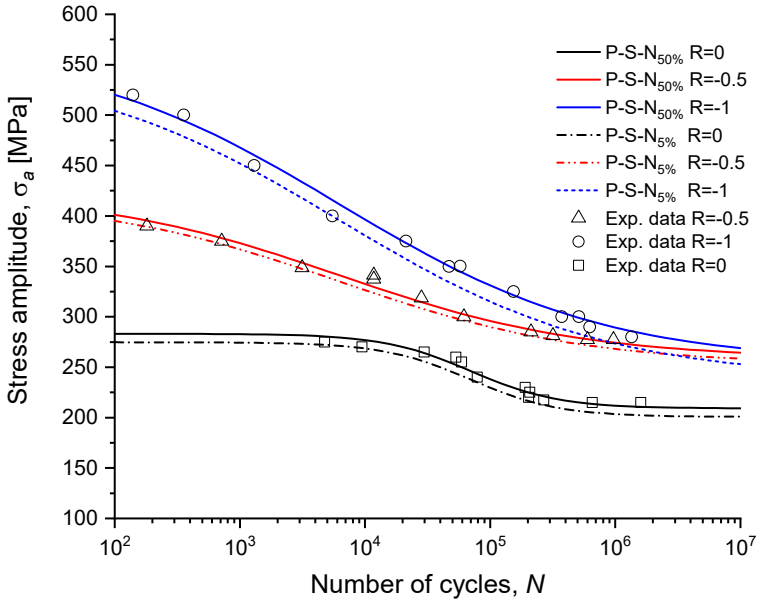

Figure 5.5: Probabilistic S-N curves based on Stüssi model combined with a Weibull distribution for the dog-bone shaped specimens made of P355NL1 steel: R=0, R=-0.5 and R=-1.

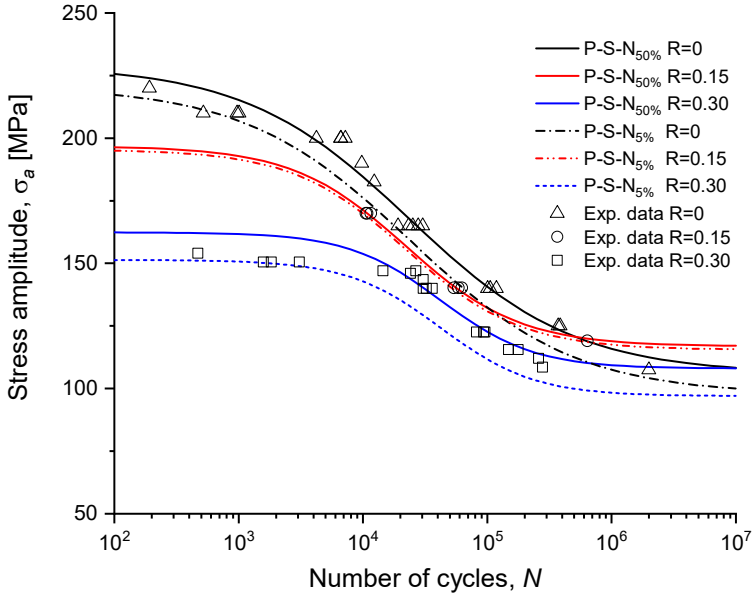

Figure 5.6: Probabilistic S-N curves based on Stüssi model combined with a Weibull distribution for the notched detail made of P355NL1 steel: R=0, R=0.15 and R=0.3.

5.4 Implementation of a machine learning artificial neural algorithm

Artificial neural networks (ANNs) emerged as a new branch of the computation, which shows remarkable performance when used in the modelling of complex linear and nonlinear relationships [25]. This computational/mathematical technique is especially useful for simulations of any correlation that is difficult to describe with physical models due to the ability to learn. Thus, the ANN can extract the existing relationship between the various variables that makes part of the application [26]. Another relevant characteristic is its generalization ability, where after a network training process is able to generalize the acquired knowledge, making possible to estimate unknown solutions. Furthermore, the ANNs are able to solve complex problems and can be used in the research activities on mechanical properties [27], fracture mechanics [25], fatigue and failure analysis and detection [28].

The artificial neural network (ANN) are computational algorithms based on biological neural networks (BNN) composed of neurons [25]. This kind of algorithms consists in three layers of neurons – an input layer, an intermediate or hidden layer and an output layer. These layers are interconnected by artificial synaptic weights [26]. The input layer

is composed of the information that will be processed through the hidden layer and finally, in the output layer the response information of the model is computed. In this work, a multi-layer Perceptron (MLP), network trained with the back-propagation algorithm with momentum terms (BPM) and structured with a topology of the artificial neural network (ANN) is presented (**Figure 5.7**) [26]. This ANN is structured with two neurons in the input layer, the mean stress (σ_m) and the number of cycles to failure (N), and a neuron in the output layer, the stress amplitude (σ_a), given by Equation (5.10).

$$\sigma_a = f(\sigma_m, N) \tag{5.10}$$

In this MLP, the topology consists only of a hidden neural layer, which allows the mapping of any continuous function in the real functions space [29]. The hidden layer will have a number of neurons defined between 2 to 30 neurons. All neurons of the hidden layer have a sigmoid activation function whereas the neuron of the output layer has a linear activation function.

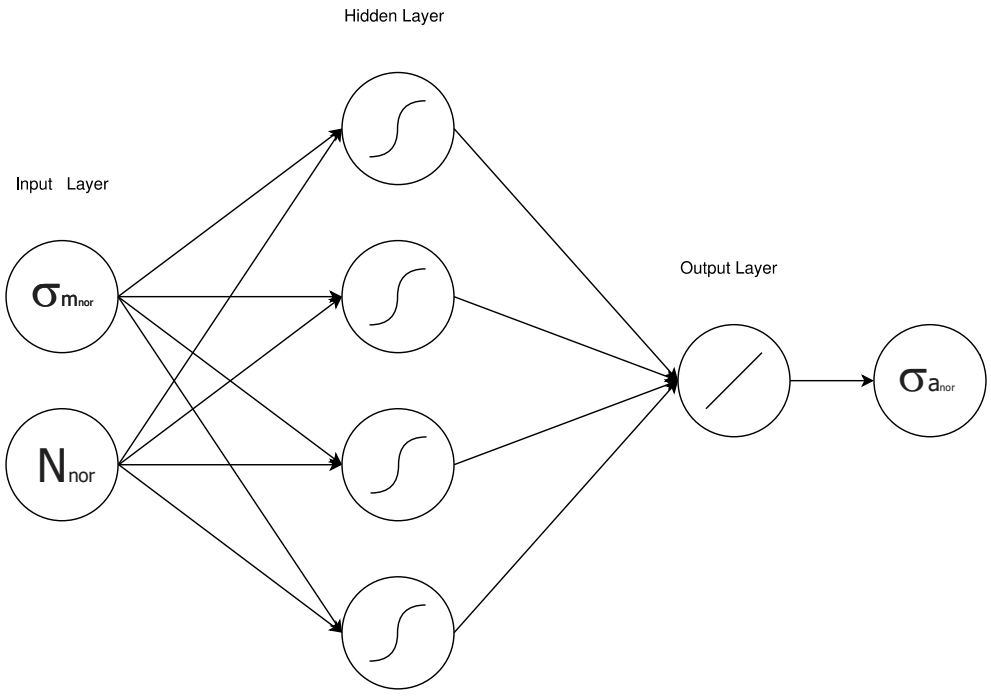

Figure 5.7: Topology of the artificial neural network used in this study.

Pre-processing is an important step that precedes the ANN training and validation phases, which aims to reduce dimensional complexity and minimize the redundancy of the input and output signals. For this, it is important to emphasize that all input and

output variables of the network must be individually normalized in relation to their respective minimum and maximum values. The normalized stress amplitude is given by:

$$\sigma_{a_{nor}} = \frac{\sigma_a}{\sigma_{a_{max}}} \quad \therefore \quad \sigma_{a_{max}} = \sigma_a^*(N = 1) = \frac{\sigma_{ult}}{2} \tag{5.11}$$

where, $\sigma_{a_{nor}}$ is the normalized stress amplitude, $\sigma_{a_{max}}$ is the maximum stress amplitude and σ_{ult_T} is the ultimate tensile stress. The normalized mean stress is written by:

$$\sigma_{m_{nor}} = \frac{\sigma_m}{\sigma_{ult}} \tag{5.12}$$

where $\sigma_{m_{nor}}$ is the normalized mean stress and σ_{ult} is the ultimate tensile strength. Thus, in order to normalize the number of cycles, first it was used logarithm transformations and then proceed with the normalization using the maximum number of cycles. The normalized number of cycles is given by:

$$N_{nor} = \log(N)/\log(N_{max}) \quad \therefore \quad N_{max} = 10^7 cycles \tag{5.13}$$

This normalization process with application of the logarithm transformations to the numbers of cycles (N) avoids the concentration of values of the number of cycles in a region close to zero. If the normalization process used in Equation (5.10) was not adopted, there would be a saturation of neurons in the neural network [17].

The training phase of the ANN requires a data set large enough for the back-propagation algorithm (BPM) performs the *forward* and *backward* steps, which allows the adjustment of the synaptic weights (w) in each interaction (training time), implying a gradual decrease in the sum of the errors produced (e) by the network responses (z) in front of the desired ones (d). The flow of these interactions from the supervised training process is illustrated in **Figure 5.8**. The assigned values to the moment and learning rate constants were 0.7 and 0.1 respectively, for any training time. It is important to note that the values attributed to the learning rate (η) expresses how quickly the network training process is driven to its convergence, and the insertion of the momentum term (θ) leaves the convergence process more efficient according to Reed & Marks analyses [30]. The η and θ values understood between $0.05 \leq \eta \leq 0.75$ and $0 \leq \theta \leq 0.9$, are normally recommended for the training of MLP networks [31].

The set of these steps ordered for the training of the ANN is called machine-learning algorithm. Throughout its application, the network will be able to extract discriminant characteristics of the fatigue behaviour of the mean stress, σ_m, as a function of the stress amplitude, σ_a, and of the number of cycles to failure to be mapped through samples that have been withdrawn from its context.

In this research work, the samples used for the ANN training were generated by three different Stüssi fatigue curves (**Figure 5.3**) from the three fatigue R-ratios (R=0, R=-0.5 and R=-1) concerning to the dog-bone shaped specimens made of P355NL1 steel (see **Figure 5.1**). The generation of these data for RNA training was made using Equation (5.9), which allows determining fatigue data for different levels of probability of failure using the geometrical and material parameters as well as Weibull distribution parameters, presented in Table 5.2. In this research, the ANN is trained for the probabilistic Stüssi fatigue data from the probabilities of failure of 50% and 5%. The obtained data from the probabilistic Stüssi fatigue data for the ANN training are ranged for the number of cycles to failure between 10^2 and 10^7 cycles, since it corresponds to the most significant domain of experimental results. The set of samples is divided into two subsets, which are called the training subset and test subset (see **Figure 5.8**). In the training subset the Stüssi fatigue data for the stress R-ratios, R=0 and R=-0.5, are used aiming the ANN learning process. In the test subset are added the Stüssi fatigue data for the stress R-ratio equal to R=-1, to be used for the validation of the assumed topology (**Figures 5.7** and **5.8**).

For each presented sample set belonging to the training subset aiming the adjustment of the synaptic weights (w_i) is called training time; and for each time, the back-propagation algorithm defines the representative function of the approximation error, whose task is to measure the deviation between the responses produced by the network output neurons (z_i) in relation to the respective desired values (d_i). Thus, considering the Q-*th* training sample for the topology shown in **Figure 5.8**, the quadratic error function is assumed to be used to measure the local performance associated with the results produced by the output neurons of the sample, i.e.:

$$RMS = \frac{1}{2Q}\sum_{1}^{Q}\sum_{i=1}^{m}(d_i - z_i)^2 \tag{5.14}$$

In **Equation (5.14)**, the variable m represents the number of output neurons, where for this study m is equal to 1. It is important to emphasize, as already mentioned in **Section 1**, that there is not a unified mathematical model capable of taking into account the mean stress effects and stress R-ratios in **Equation (5.1)**. Thus, trained ANN (**Figures 5.7** and **5.8**) will be able to generalize the fatigue behaviour of metallic materials and details to any value of constant mean stress as well as will allows the modelling of the Haigh Diagram for any probability of failure (in fatigue design for a probability of failure of 5%).

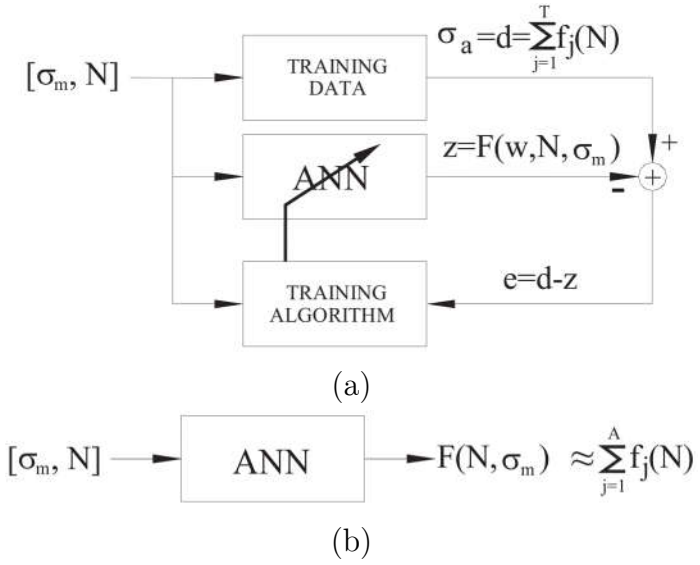

Figure 5.8: (a) ANN training method; (b) Model obtained with the training of the ANN.

5.5 Procedure for estimating the fatigue resistance reduction factor

The geometric discontinuities causes a considerable increase in the value of the nominal stresses acting in the vicinity of the stress concentrators of notched details. Thus, there is a direct influence on reducing the fatigue strength of the notched detail when compared to the fatigue data of the smooth specimens (for the same material concerned) at the same levels of the number of cycles. The notch effects on fatigue resistance can be evaluated by the relationship between the experimental fatigue data or deterministic

fatigue curves from the smooth specimens and notched details allowing to estimate the fatigue strength reduction factor, K_f, given by:

$$K_f = \frac{\Delta\sigma_{smooth}}{\Delta\sigma_{notch}} \tag{5.15}$$

where $\Delta\sigma_{smooth}$ is the smooth fatigue strength and $\Delta\sigma_{notch}$ is the notch component fatigue strength, both for the same levels of the number of cycles to failure. The fatigue strength reduction factor K_f has an asymptotic behaviour for high-cycle fatigue regions [32]. According to Ciavarella & Meneghetti [33], the classical values of K_f are included in local approaches proposed by Neuber [34], Peterson [35] and Heywood [36]. These approaches are widely used in books and design codes [37–39], where the formulations for the fatigue resistance reduction factor, K_f, is required. However, there are no empirical equations for K_f that consider the effects of a loading level, material properties, shape and size of manufacturing defects, size and geometry of the notched detail, stress gradient, number of cycles to failure, stress amplitude and mean stress, among others [35]. Lee and Taylor [40] proposed a relationship between K_f and the number of cycles, where the fatigue strength reduction factors K_f' and K_f can be provided for a component at 10^3 cycles and the fatigue limit (10^6cycles) respectively, and given by:

$$\frac{\log(10^3) - \log(10^6)}{\log(K_f') - \log(K_f)} = \frac{\log(10^3) - \log(N)}{\log(K_f') - \log(K_{f,N})} \tag{5.16}$$

This approach has been widely used in multiaxial states of stresses [40]. In order to simplify and contribute to the development of new estimation methods for the fatigue strength reduction factor, a sensitivity analysis of K_f from low-cycle (LCF) to high-cycle fatigue (HCF) regions is carried out. The influence of the variables, number of cycles to failure and mean stress, are considered to evaluate K_f. In this analysis, a comparison between the values of the stress amplitudes obtained from the Stüssi fatigue results and the obtained values from the ANN for the stress R-ratios, R=0 and R=-0.5, of the P355NL1 steel are carried out. In this way, a hybrid ANN-Stüssi model to determine the fatigue strength reduction factor, K_f, where the stress amplitude as a function of the number of cycles ($\sigma_{s,ANN}(N)$) of the P355NL1 steel are generated for the ANN fatigue model and for the notched detail are evaluated according to Stüssi fatigue model ($\sigma_{d,Stussi}(N)$) is proposed and illustrated in **Figure 5.9**. This new hybrid ANN-Stüssi model (see **Figure 5.9**) is given by:

$$K_f = K_f\left(\sigma_{s,ANN}, \sigma_{d,Stussi}\right) = \frac{\sigma_{s,ANN}(N)}{\sigma_{d,Stussi}(N)} \tag{5.17}$$

A generalized ANN-Stüssi formulation for the K_f values combining the ANN fatigue data (**Figures 5.7** and **5.8**) for the P355NL1 steel and the probabilistic Stüssi fatigue data (Equation (5.9)) for the notched detail are given by the following equation:

$$K_f = \frac{\sigma_{s,ANN}(N)}{\sigma_{d,Stussi}(N)} = \frac{\sigma_{s,ANN}(N)}{\beta[-(\ln(1-p))^{1/\delta}] + \frac{R_m + aN^b \cdot \Delta\sigma_\infty}{1 + aN^b} + \alpha} \tag{5.18}$$

The geometrical and detail parameters as well as the Weibull distribution parameters of the probabilistic Stüssi fatigue model are evaluated according the recommendations of **Section 5.3**. These parameters estimated for the fatigue data of the notched detail are presented in **Table 5.2**.

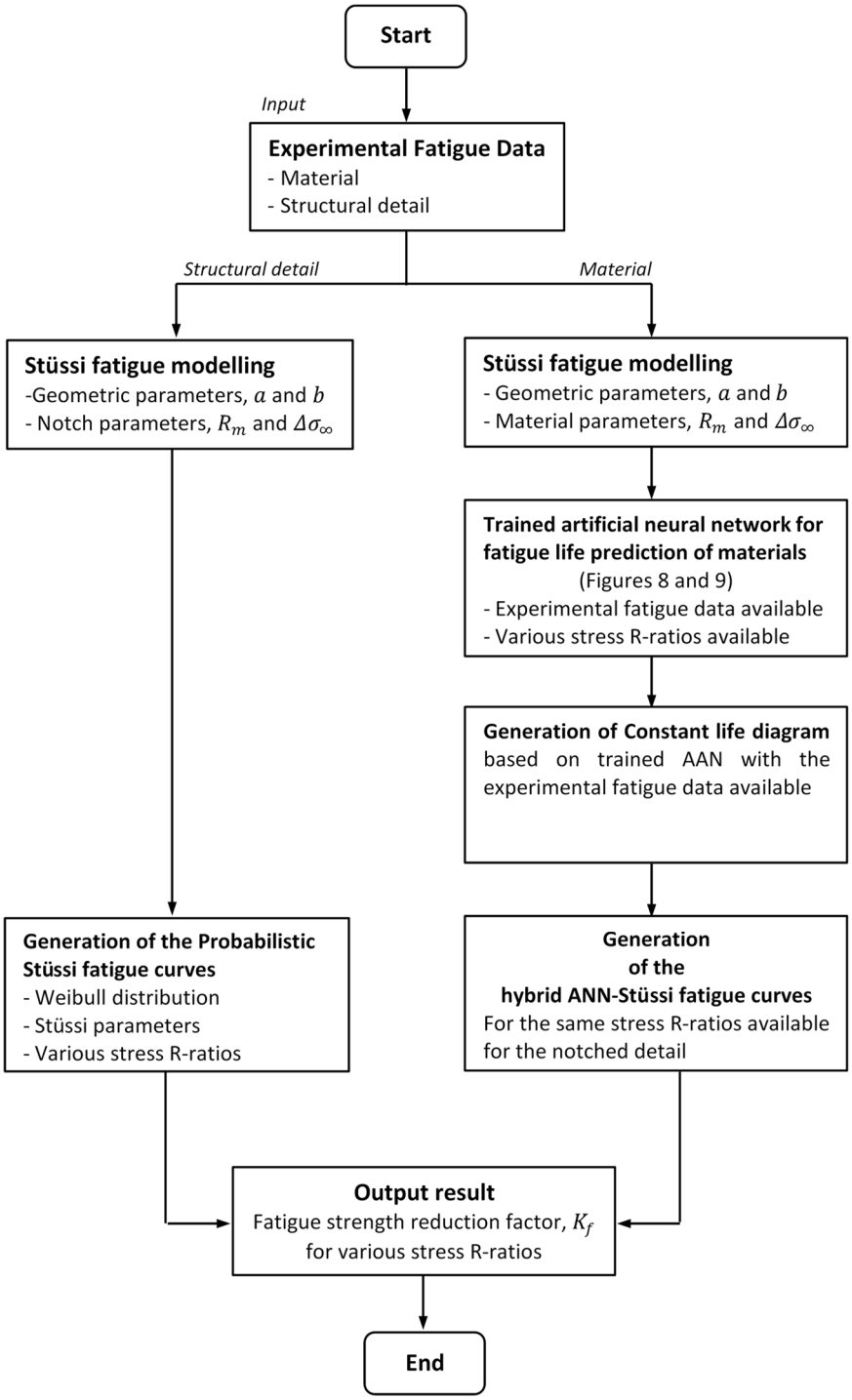

Figure 5.9: Workflow for estimating the fatigue strength reduction factor, K_f, for the fatigue life prediction of materials and components of extrapolation regions based on machine learning artificial neural network algorithm.

5.6 Results and Discussion

5.6.1 Artificial neural network based constant life diagram

The artificial neural network-based constant life modelling was proposed according to the ANN topology and training method, **Figures 5.7** and **5.8** of **Section 5.4**, respectively. In this analysis, the constant life diagrams (CLD) are presented in a format of three axes related to the mean stress, σ_m, the stress amplitude, σ_a, and the number of cycles to failure, N_f (see **Figures 5.12** and **5.13**). Firstly, the probabilistic Stüssi fatigue model is applied to the experimental fatigue data of the P355NL1 steel (**Figure 5.3**) aiming to determine the limits of the fatigue resistance as well as the Weibull distribution parameters, and their results are presented in **Table 5.2** and **Figure 5.5**. Secondly, the ANN training method (**Figure 5.8**) is implemented based on the ANN topology (**Figure 5.7**). The obtained ANN results are evaluated and compared with the experimental fatigue data. In this step, the constant life diagrams (CLD) based on proposed methodology for the P355NL1 steel taking into account the various stress R-ratios (R=0, R=-0.5 and R=-1) are generated. Finally, sensitivity analysis by means of the mean square error (**Equation (5.14)**) is performed on obtained CLD results based on the ANN topology and training method.

The probabilistic Stüssi fatigue curves obtained for the experimental fatigue data of the P355NL1 steel, for each stress R-ratios under consideration, are presented in **Figure 5.5** (S**ection 5.3**). In **Table 5.2** (**Section 5.3**), the geometrical and material parameters as well as the Weibull distribution parameters are showed. This information is required to obtain the constant life diagrams (CLD) based on the ANN method (see **Figure 5.8**, **Section 5.4**) for the failure probabilities of 50% and 5%.

In **Figures 5.10** and **5.11**, the constant life diagram (CLD) generated based on ANN topology (**Figure 5.7**) and training method (**Figure 5.8**) for the P355NL1 steel, for the failure probabilities of 50% and 5%, respectively, are illustrated. In these diagrams, the relationship between the stress amplitude and mean stress for each number of cycles (N_f), 10^4, 10^5, 10^6 and 10^7, are illustrated. For the stress amplitudes below the CLD curves (**Figures 5.10** and **5.11**), safety operation regions are considered. Additionally, according to **Figures 5.10** and **5.11**, for failure probabilities of 50% and 5%, respectively, it is possible to estimate the fatigue strength limits for any stress R-ratio. The trained

ANN taking into account the probabilistic Stüssi fatigue data makes possible the development of constant life diagrams (CLDs) for any failure probability, as can be seen in **Figure 5.11**, where the CLD for a failure probability of 5% is shown. These generated constant life diagrams obtained a good convergence for the results of the ultimate tensile strength of 568MPa ($\sigma_a = 0$ or $R = -1$), for failure probabilities of 50%, when compared with experimental data presented in **Table 5.1**. In **Figures 5.12** and **5.13**, artificial fatigue life surfaces (σ_a, N, σ_m) for the dog-bone shaped specimens made of P355NL1 steel for the failure probabilities of 50% and 5% are shown. They can be used to estimate the mean stress effects on fatigue strength for any number of cycles to failure.

The performance of the back-propagation algorithm with momentum (BPM) is measured by means of the mean square error, RMS, (Equation (5.14)) between the network output (z) and the desired value (d), for the trained ANN with the Stüssi fatigue data and for failure probabilities of 50% and 5%. The smallest RMS values were obtained for the trained ANN with 28 and 7 neurons in the hidden layer, respectively, for the probabilistic Stüssi fatigue data of 50% e 5%. In **Table 5.3**, the performance of the obtained ANN, in terms of RMS and r, using the Stüssi fatigue data at the failure probabilities of 50% and 5%, is showed. In **Figures 5.14** and **5.15**, the estimated RMS results during the ANN training process are presented. The minimum RMS value is obtained when the training set reaches its lowest value. According to the obtained RMS results and exhibited in **Figure 5.14**, the use of the training algorithm (see **Figure 5.8**) with 28 hidden neurons leads to the training epoch of 79 that corresponds to minimum RMS value equal to 0.00329. For the use of the training algorithm with 7 hidden neurons, the minimum RMS value equal to 0.00327 is obtained for a training epoch of 109 (see **Figure 5.15**).

The proposed methodology (**Figures 5.7** and **5.8**) for the artificial neural network-based constant life modelling was able to estimate the mean stress effects in the stress amplitude combined with the number of cycles to failure, for any stress R-ratio predominantly in the tensile loading region. The obtained constant life diagrams and surfaces (CLD) proved to be satisfactory considering the small estimation errors and the reduced amount of experimental fatigue data available. In this proposed methodology based on the artificial neural network (ANN), according to the **Figures 5.7** and **5.8**, were only used fatigue data of the P355NL1 steel for the stress R-ratios, R=0, R=-0.5 and R=-1, in a total of 36 experimental fatigue samples.

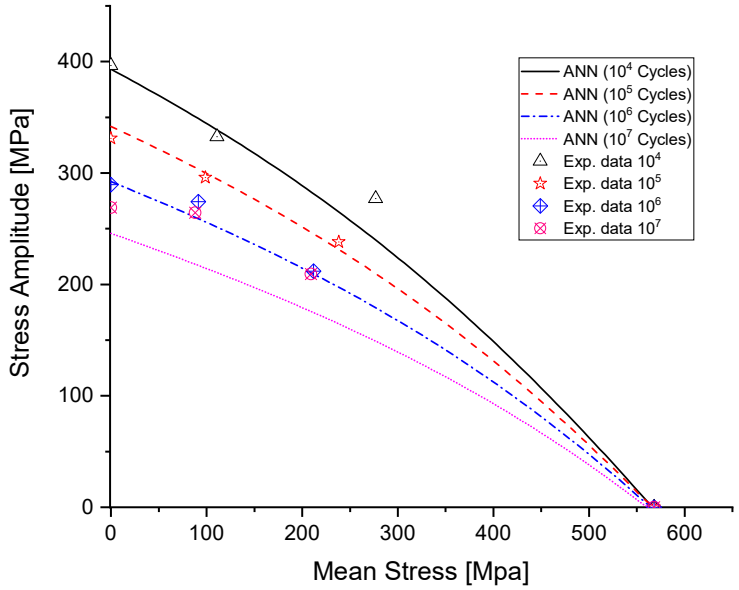

Figure 5.10: Artificial constant life diagram for the dog-bone shaped specimens made of P355NL1 steel obtained by a machine learning artificial neural network algorithm: failure probability of 50% (regions below the curves are considered safety zones).

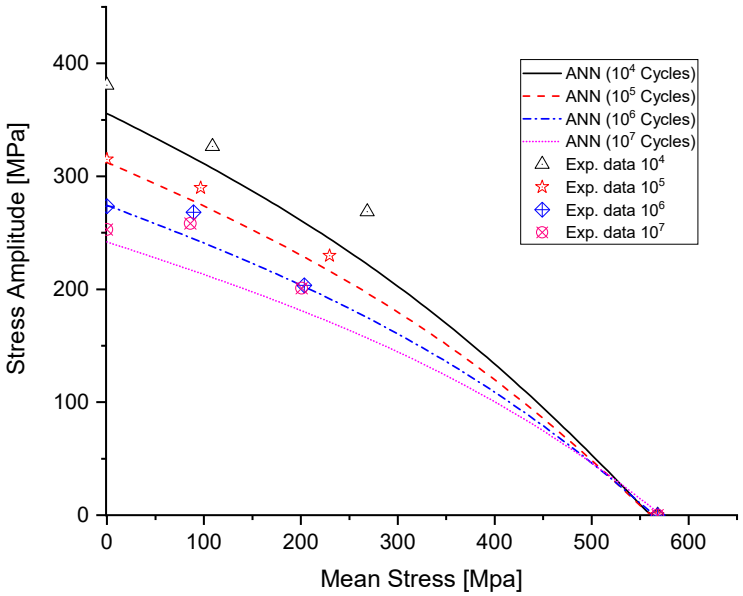

Figure 5.11: Artificial constant life diagram for the dog-bone shaped specimens made of P355NL1 steel obtained by a machine learning artificial neural network algorithm: failure probability of 5% (regions below the curves are considered safety zones).

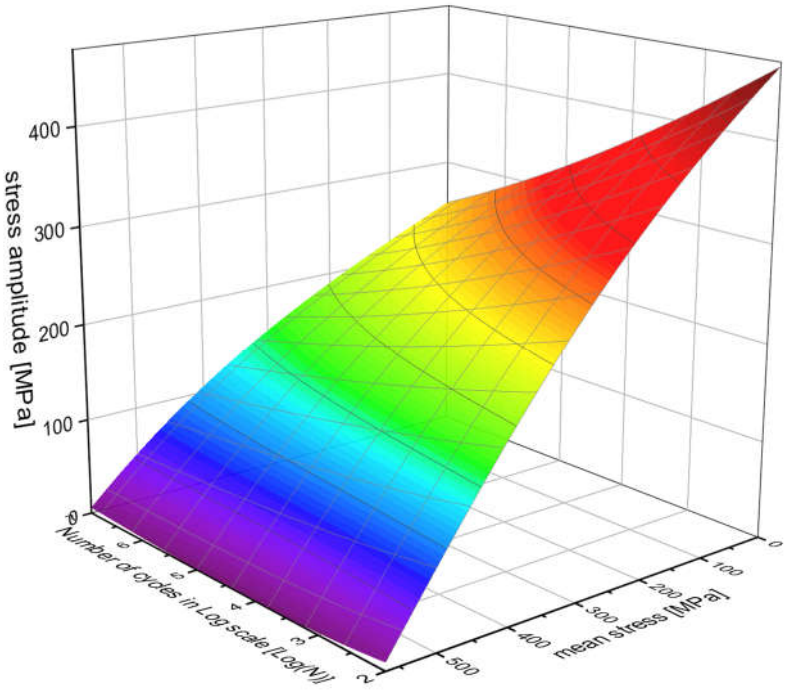

Figure 5.12: Artificial fatigue life surface for the dog-bone shaped specimens made of P355NL1 steel for the failure probability of 50% (50% confidence level).

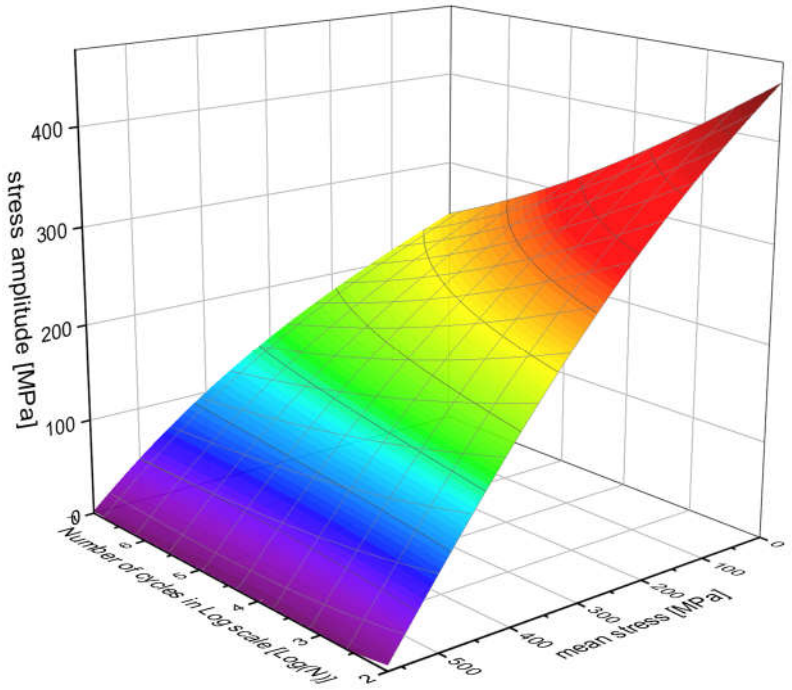

Figure 5.13: Artificial fatigue life surface for the dog-bone shaped specimens made of P355NL1 steel for the failure probability of 5% (95% confidence level).

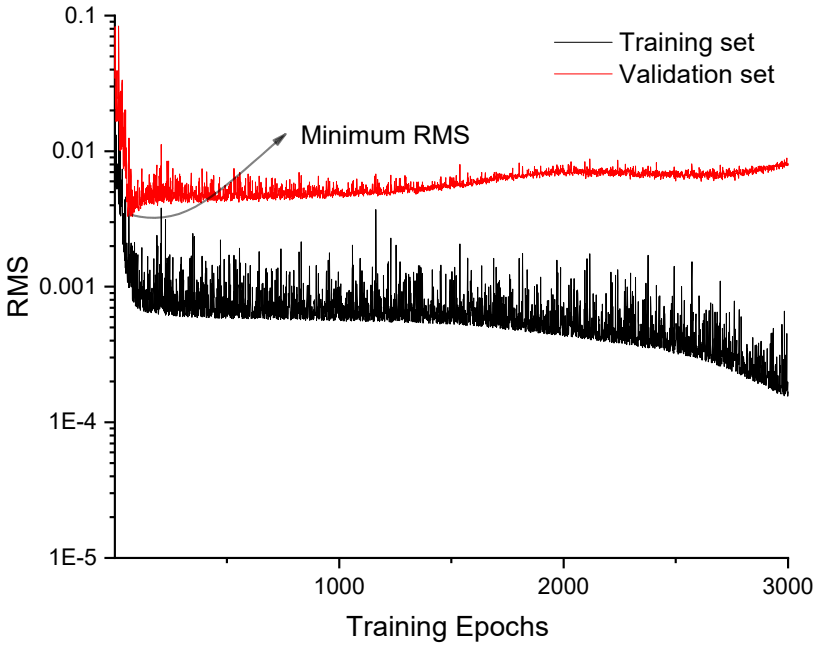

Figure 5.14: RMS curves as a function of training epoch obtained for the ANN with 28 hidden neurons and considering the three stress R-ratios under consideration (R=-1, R=-0.5, R=0), for the Stüssi fatigue data at the 50% probability of failure.

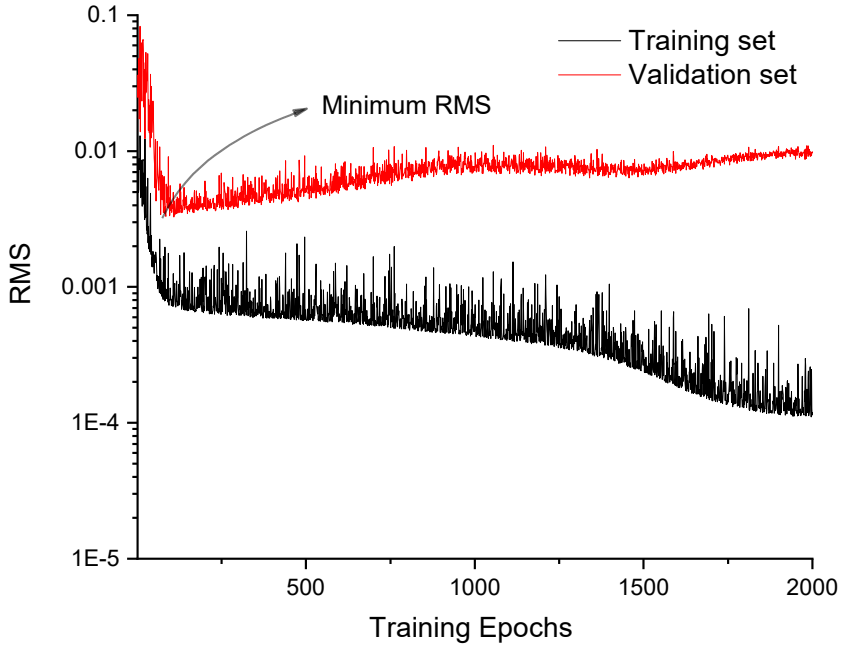

Figure 5.15: RMS curves as a function of training epoch obtained for the ANN with 7 hidden neurons and considering the three stress R-ratios under consideration (R=-1, R=-0.5, R=0), for the Stüssi fatigue data at the 5% probability of failure.

Table 5.3: ANN training estimation results that correspond to the lowest RMS and r values for the validation data set (R=-1, R=-0.5, R=0).

Stress R-ratios	Data Set	Training set		Validation set		Hidden Neuron	Training Epochs
		RMS	r	RMS	r		
-1, -0.5, 0	Stüssi fatigue data for $p = 50\%$	0.00081	0.9969	0.00329	0.9845	28	79
	Stüssi fatigue data for $p = 5\%$	0.00082	0.9924	0.00327	0.9812	7	109

5.6.2 New hybrid ANN-Stüssi modelling to evaluate K_f values

The topology of the artificial neural network algorithm according to **Figure 5.7** and training method proposed in **Figure 5.8** were used to generate the ANN fatigue curves for the fatigue stress R-ratios, R=0, R=0.15 and R=0.3, of the P355NL1 steel. In **Figure 5.16**, the ANN fatigue curves, for the stress R-ratios of R=0, R=0.15 and R=0.3, as well as the experimental fatigue results, for the stress R-ratios equal to R=-1, R=-0.5 and R=0, are illustrated. The ANN fatigue curves were estimated based on trained ANN using the experimental fatigue data for stress R-ratios equal to R=-0.5 and R=0, and validated for R=-1 (see **section 5.6.1**). According to Equation (5.15), the K_f values can be estimated based on smooth specimen ($\Delta\sigma_{smooth}$) and detail fatigue strengths ($\Delta\sigma_{notch}$) for each number of cycles to failure and for the same stress R-ratios. The fatigue data for the notched detail presented in **Figure 5.4** were used to apply the probabilistic Stüssi fatigue model to be used in this new approach (see **Figure 5.9**), according to Equations (5.17) and (5.18), and then estimate the K_f values for the notched detail (see **Figure 5.2**). In this way, the workflow for estimating the fatigue resistance reduction factor, K_f, presented in **Figure 5.9**, aiming at being used in studies concerning the fatigue life prediction of materials and details of extrapolation regions based on the ANN algorithm was applied. Therefore, by applying the approach presented in **Figure 5.10**, K_f values were estimated for the mean values (p equal to 50% and 5%) of the experimental fatigue data. In **Table 5.4**, the K_f values for $10^3 \leq N \leq 10^6$ are presented. According to **Figure 5.17a** and **Table 5.4**, the K_f values are very similar in the quasi-static to low-cycle fatigue regimes for all stress R-ratios under consideration, for the failure probability of 50%. In finite life to high-cycle fatigue regimes, for all stress R-ratios under consideration, the K_f values are increasing and tend to stabilize to values of number of cycles to failure

of 10^6. In **Figure 5.17a**, it is also possible to observe that the K_f values for $R = 0$ are higher when compared to R= 0.15 and R=0.30. Another conclusion can be obtained by observing the results obtained, the K_f values decrease with the increase of the mean stress values. In fatigue design, the K_f values for the failure probability of 5% are presented in **Figure 5.17b**.

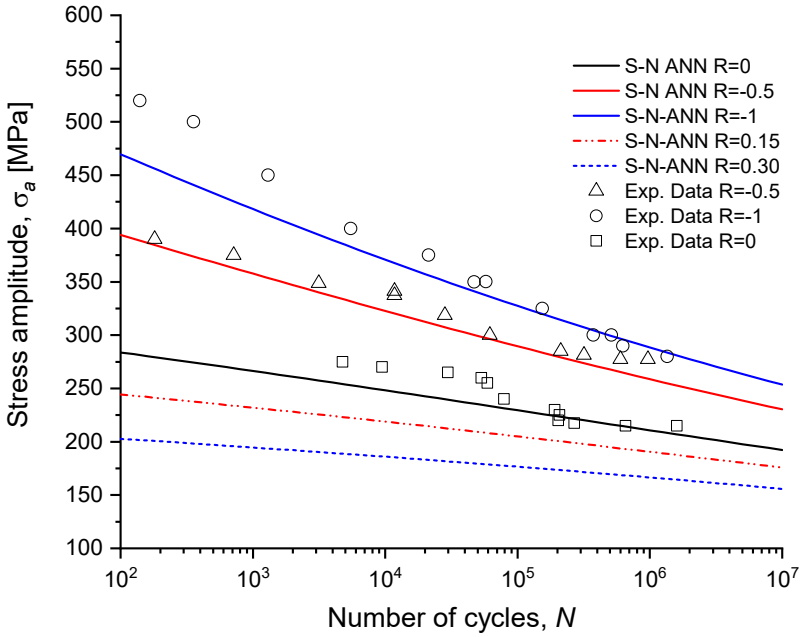

Figure 5.16: ANN fatigue curves, for the stress R-ratios 0, 0.15 and 0.3, as well as the experimental fatigue data, for the stress R-ratios equal to -1, -0.5 and 0.

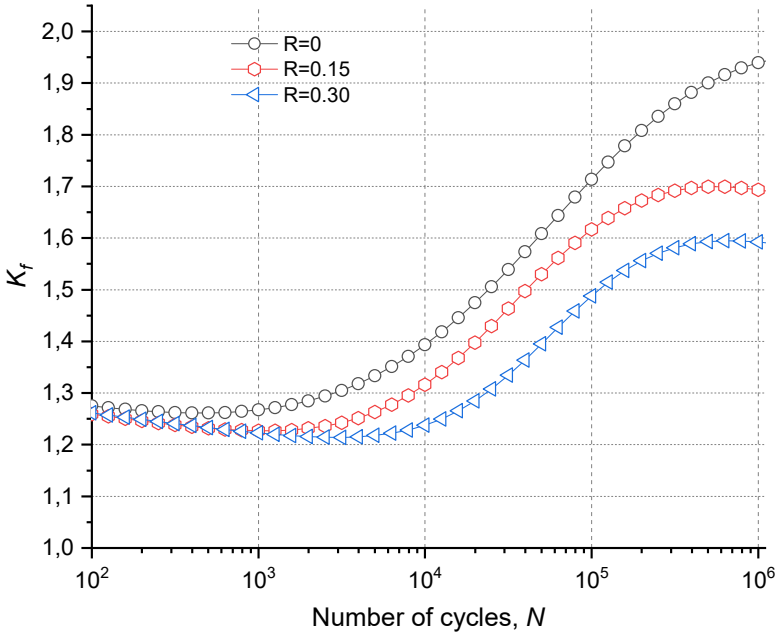

(a)

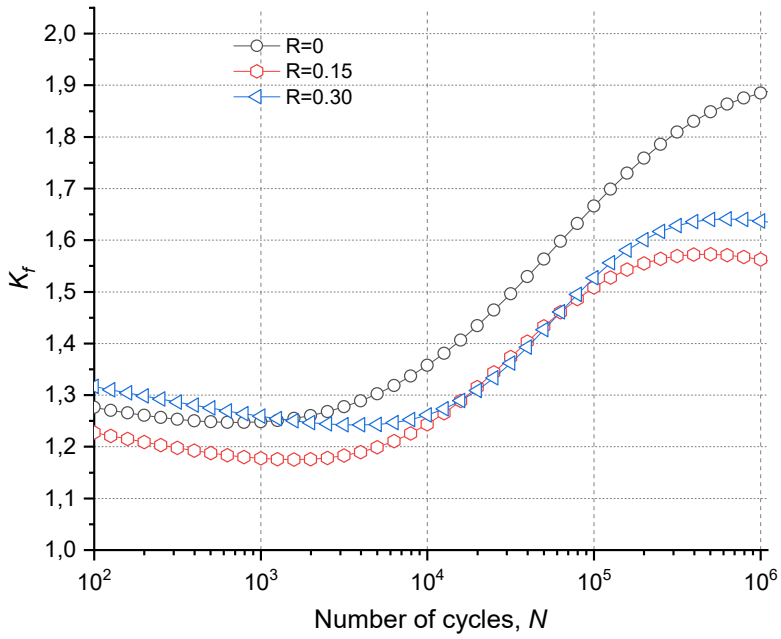

(b)

Figure 5.17: Fatigue strength reduction factor *versus* number of cycles to failure for the failure probabilities of 50% **(a)** and 5% **(b)** of notched detail under consideration.

Table 5.4: Fatigue strength reduction factors for the notch detail under consideration.

N	K_f (p=50%)		
	R=0	***R=0.15***	***R=0.30***
1000	1.267	1.227	1.223
10000	1.393	1.316	1.238
100000	1.713	1.617	1.488
1000000	1.939	1.694	1.592

5.7 Conclusions

In this research work, a new constant life diagram (CLD) based on a machine learning artificial neural network algorithm was developed and trained with probabilistic S-N curves based on the Stüssi model, for various stress R-ratios, using fatigue data from the P355NL1 steel. The trained artificial neural network was able to describe the reliability regions for the fatigue data of the P355NL1 steel in term of mean stress, stress amplitude and stochastic behaviour of the number of cycles until to failure. The proposed

probabilistic constant life diagram was also used to evaluate the mean stress effects on fatigue behaviour as well as to estimate its maximum value as a function of the stress amplitude and number of cycles until to failure. In addition, it was possible to estimate the fatigue strength reduction factors corresponding to the fatigue limit of the notched detail under consideration for any stress R-ratio of the experimental data.

Finally, it is possible to conclude that this new probabilistic constant life diagram (CLD) based on an artificial neural network algorithm allows designers to determine the fatigue resistance limits for any stress R-ratio, with a small amount of experimental fatigue data.

5.8 References

[1] Zhu SP, Lei Q, Huang HZ, Yang YJ, Peng W. Mean stress effect correction in strain energy-based fatigue life prediction of metals. Int J Damage Mech 2017;26:1219–41. doi:10.1177/1056789516651920.

[2] Ince A. A mean stress correction model for tensile and compressive mean stress fatigue loadings. Fatigue Fract Eng Mater Struct 2017;40:939–48. doi:10.1111/ffe.12553.

[3] Lu S, Su Y, Yang M, Li Y. A Modified Walker Model Dealing with Mean Stress Effect in Fatigue Life Prediction for Aeroengine Disks. Math Probl Eng 2018;2018:1–12. doi:10.1155/2018/5148278.

[4] Lanning DB, Nicholas T, Haritos GK. On the use of critical distance theories for the prediction of the high cycle fatigue limit stress in notched Ti-6Al-4V. Int J Fatigue 2005;27:45–57. doi:10.1016/j.ijfatigue.2004.06.002.

[5] Dowling NE. Mean Stress Effects in Stress-Life and Strain-Life Fatigue. SAE Tech Pap Ser 2010;1. doi:10.4271/2004-01-2227.

[6] Gerber H. Bestimmung der zulässigen spannungen in eisen-constructionen. 6th ed. Wolf; 1874.

[7] Goodman J. Mechanics Applied to Engineering. 9th ed. London: Longmans Green and Co; 1930.

[8] Soderberg CR. Factor of Safety and Working Stress. ASME Trans 1930;52:13–28.

[9] Morrow J. Fatigue properties of metals. In: Halford GR, Gallagher and JP, editors.

Fatigue Des. Handb. Pub, SAE: Warrendale; 1968.

[10] Smith, K. N., Watson, P. and Topper TH. A stress-strain function for the fatigue of materials. J Mater 1970;5:767–78.

[11] Pallarés-Santasmartas L, Albizuri J, Avilés A, Avilés R. Mean Stress Effect on the Axial Fatigue Strength of DIN 34CrNiMo6 Quenched and Tempered Steel. Metals (Basel) 2018;8:213. doi:10.3390/met8040213.

[12] Niesłony A, Böhm M. Mean stress effect correction using constant stress ratio S-N curves. Int J Fatigue 2013;52:49–56. doi:10.1016/j.ijfatigue.2013.02.019.

[13] Correia JAFO, Huffman PJ, De Jesus AMP, Cicero S, Fernández-Canteli A, Berto F, et al. Unified two-stage fatigue methodology based on a probabilistic damage model applied to structural details. Theor Appl Fract Mech 2017;92:252–65. doi:10.1016/J.TAFMEC.2017.09.004.

[14] Koutiri I, Bellett D, Morel F. The effect of mean stress and stress biaxiality in high-cycle fatigue. Fatigue Fract Eng Mater Struct 2018;41:440–55. doi:10.1111/ffe.12699.

[15] Barbosa JF, Montenegro PA, Lesiuk G. A comparison between S-N Logistic and Kohout-Věchet formulations applied to the fatigue data of old metallic bridges materials 2019;48:400–10. doi:10.3221/IGF-ESIS.48.38.

[16] Carlos R, Freire S, Maria E, Aquino F De. Building of constant life diagrams of fatigue using artificial neural networks 2005;27:746–51. doi:10.1016/j.ijfatigue.2005.02.003.

[17] Carlos R, Freire S, Duarte A, Neto D, Maria E, Aquino F De. Comparative study between ANN models and conventional equations in the analysis of fatigue failure of GFRP. Int J Fatigue 2009;31:831–9. doi:10.1016/j.ijfatigue.2008.11.005.

[18] Pestana MS, Kalombo RB, Carlos R, Freire S, Jorge J, Almeida L, et al. Use of artificial neural network to assess the effect of mean stress on fatigue of overhead conductors 2018;12:1–10. doi:10.1111/ffe.12858.

[19] Jesus AMP De, Ribeiro AS. Low and High Cycle Fatigue and Cyclic Elasto-Plastic Behavior of the P355NL1 Steel. J Press Vessel Technol 2006;128:298–304. doi:10.1115/1.2217961.

[20] Toasa Caiza PD, Ummenhofer T. A probabilistic Stüssi function for modelling the S-N curves and its application on specimens made of steel S355J2+N. Int J Fatigue

2018. doi:10.1016/j.ijfatigue.2018.07.041.

[21] Barbosa JF, Correia J, Freire Junior RCS, Zhu S-P, De Jesus AM. Probabilistic S-N fields based on statistical distributions applied to metallic and composite materials: State of the Art. Adv Mech Eng 2019;11:1–22. doi:10.1177/1687814019870395.

[22] Castillo E, Fernández-Canteli A. A unified statistical methodology for modeling fatigue damage. Springer Science & Business Media; 2009.

[23] Castillo E, Hadi AS. Parameter and quantile estimation for the generalized extreme-value distribution. Environmetrics 1994;5:417–32.

[24] Dario P, Caiza T, Ummenhofer T. General probability weighted moments for the three-parameter Weibull Distribution and their application in S – N curves modelling. Int J Fatigue 2011;33:1533–8. doi:10.1016/j.ijfatigue.2011.06.009.

[25] Nasiri S, Khosravani MR, Weinberg K. Fracture mechanics and mechanical fault detection by artificial intelligence methods: A review. Eng Fail Anal 2017;81:270–93.

[26] Genel K. Application of artificial neural network for predicting strain-life fatigue properties of steels on the basis of tensile tests. Int J Fatigue 2004;26:1027–35. doi:10.1016/j.ijfatigue.2004.03.009.

[27] Asteris P, Roussis P, Douvika M. Feed-forward neural network prediction of the mechanical properties of sandcrete materials. Sensors 2017;17:1344.

[28] The use of intelligent computational tools for damage detection and identification with an emphasis on composites – A review. Compos Struct 2018;196:44–54. doi:10.1016/J.COMPSTRUCT.2018.05.002.

[29] Artificial neural network modeling on the relative importance of alloying elements and heat treatment temperature to the stability of α and β phase in titanium alloys. Comput Mater Sci 2015;107:175–83. doi:10.1016/J.COMMATSCI.2015.05.026.

[30] Reed R, MarksII RJ. Neural smithing: supervised learning in feedforward artificial neural networks. Mit Press; 1999.

[31] Rumelhart DE, Hinton GE, Williams RJ. Learning representations by back-propagating errors. Nature 1986;323:533–6. doi:10.1038/323533a0.

[32] Pluvinage G. Fracture and Fatigue Emanating from Stress Concentrators. Springer

Science & Business Media; 2007.

[33] Ciavarella M, Meneghetti G. On fatigue limit in the presence of notches: classical vs. recent unified formulations. Int J Fatigue 2004;26:289–98. doi:10.1016/S0142-1123(03)00106-3.

[34] Neuber H. Kerbspannungslehre. Springer-Verlag Berlin Heidelberg; 1937. doi:10.1007/978-3-662-36565-6.

[35] Pilkey WD, Pilkey DF, Peterson RE. Peterson's stress concentration factors. John Wiley; 2008.

[36] Heywood RB. Designing against fatigue. 1st ed. Springer US; 1962.

[37] Solland G. Code requirements to structures documented by non-linear FE-methods. Ce/Papers 2017;1:455–60.

[38] Yamada Y, Kuwabara T. Materials for springs. Springer Science & Business Media; 2007.

[39] Dowling NE. Mechanical behavior of materials: engineering methods for deformation, fracture, and fatigue. Pearson; 2012.

[40] Lee Y-L, Taylor D. Stress-Based Fatigue Analysis and Design. Fatigue Test. Anal. Theory Pract., United States of America: Butterworth Heinemann; 2005, p. 416.

Chapter VI

Conclusions and Future Works

6.1 Concluding remarks

The conclusion of this thesis is consolidated in the integration between the Part A – review, computational implementation, analysis and comparison – which was based on a comparative analysis and discussion of probabilistic fatigue models [1], such as Basquin [2], Sendeckyj [3], ASTM E739 [4], Castillo & Fernández-Canteli [5], Logistic [6] and Stüssi [7], applied to metallic and composite materials, as well as a comparison and performance of least squares (LS), least squares weighted (WLSE), maximum likelihood (MLE) and momentum method (MOM), with aims to obtain a better performance in fatigue life behaviour for small samples [8], and, Part B (purposeful research) on a new proposed methodology for the fatigue life prediction for metallic materials and details based on the probabilistic Stüssi model and trained artificial neural network (ANN) [9]. The development of a constant life diagram based on the probabilistic Stüssi fatigue model and trained artificial neural network (ANN) was proposed. Additionally, a procedure for estimating the fatigue strength reduction factor, K_f, for the fatigue life prediction of materials and components of extrapolation regions based on machine learning artificial neural network algorithm was also proposed. According to Part 1 of the proposed scheme in **Figure 1.1** of this Ph.D. thesis, the probabilistic Stüssi fatigue models applied to metallic materials is more suitable for the development, training, and validation of an artificial neural network (ANN) – **Figures 5.8** and **5.9** – with aim to estimate constant life diagram to high cycle fatigue regions and extrapolate for unknown loading regions.

The fatigue life prediction assumes that the failures do not follow a deterministic law but rather a stochastic process. With aims to quantify the uncertainty associated with the moment of failure, it is necessary to obtain experimental fatigue data for different levels of stress ranges and to associate it with a probability distribution. This kind of research uses fatigue curve models based on probability distribution functions to estimate the fatigue behaviour for the low cycle to high cycle fatigue regions. It turns out that the phenomenon of randomness changes completely depending on the type of material analysed and the fatigue ratio of the test. Composite materials tend to have a greater dispersion of fatigue data when compared to metallic materials, which directly influence the choice of the fatigue model that best represents it.

A state of the art on probabilistic fatigue models based on statistical distributions applied to metallic and composite materials was made [1]. In this study, a comparative study between probabilistic fatigue models such as ASTM E739 standard, Sendeckyj, Castillo & Fernández-Canteli, and Stüssi applied to the metallic and composite materials are presented. For the metallic material, all models exhibit good adjustment when compared with the experimental data from low-cycle to high-cycle fatigue regimes, excluding the Sendeckyj model, which not presented a good fit for the high-cycle fatigue region. For all fatigue regions, only the probabilistic Stüssi model presented very good adjustment results when compared with experimental data. While for the composite material, the probabilistic Stüssi and Sendeckyj fatigue models reveal to be effective for all fatigue regions.

For the formulations of the S-N curves, using Logistic method, Kohout-Věchet model, Power Law and ASTM E739 standard, applied to the metallic materials, obtained different performances mainly in the LCF and HCF regions [10]. Therefore, the obtained results showed that the S-N curve formulation using the Logistic and Power Law equations obtained a better performance in the LCF and HCF regions, corresponding to the lower MSE values when compared to the generalized Power Law formulations and the ASTM E739 standard. In addition, it was also concluded that the Logistic, Kohout-Věchet and Power Law equations obtained smaller errors for the cases with a reduced number of experimental data.

Concerning to a comparison and performance of least squares (LS), weighted least squares (WLSE), maximum likelihood (MLE) and momentum method (MOM), with aims to obtain a better performance in fatigue life behaviour for small samples; it can be

concluded that using the weighted least squares method (WLSE) is more suitable for high-cycle fatigue tests for composites materials [8].

A new constant life diagram (CLD) based on a machine learning artificial neural network algorithm using a multilayer perceptron network trained with the back-propagation algorithm was suggested [9]. This proposed CLD uses the probabilistic S-N curves based on the Stüssi model, for various stress R-ratios, using fatigue data from the P355NL1 steel. The trained artificial neural network, used in this study, was able to describe the reliability regions for the fatigue data of the P355NL1 steel in term of mean stress, stress amplitude and stochastic behaviour of the number of cycles until to failure. Additionally, it was possible to estimate the fatigue strength reduction factors corresponding to the fatigue limit of the notched detail under consideration for any stress R-ratio of the experimental data.

In this way, with the research work proposed in this Ph.D. thesis, it can be concluded that this new probabilistic constant life diagram (CLD) based on an artificial neural network algorithm allows to designers the determining the fatigue resistance limits for any stress R-ratio, with a small amount of experimental fatigue data.

6.2 Future works

The future work after this thesis will consist in the following:

- To perform fatigue tests of metallic materials for different stress R-ratios with the purpose of extending the applicability of the CLD model based on ANN;
- Proposed CLD model based on ANN can be extended to other fatigue damage parameters (strain, SWT, energy, etc.) with aims to predict the fatigue life of structural details supported by finite element method or Neuber rule;
- Generalization of the Stüssi model for other local damage parameters (stress, strain, SWT, energy, etc.);
- Evaluation of the results from the probabilistic fatigue models, such as exponential and Power laws equations, comparing with probabilistic outcomes of each individual stress level applied to metallic materials or details.

6.3 References

[1] Barbosa, J. F. et al. Probabilistic S-N fields based on statistical distributions applied to metallic and composite materials: State of the Art. Advances in Mechanical Engineering, v. 11, n. 8, p. 1-22, 2019.

[2] Basquin OH. The exponential law of endurance tests. Proc Am Soc Test Mater, vol. 10, 1910, p. 625–30.

[3] Sendeckyj GP. Fitting Models to Composite Materials Fatigue Data. ASTM STP 734 1981:245–60. doi:10.1520/STP29314S.

[4] ASTM E739-10(2015). Standard Practice for Statistical Analysis of Linear or Linearized Stress-Life (S-N) and Strain-Life (ε-N) Fatigue Data. ASTM Int West Conshohocken, PA, USA 2015. doi:10.1520/E0739-10.2.

[5] Castillo E, Fernández-Canteli A. A unified statistical methodology for modeling fatigue damage. Springer Science & Business Media; 2009.

[6] Mu PG, Wan XP, Zhao MY. A New S-N Curve Model of Fiber Reinforced Plastic Composite. Key Eng Mater 2011;462–463:484–8.

[7] Toasa Caiza PD, Ummenhofer T. A probabilistic Stüssi function for modelling the S-N curves and its application on specimens made of steel S355J2+N. Int J Fatigue 2018.

[8] Barbosa, J.F. et al. Analysis of the fatigue life estimators of the materials using small samples. The Journal of Strain Analysis for Engineering Design, v. 53, n. 8, p. 699-710, 2018.

[9] Barbosa, J. F., et al. Fatigue life prediction considering the mean stress effects through an artificial neural network applied to metallic materials. International Journal of Fatigue, 2019, [accept].

[10] Barbosa, J. F. et al. A comparison between SN Logistic and Kohout-Věchet formulations applied to the fatigue data of old metallic bridges materials. Frattura ed Integrità Strutturale, v. 13, n. 48, p. 400-410, 2019.